



# A Review of Australian and New Zealand Investigations on Aeronautical Fatigue During the Period April 2003 to March 2005

*Graham Clark*

**Air Vehicles Division**  
Platforms Sciences Laboratory

DSTO-TN-0624

## **ABSTRACT**

This document has been prepared for presentation to the 29th Conference of the International Committee on Aeronautical Fatigue scheduled to be held in Hamburg, Germany, 6th and 7th June 2005. Brief summaries and references are provided on the aircraft fatigue research and associated activities of research laboratories, universities, and aerospace companies in Australia and New Zealand during the period April 2003 to March 2005. The review covers fatigue-related research programs as well as fatigue investigations on specific military and civil aircraft.

## **RELEASE LIMITATION**

*Approved for public release*

*Published by*

*DSTO Platforms Sciences Laboratory  
506 Lorimer St  
Fishermans Bend, Victoria 3207 Australia*

*Telephone: (03) 9626 7000  
Fax: (03) 9626 7999*

*© Commonwealth of Australia 2005  
AR- 013-387  
May 2005*

**APPROVED FOR PUBLIC RELEASE**

# A Review of Australian and New Zealand Investigations on Aeronautical Fatigue During the Period April 2003 to March 2005

## Executive Summary

The Australasian delegate to the International Committee on Aeronautical Fatigue (ICAF) is responsible for preparing a review of aeronautical fatigue work in Australia and New Zealand for presentation at the biennial ICAF conference. The Defence Science and Technology Organisation (DSTO) has traditionally provided the Australasian delegate to ICAF and publishes the review as a DSTO document. This document later forms a chapter of the ICAF conference minutes published by the conference host nation. The format of the review reflects ICAF requirements.

# Contents

<b>8. AUSTRALASIAN REVIEW .....</b>	<b>8-1</b>
<b>8.1 Introduction .....</b>	<b>8-1</b>
<b>8.2 Fatigue Investigations On Military Aircraft.....</b>	<b>8-2</b>
8.2.1 Completion of F/A-18 Aft Fuselage Test (L. Molent and S. Barter, DSTO).....	8-2
8.2.2 Flaw IdeNtification through the Application of Loading (FINAL) (B. Dixon, S. Barter and L. Molent, DSTO) .....	8-2
8.2.3 The Effective Block approach to Crack Growth Modelling (L. Molent, M. McDonald, S. Barter, P. White, DSTO).....	8-3
8.2.4 The F/A-18 Fatigue Crack Growth Data Compendium (L. Molent, J. Sun and A.J. Green, DSTO) .....	8-4
8.2.5 F/A-18 Aircraft Structural Integrity Support (Mr Juergen Moews, Aerostructures).....	8-6
8.2.6 F-111 Sole Operator Program – F-111F Wing Economic Life Determination (Thomas van Blaricum, DSTO) .....	8-7
8.2.7 F-111 Aircraft Structural Integrity Sole Operator Program (G. Swanton, K. Walker, DSTO) .....	8-12
8.2.8 Structural integrity assurance for the F-111 outer lower wing skin through a condition assessment program (K. Walker, J. Walker and G. Swanton, DSTO) ...	8-13
8.2.9 Fatigue Cracking of F-111 FS 496 Nacelle Former (K. Walker, G. Swanton, G. Chen, DSTO, V. Sridhar Aerostructures) .....	8-16
8.2.10 Fatigue assessment of critical features in the F-111 Wing Pivot Fitting (K. Walker, J. Walker, DSTO) .....	8-17
8.2.11 Development of a predictive tool for the analysis of fatigue crack growth involving notch plasticity (Weiping Hu, DSTO) .....	8-19
8.2.12 Support of the ADF F-111 Safety By Inspection Program (Rahul Kashyap and Michael Houston, Aerostructures) .....	8-21
8.2.13 Build Quality Assessment of F-111 Wings (C.A. Harding, M.W. Hobson and G.R. Hugo, DSTO) .....	8-22
8.2.14 Automated Ultrasonic Inspection for Cracks in F-111 Wing Planks (G. Hugo, C. Harding, S. Bowles, H. Morton, DSTO, G. Craven, D. Ward, J. Duncombe, RAAF NDTSL) .....	8-23
8.2.15 F-111 Strake failures (G. Redmond, DGTA).....	8-24
8.2.16 Extended Testing of a P-3 Empennage at DSTO, Melbourne (P Jackson, DSTO).....	8-26
8.2.17 P3 Orion Flap Track (G. Redmond, DGTA).....	8-27
8.2.18 C130J Structural Life (L. Meadows, R. Ogden, DSTO).....	8-29
8.2.19 LIF Fatigue Test (T. Bussell, DSTO).....	8-31
8.2.20 Helicopter Structural Integrity - Flight Data Recorder (FDR) Trials (Chris Knight, DSTO) .....	8-32
8.2.21 Automatic Synthesis of Transfer Functions to Predict Helicopter Dynamic Component Loads from Fixed System Parameters (Luther Krake, DSTO).....	8-33
<b>8.3 Fatigue of Civil Aircraft .....</b>	<b>8-33</b>
8.3.1 Piper Brave - New Long Life Spar (Juergen Moews, Aerostructures) .....	8-33
8.3.2 The ‘Damage Tolerance’ of Civil Aircraft (S. Swift, CASA).....	8-34
<b>8.4 Fatigue-Related Research Programs.....</b>	<b>8-37</b>
8.4.1 In situ Structural Health Monitoring of an Impact Damaged F/A-18 Horizontal Stabilator (A.P. Walley, N. Rajic, DSTO). .....	8-37
8.4.2 Use of Sonic Thermography as a Non-destructive evaluation technique (Kelly A. Tsoi and Nik Rajic, DSTO).....	8-38
8.4.3 Aircraft Forensic Engineering – Investigations (N Athinotis, DSTO) The following sections contain examples of investigations undertaken in the last two years: .....	8-40
8.4.4 The effect of pitting corrosion on the position of aircraft structural failures (B.R. Crawford, C. Loader and P.K. Sharp, DSTO).....	8-46
8.4.5 Shape optimisation of holes for multiple-peak stress minimisation (W. Waldman and M. Heller, DSTO) .....	8-53
8.4.6 Risk and Reliability Assessment Methods (K. Watters and P. White, DSTO) .....	8-54
8.4.7 Shape optimisation for life extension of holes in lower wing stiffeners in P-3C Aircraft (R. Evans, R. Braemar and M.Heller) .....	8-55
8.4.8 Computational shape optimization with stress robustness constraints (R. Braemar, M. McDonald, and M. Heller, DSTO).....	8-56

8.4.9	Stress analysis of near optimal surface notches in 3D plates (R. Wescott, B. Semple, and M. Heller, DSTO).....	8-57
8.4.10	Effects of Corrosion Prevention Compounds on the Fatigue Life of a Typical Transport Aircraft Skin Splice (S. Russo, Bob. Clark <sup>a</sup> , P. Nolan <sup>a</sup> , B.R.W. Hinton, K. Shankar <sup>a</sup> , DSTO, <sup>a</sup> School of Aerospace and Mechanical Engineering, ADFA, Canberra, Australia).....	8-58
8.4.11	Fractographic study of 7xxx Aluminium alloys (P. White, DSTO).....	8-59
8.4.12	Comparative Vacuum Monitoring (CVM™) A tool for Structural Health Monitoring of aircraft (D P Barton, Structural Monitoring Systems Ltd, Australia).....	8-63
8.4.13	Laser Shock Peening of Aluminium alloys (Q Liu, DSTO) .....	8-65
8.4.14	Modelling of Defects and Damage in Aerospace Composite Structures (M. Scott, CRC-ACS) .....	8-69
8.4.15	Damage Resistance and Tolerance of Composite Replacement Panels (M. Scott, CRC-ACS) .....	8-70
<b>8.5</b>	<b>Fatigue Investigations in New Zealand .....</b>	<b>8-72</b>
8.5.1	C-130 Hercules: Fleetwide Cracking of Lower Wing Spar (M. L. Stevens, S. K. Campbell, P. C. Conor, G. Murphy, DTA, New Zealand).....	8-72
8.5.2	Development of an Operational Usage Monitoring System using Commercial Data Recorders (M. J. Hollis, S. K. Campbell, D. C. Scott, J. D. Williams).....	8-73
8.5.3	Failure Investigation of Civilian UH-1H Main Rotor Blade, (A. D. James, P. C. Conor) .....	8-74

## 8. Australasian Review

### 8.1 INTRODUCTION

This document presents a review of Australian and New Zealand work in fields relating to aeronautical fatigue in the period 2003 to 2005, and comprises inputs from the organisations listed below. The author acknowledges these contributions with appreciation. Enquiries should be addressed to the person identified against the item of interest.

DSTO	Defence Science and Technology Organisation, 506 Lorimer Street, Fishermans Bend VIC 3207, Australia
ADFA	Australian Defence Force Academy, University of New South Wales, Canberra, Australia
CASA	Civil Aviation Safety Authority, Northbourne Ave, Civic, Canberra 2601, Australia.
DTA	Defence Technology Agency, Auckland, New Zealand
CRC-ACS	Cooperative Research Centre for Aerospace Composite Structures. 506 Lorimer Street, Fishermans Bend, VIC 3207, Australia.
Aerostructures Australia	Level 14, 222 Kingsway, South Melbourne, VIC 3205, Australia.
Structural Monitoring Systems Ltd	Level 1, 5/15 Walters Drive, Osborne Park, Western Australia, 6017, Australia.
DGTA	Director General Technical Airworthiness, RAAF Williams, Laverton Vic 3207, Australia

## **8.2 FATIGUE INVESTIGATIONS ON MILITARY AIRCRAFT**

### **8.2.1 Completion of F/A-18 Aft Fuselage Test (L. Molent and S. Barter, DSTO)**

The F/A-18 is an extremely manoeuvrable and high performance fighter/attack aircraft. The inner wing leading edge extension (LEX) provides fuselage and inner wing lift enabling it to achieve angles of attack (AOA) in excess of 60 degrees. The twin vertical tails canted slightly outward exploit the high-energy vortices generated by each LEX during high AOA flight. This provides good directional stability during these high AOA conditions. However, these vortices break down at  $AOA > 10$  degrees, buffeting the structure and exciting the resonant frequencies of the empennage. This produces high acceleration levels resulting in high stresses in many key structural components, which are synergistic with the quasi-static manoeuvre loading with respect to fatigue damage.

To address this difficult fatigue life problem the Australian part of the F/A-18 International Follow-On Structural Test Project was to carry out an empennage test (FT46) using loading such that test article dynamic response matched as closely as possible that of an aircraft in flight. This required a high degree of load fidelity and a high rate of test load application. This was accomplished by combining a manoeuvre loading system (that did not significantly affect the dynamic characteristics of the structure) with a high frequency dynamic loading system. The fatigue phase of this test has now been completed with over 23,000 simulated flight hours applied.

Following the fatigue portion of the testing a complex residual strength test was undertaken using loads predicted from in service flight data rather than design load cases. This not only tested the structure in the state of damage at the end of fatigue testing but also with removal of several of the repairs that had been applied during testing. This produced valuable quasi-damage tolerance information. In addition damage was introduced to several areas to simulate the condition of structural damage, revealed through other testing and service experience but had failed to occur on FT46 [1,2].

### **8.2.2 Flaw Identification through the Application of Loading (FINAL) (B. Dixon, S. Barter and L. Molent, DSTO)**

The teardown and inspection of aircraft, which have completed a significant period of service, is a central requirement of many Aircraft Structural Integrity Management Plans (ASIMP). The reasons for this include a need to inspect for the potential onset of widespread fatigue damage and to assess the impact of corrosion and in-service mechanical damage. Furthermore, service life data from fleet aircraft are required to confirm laboratory fatigue test results and substantiate the assumptions made during safe-life calculations or probabilistic risk and reliability studies. A teardown and inspection of the fracture critical F/A-18 wing attachment bulkheads (or centre barrel - CB) has been initiated to achieve these goals for the RAAF's F/A-18 fleet. Use is being made of ex-service CBs supplied from the Canadian Forces and U.S. Navy (USN) CB replacement programs.

Investigations suggest that the largest "likely" cracks in the critical bulkheads will be less than 1 mm deep at the time a CB is replaced. Since the detectable crack depth threshold for current NDI (using high frequency eddy current (HFEC) detection) is 1.0 mm or greater, these cracks may not be found.

To significantly improve the probability of detecting cracks that are below the lower threshold of NDI, an increase in their size by accelerated fatigue testing of the CBs has been implemented. Cyclic loads (using the mini-FALSTAFF spectrum) are applied to the wing attachment lugs of ex-service CBs in a test rig to simulate in-flight wing loads. The loading is of sufficient magnitude and duration to ensure that any existing cracks will be grown to a size that ensures their detection under laboratory conditions. Quantitative fractography has been performed on observed cracking to obtain crack growth data and to determine the size, nature and cause of discontinuities that initiate fatigue cracking. Three CBs have been tested and torn-down and a fourth is currently cycling [3,4,5].

### 8.2.3 The Effective Block approach to Crack Growth Modelling (L. Molent, M. McDonald, S. Barter, P. White, DSTO)

Accurate fatigue prediction tools are essential for fatigue life management. In the case of the RAAF F/A-18 there is a wealth of crack growth data generated through quantitative fractography (QF) [6-10]. Unfortunately conventional damage models (eg AFGROW, Fastran etc) provided poor representations of these data [11], and this prompted the development of a predictive method tailored to variable amplitude data.

A key concept used is one where a repeating “block” of loading is applied throughout the fatigue life, sufficiently often that the blocks can be treated in a similar manner to single cycles in constant-amplitude loading. This characteristic approach to fatigue life prediction was first proposed by Paris [12]. The basic hypothesis is that the variations of the crack tip fields are describable in terms of some characteristic stress-related measure, for example, Root Mean Squared (RMS) of the stress intensity factor range ( $\Delta K_{RMS}$ ) (or the peak value).

Analysis of fatigue cracking over many decades has provided DSTO with a capability to produce detailed crack growth information for variable-amplitude loading under service conditions or laboratory conditions which closely resemble real service conditions. The methods being developed capitalize on the quality of this data and are aimed at providing useful tools for fatigue management. They have been reviewed in detail, recently by McDonald [15], and this approach has been used successfully on F/A-18 representative steel (AF1410) coupon specimens at different stress levels [13] to life a fracture critical component. It has also been used to predict the results from coupon fatigue tests [6,7,8] and to help assess the fatigue life of the inner wing [14].

One simple formulation is to use the well-known Paris equation and apply it to variable amplitude loading:

$$\frac{da}{dt} = C(K_{ref})^m$$

where  $K_{ref}$  is the parameter containing the reference stress.

The first step in the process was to derive a crack growth resistance relationship based on the quantitative fractography (QF) coupon data for several fighter aircraft load sequences. To do this, the crack growth gradient ( $da/dN$ ) and  $\Delta K_{RMS}$  were calculated for each consecutive QF data point.

The crack growth gradients ( $da/dN$ ) were obtained from a linear best fit of crack depth versus test hours smoothed over nine experimental data points. The cycles/hour conversion factors for each spectrum were used in order to ascertain the “average” crack growth *per cycle*.

In this example, an RMS stress intensity factor range ( $\Delta K_{RMS}$ ) was adopted as the parameter representing the characteristic stress, and was calculated using the following equation:

$$\Delta K_{RMS} = \beta \Delta \sigma_{RMS} \sqrt{\pi a}$$

Notes:

- For each  $\Delta K_{RMS}$  calculation, the beta value was obtained by means of a look-up table extracted from the crack growth program AFGROW. The beta ( $\beta$ ) value is only a function of crack and specimen geometry.
- The RMS stress range,  $\Delta \sigma_{RMS}$ , was a fixed value calculated for each spectrum/reference stress combination.

Typical results for two F/A-18 spectra are shown in Figure 1. Here the slope (equivalent to a Paris CA exponent  $m$ ) was found to be 2 and the intercept ( $C$ ) varied with the spectrum (with material and geometry constant).



A key outcome from this analysis is that by determining  $C$  and  $m$ , it appears to be possible to use these parameters, determined using one particular fighter sequence, to predict behaviour under a different sequence. This involves coupon-derived data similar to that in Figure 1, derived for just one sequence, and the use of conventional fatigue prediction models – which can be fairly inaccurate in direct prediction – simply as a transfer tool. The extent to which this approach (described in [15]) may be applied (eg. over what type of VA sequence) has not yet been established, and will be the subject of further work.

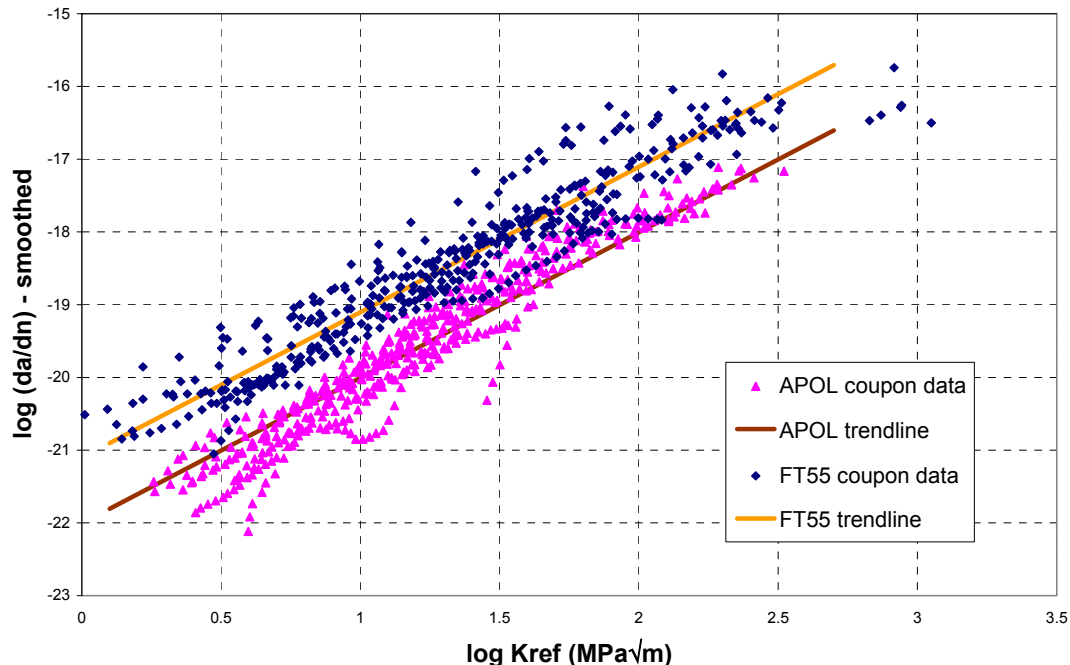


Figure 1: Crack growth resistance curve for two fighter aircraft load spectra, determined using the characteristic stress approach for all coupon specimens tested

#### 8.2.4 The F/A-18 Fatigue Crack Growth Data Compendium (L. Molent, J. Sun and A.J. Green, DSTO)

One of the primary factors that limit the life of metallic aircraft structures is fatigue cracking under variable amplitude cyclic loading. In highly-stressed fighter aircraft, material defects or flaws are often initiators of fatigue cracking, and initial flaws typically 0.01mm in size are widespread. Rarer flaws substantially larger than this (in extreme cases, of mm size) are the ones which need to be considered to provide limits to fatigue life of the fleet aircraft. During the application of flight loads, these fatigue cracks propagate at approximately an exponential rate with time in service.

Various types of ‘fatigue initiating mechanisms’ have been known to commence the fatigue cracking. These include inter-metallic particles; etch pits and material folds due to bead shot peening. The fatigue life of any given metallic structure correlates to what is known as the Equivalent Pre-crack Size (EPS) of these fatigue crack-initiating defects.

A better understanding of the factors that influence EPS has the potential to facilitate more accurate predictions of fatigue life, and thus the potential to extend the safe life of aircraft structures and enhance Australian Defence capability.

Many aluminium alloy 7050-T7451 coupons have been fatigue tested at the Air Vehicles Division of DSTO. During these tests, various F/A-18 representative spectra were repeatedly applied to the coupons, at various stress levels, until failure. In addition, much data are available from cracks in various F/A-18 full-scale structural fatigue tests.

Quantitative fractography was conducted for many of these specimens, producing crack growth data that have been considered useful in fatigue analysis. A completed report presents a collation of DSTO F/A-18 crack growth information known as the F/A-18 Fatigue Crack Growth Data Compendium [16]. Using the data in this compendium, various techniques were used to estimate the EPS. The report presents an assessment of the size of fatigue-crack initiating defects and damage types found in these specimens. Further it was determined that the applied stress appeared to have little bearing on the initial defect size or the damage type. However, the surface finish appeared to have decisive influence in governing the type of fatigue damage induced. A key element of further work is to identify the larger flaws which have the potential to give short service lives in fleet aircraft.

A sound understanding of the factors influencing the EPS is important to the task of predicting the fatigue life of aircraft structures and thus, the outcome of this investigation is valuable for the enhancement of Australian defence capability. The probabilistic risk assessment method [17] can make use of the data derived within the compendium.

#### References.

1. Molent, L., Barter, S., White, P. and Conser, D., "Overview of the F/A-18 Aft Fuselage Combined Manoeuvre and Dynamic Buffet Fatigue Test", Proc. USAF Aircraft Structural Integrity Program Conference, Savannah, Georgia, 10-12 Dec 2002.
2. Barter, S., Molent, L., Landry, N., Klose, P. and White, P., "Overview of the F/A-18 Aft Fuselage Combined Manoeuvre and Dynamic Buffet Fatigue and Residual Strength Testing", Proc. Australian International Aerospace Congress, Brisbane Aust., July 29 – 1 Aug 2003.
3. Dixon, B., Molent, L. and Barter, S.A., Flaw Identification through the Application of Loads: Teardown of the Centre Barrel from CF-18 188747, DSTP-TR-1660, Dec 2004.
4. Dixon, B., Molent, L. and Barter, S.A., The FINAL program of enhanced teardown for agile aircraft structures, Proc. 8th NASA/FAA/DOD Conference on Aging Aircraft, Palm Springs, 31 Jan – 3 Feb 2005.
5. Molent, L., Dixon, B. and Barter, S., "Flaw Identification through the Application of Loading", Proc. Structural Integrity and Fracture Conference 2004, Brisbane, 26-29 Sept 2004.
6. Pell, R.A., Molent, L., and Green, A.J., "The Fractographical Comparison of F/A-18 Aluminium Alloy 7050-T7451 Bulkhead Representative Coupons Tested Under Two Fatigue Load Spectra at Several Stress Levels", DSTO-TR-1547, Feb 2004.
7. Pell, R.A., Molent, L., and Green, A.J., "The Fractographic Examination of F/A-18 Aluminium Alloy 7050-T7451 Bulkhead Representative Coupons Tested Under Two Service Spectra and Two Stress Levels", DSTO-TR-1629, Oct 2004.
8. Molent, L., Barter S.A. and Green, A.J., Comparison of Two F/A-18 Aluminium Alloy 7050-T7451 Bulkhead Coupon Fatigue Tests, DSTO-TR-1646, Nov 2004.
9. Cox, A.F. and Barter, S.A., "F/A-18 Horizontal Stabilator Spindle Coupon Test Program", DSTO-TR-1443, June 2003.
10. Barter, S.A., "Fatigue Crack Growth in 7050T7451 Aluminium Alloy Thick Section Plate with a Surface Condition Simulating Some Regions of F/A-18 Structure", Defence Science and Technology Organisation, DSTO-TR-1458, July 2003.
11. Barter S.A., Molent L., Goldsmith, N.T. and Jones, R., "An experimental evaluation of fatigue crack growth." Journal of Engineering Failure Analysis, Vol 12/1 pp 99-128, 2005.
12. Paris P.C., "The Growth of Cracks due to Variation in Loads", Ph.D. Thesis, Lehigh University, Bethlehem, Pennsylvania, 1960.
13. McDonald, M. and Molent, L., "Fatigue Assessment of the F/A-18 Horizontal Stabilator Spindle", DSTO-TR-1620, Oct 2004.

14. Huynh, J., Molent, L. and Barter, S.A., "F/A-18 Inner Wing Lifing Investigation", DSTO-TR-1641, Nov 2004.
15. McDonald, M., "Fatigue Crack Growth Methodologies in Structural Life Assessment", Discussion Paper, DSTO-DP-in preparation, 2005.
16. Molent, L., Sun, Q., and Green, A.J., "The F/A-18 Fatigue Crack Growth Data Compendium", DSTO-TR-1677, Feb 2005.
17. White, P., Molent, L. and Barter, S.A., "Interpreting fatigue test results using a probabilistic fracture approach" International Journal of Fatigue 27/7, pp 752-767 (2005).

## **8.2.5 F/A-18 Aircraft Structural Integrity Support (Mr Juergen Moews, Aerostructures)**

### **8.2.5.1 F/A 18 Fatigue Test Interpretation**

The F/A-18 International Follow-On Structural Test Program (IFOSTP) was established to determine the F/A-18 safe life under RAAF usage. With the completion of this program, test interpretation now establishes where critical structure suffered damage and how it can be managed in service.

Using DEF STAN 00-970, Aerostructures developed a fatigue management methodology for the aft fuselage and empennage which combines safe life and safety by inspection methodologies. Critical structure with damage during fatigue testing was the priority.

Using mean and safe SN curves, developed in accordance with DEF STAN 00-970, scatter factors were calculated that determined whether fatigue test results demonstrated sufficient safe life. Where necessary, residual strength calculations were made to extend the safe life using a simplified crack growth model and fractographic crack growth rates. For inspectable maintenance critical parts with inadequate safe life, inspection intervals were established.

These test interpretation activities allow results of the long running F/A-18 fatigue test program to be applied in support of the RAAF fleet, enabling safe operations to their planned withdrawal date.

### **8.2.5.2 F/A-18 Ageing Aircraft Audit**

The Royal Australian Air Force (RAAF) F/A-18 fleet has reached its anticipated mid-service life. In accordance with Australian Defence Force (ADF) airworthiness doctrine, an Ageing Aircraft Audit (AAA) was conducted to provide advice on the management of the airframe given the structural condition of the ageing fleet. A key aspect of the AAA is to provide fleet condition data to supplement and support IFOSTP test interpretation activities.

The structural condition data required for an effective AAA was acquired via a desk-top audit of historical maintenance records and a physical audit of a representative aircraft. All data was stored in an SQL database with a web-based data retrieval system. For the desk-top audit, all available defect and repair information was extracted and analysed to establish meaningful trends within the fleet, including assessments with respect to defect cause, location, high defect parts and distribution by material type. The distribution of defects by servicing type, tail number, model and production block was also considered.

The physical audit involved deeper level inspection of targeted locations not considered during routine RAAF maintenance. One of the key drivers for the selection of locations were critical areas that have experienced fatigue cracking during IFOSTP. These inspections sought to determine whether these locations may also be prone to various forms of environmental degradation. The results of depot level maintenance activity and physical audit programs carried out by foreign operators of the F/A-18 were also considered for the selection of candidate inspection locations.

Several defects on critical components were detected during the physical audit, which indicated the need for further action in the fleet. Furthermore the requirement for a regularly updated Condition Monitoring Database was highlighted. Further steps to conclude the AAA are under consideration.

### 8.2.5.3 F/A-18 HUG

The RAAF Hornet Upgrade (HUG) project is an undertaking by Australia to maintain and improve the leading edge capability of the F/A-18 aircraft through various systems and structural upgrades and modifications. Part of that activity includes HUG Phase 3 which is the structural modification and refurbishment program aimed at ensuring the fleet can safely achieve the planned withdrawal date.

Aerostructures was requested to assist the Commonwealth in reviewing engineering issues and making recommendations to the Phase 3 project team. The aim is to provide independent validation that the envisaged technical solutions represent value for money, or to suggest alternative management strategies.

Aerostructures is supporting the HUG Phase 3 project team by providing engineering support to specific tasks and in a more general sense ensure continuity of engineering knowledge from IFOSTP test interpretation activities through to implementation of management solutions. Activities are underpinned by a methodology for the systematic assessment of damaged structure including test interpretation, review of classification, configuration, accessibility, estimation of expected fleet defects, cost benefit analysis for preventative modifications, technical requirements and impact on operations.

### 8.2.6 F-111 Sole Operator Program – F-111F Wing Economic Life Determination (Thomas van Blaricum, DSTO)

An F-111C Wing Damage Enhancement Test (WDET) article (Wing S/N A15-5) failed on test at DSTO in Feb 2002 [1]. The failure occurred largely as a result of build quality deficiencies in Taperlok bolt holes in the lower wing skin. The RAAF sourced replacement F-111F and F-111D wings from the Aircraft Maintenance and Regeneration Centre (AMARC) as there were concerns that similar flaws could be present in other C model wings. One of the reasons for the WDET test was to confirm a view that there were gaps in the structural certification basis of both the F-111 long wing and short wing configurations for the RAAF and USAF operational environments. The wing test conducted by the Original Equipment Manufacturer (OEM) set a life of 10,000 flying hours, however both RAAF operations (long configuration) and USAF operations (short configuration) have historically been significantly more severe than the loading applied during that OEM wing test. In addition, truncation of the test spectrum by the OEM further undermined confidence in the test result when applied to the lower wing skin. Consequently any economic life based on the test result, and some aspects of the certification basis pertaining to fatigue strength, were no longer seen to provide valid support for continued operation of any of the RAAF wings up to the planned withdrawal date (PWD).

As a result of the identified concerns about the wing certification basis, and significant deviation from the test verification basis which became evident when DSTO assessed USAF usage data on wings recently purchased from the USAF, DSTO was tasked to undertake an additional wing test to determine the economic life of F-111F and F-111D model wings. This test has been titled as the F-111F Wing Economic Life Determination (F-WELD) (Figure 1) and forms part of the F-111 Sole Operator Program.

The primary objectives of the F-WELD fatigue test are to:

- a. determine the economic fatigue life of the F-111F and D model wings
- b. contribute to the development of a revised certification basis and structural management plan for the ongoing structural integrity management of F-111F and D model wings through to PWD, and
- c. provide an opportunity to conduct Non Destructive Inspection (NDI) procedure development activities utilising an SAIC Ultra Image international UltraSpect-MP automated ultrasonic inspection system

The RAAF have purchased a SAIC<sup>1</sup> automated NDT system and this will be used to inspect the F-WELD test article lower wing skin Taperlok bolt holes to assist in the development of procedures that will help facilitate on going management of the wings on the basis of safety-by-inspection.

---

<sup>1</sup> The UltraSpect-MP system can simultaneously acquire ultrasonic and eddy current data in a single scan. It provides full A-scan capture for all ultrasonic data. This system consists of a laptop computer for software control, a separate Data Acquisition System (DAS), which contains the appropriate inspection hardware, such as ultrasonic cards, eddy current cards, etc. Other inspection techniques integrated into the inspection system include Sonic BondMaster and Phased Array Ultrasonics.

The F-WELD (Figure 1) is a full-scale load sequenced fatigue test. Testing is being conducted on a short configuration F-111F wing designated A15-80L using a flight-by-flight 1,000 AFHR blocked spectrum representative of previous USAF in-service operations; in effect, the wing's usage is being continued to failure, providing a sound basis for further consideration of RAAF usage and other configurations. The test sequence consists of the application of two blocks of manoeuvre loading followed by Non Destructive Inspection (NDI) followed by the application of Cold Proof Load Test<sup>2</sup> (CPLT) prior to the application of a further two blocks of loading.



Figure

1: F-WELD Test Article Undergoing Cold Proof Load Test

The F-WELD test article is a port F-111F (short) wing, serial number A15-80L, obtained from AMARC after 6,033.9 flying hours. The wing box is manufactured from 2024-T851 aluminium, while the wing pivot fitting is manufactured from D6ac steel.

Although A15-80L saw service at several USAF bases, the aim of the test is to provide an economic life and certification basis for F and D wings by replicating Cannon Air Force Base (AFB) usage. This is because the Cannon usage is considered to conservatively cover the prior usage of the ex-USAF F-111 D and F wings. The total service hours were therefore converted to an equivalent total of 4,500 Cannon hours to provide a valid starting baseline for the test.

The only data still available for Cannon AFB usage comprised of exceedance diagrams. The Cannon AFB spectrum was thus derived from a combination of Multi Channel Recorder (MCR) data (used previously in the development of the 4.5g limited DADTA2b spectrum used for the previous wing test) and recorded output from the F-111 Flight Simulator (SIM). The SIM was used to provide for manoeuvres of up to 6.5g.

Parametric data from both MCR and SIM flights were run through short wing load equations, providing target bending (BM), shear (SH) and torque (TQ) distributions across the wing. The target distributions were then converted into a set of actuator, or achieved, loads (within the limitations of the number and size of actuators on the test rig) via a combination of double shear and Legrangian constraint routines.

The spectrum was generated by composing a mix of MCR and SIM flights to match the Cannon AFB Bending Moment (BM) exceedance diagrams (at two locations: Wing Root and the Outboard Pivot Pylon (OPP)). Figures 2 and 3 contain BM exceedance plots of Cannon versus F-WELD Test spectra for the wing root and OPP respectively.

<sup>2</sup> Cold Proof Load Test (CPLT) to design limit load at minus 40 Degrees Celsius forms an integral part of the safety-by-inspection program used to ensure the structural integrity of the F-111 aircraft. CPLT is a safety measure to ensure that any critical size defects in high strength D6ac steel components, which may have been missed during NDI, are detected by actual failure of the component part.

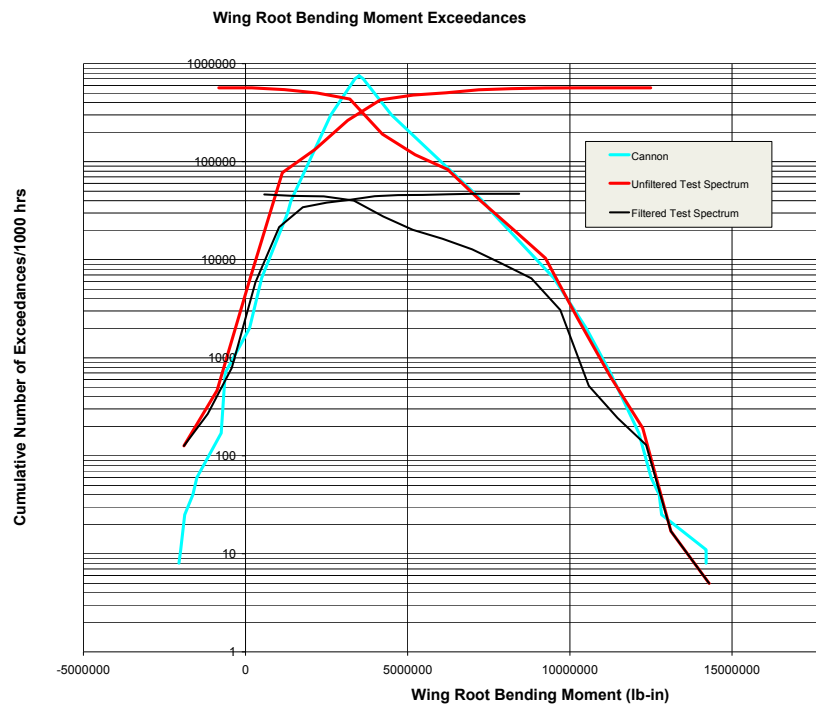


Figure 2: Wing Root Bending Moment Exceedance Diagrams

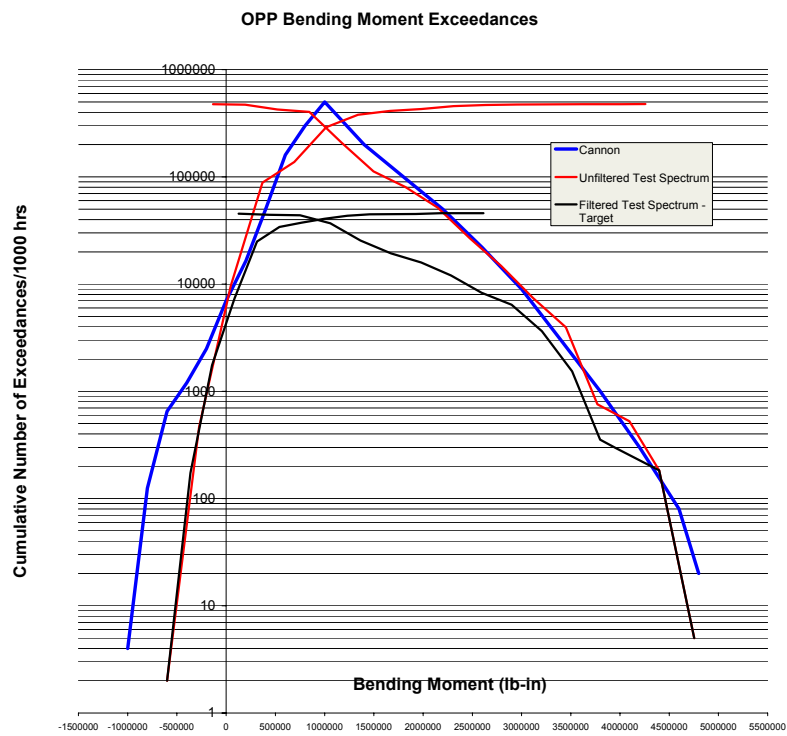
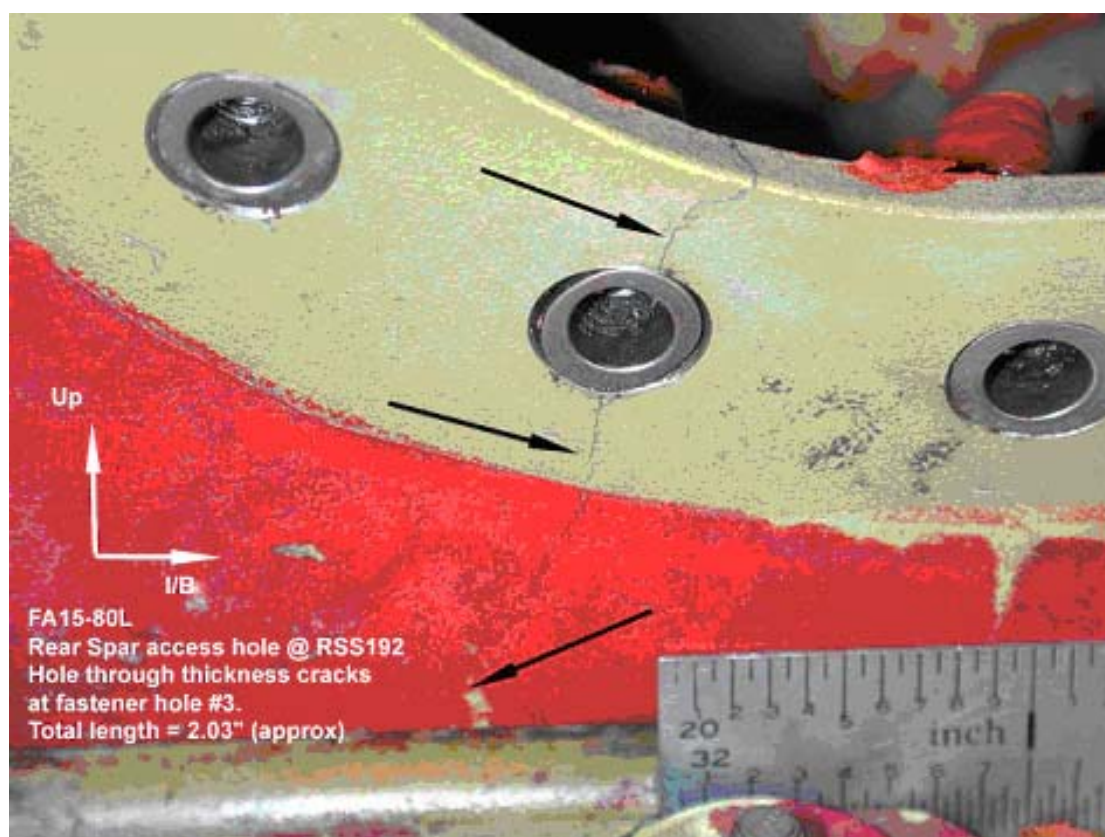


Figure 3: OPP Bending Moment Exceedance Diagrams

In considering the load distribution the priority for loading accuracy was deemed to be bending moment followed by shear and torsion. The priority for loading fidelity was deemed to be wing pivot fitting to aluminium wing box splice followed by the wing pivot fitting and forward auxiliary spar at 226 inches from the pivot.

### Test Progress to Date

From the starting point of 4,500 Cannon AFB hours the test has progressed in a satisfactory manner although not without incident. During inspection of the test article at 5,500 flying hours a crack was detected at an inspection opening in the rear spar at a location known as Durability and Damage Tolerance (DADTA) item 73; this is a location known to crack in service. The crack had grown from an anchor nut hole (See Figure 4) across the spar web and the low spar cap. Stainless steel doublers were used to restore the spar web and to reinforce the lower wing skin to prevent further cracking of the lower spar cap as shown in Figure 5. To date this repair has performed satisfactorily with no further crack growth being evident.



*Figure 4: Rear Spar Crack at DADTA Item 73*



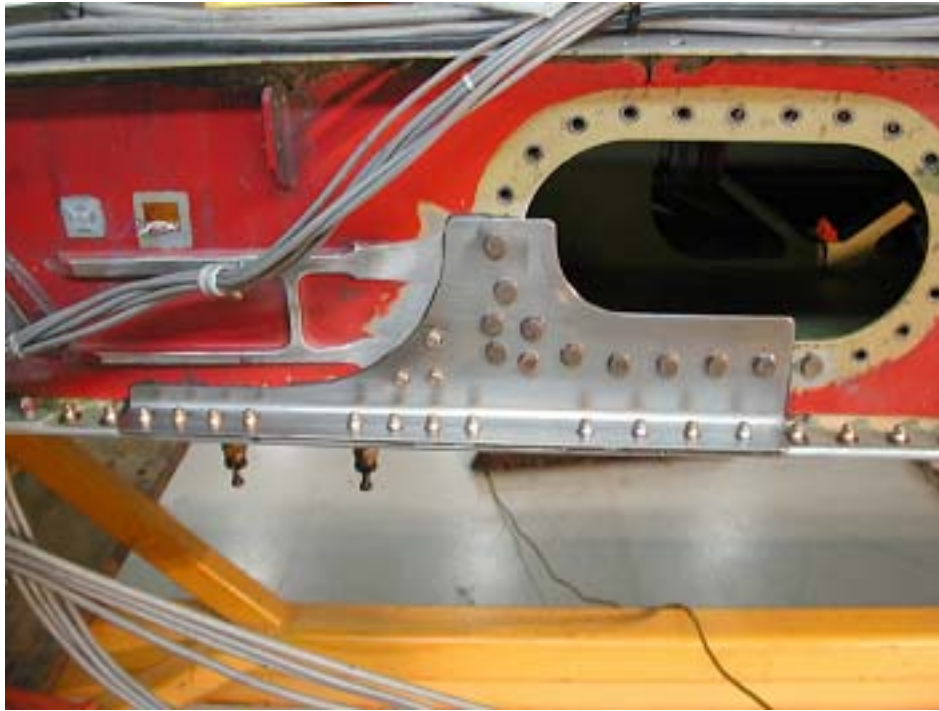


*Figure 5: Repair of Rear Spar Web at DADTA Item 73*

There are two major milestones associated with the F-WELD test; the first is to reach 22,400 hours such that the current restriction on wing flight hours can be lifted. Based on a safety factor of 3.2 the wings will then have a safe-life of 7000 hours. The second milestone is to reach 30,000 hours. This will provide a safety factor of 4 and a safe life of 7,500, which will verify that the wings have sufficient life to enable the aircraft to reach PWD. The ultimate aim is to fail the wing in fatigue preferably beyond 30,000 hours and then to conduct a comprehensive teardown inspection to identify all fatigue crack locations. It is envisaged the test program will be completed by June of 2006. That teardown and inspection will assist in the management of the remaining significant issue with F-111 wings, namely build quality concerns – the management approach being pursued is development of appropriate inspection systems and procedures.

#### References

1. Thomas van Blaricum, David Ord, Robert Koning and Martin Hobson, Damage Enhancement Testing of RAAF F-111C Wing A15-5, DSTO Technical Report 1614, March 2005.



### 8.2.7 F-111 Aircraft Structural Integrity Sole Operator Program (G. Swanton, K. Walker, DSTO)

In light of the retirement of the United States Air Force (USAF) F-111 fleet in 1998, and the subsequent diminished support from the Original Equipment Manufacturer (OEM), (General Dynamics, now Lockheed Martin), there was a necessity to establish an indigenous capability of applied research and engineering to support the Royal Australian Air Force (RAAF) F-111 fleet through to planned withdrawal date. The F-111 Sole Operator Program (SOP) was therefore initiated to identify and perform the actions required for this capability development. The SOP effectively forms the F-111 Aircraft Structural Integrity Program (ASIP) development activity, covering a large range of issues such as; establishing Australia as the sole operator, assuring ongoing technical airworthiness, conducting research into corrosion/ageing aircraft effects, and the transition of structural integrity capability and tools to Australian Industry.

The SOP is now a mature program and further capability developments have been made beyond the five original tasks that were carried out in conjunction with the OEM several years ago. To recap, the five original tasks were:

- (1) construction of a finite element model (FEM) of the entire F-111 structure,
- (2) establishing an indigenous Durability and Damage Tolerance Analysis (DADTA) capability,
- (3) structurally significant items study,
- (4) modelling of multi-site crack initiation problems, and
- (5) characterisation of external aircraft loads.

A DADTA capability and the FEM have now been transitioned to industry, which satisfies one of the goals of the SOP. New external load equations have also been developed, whilst other work is focussed on creating an improved elastic-plastic DADTA software code in-country.

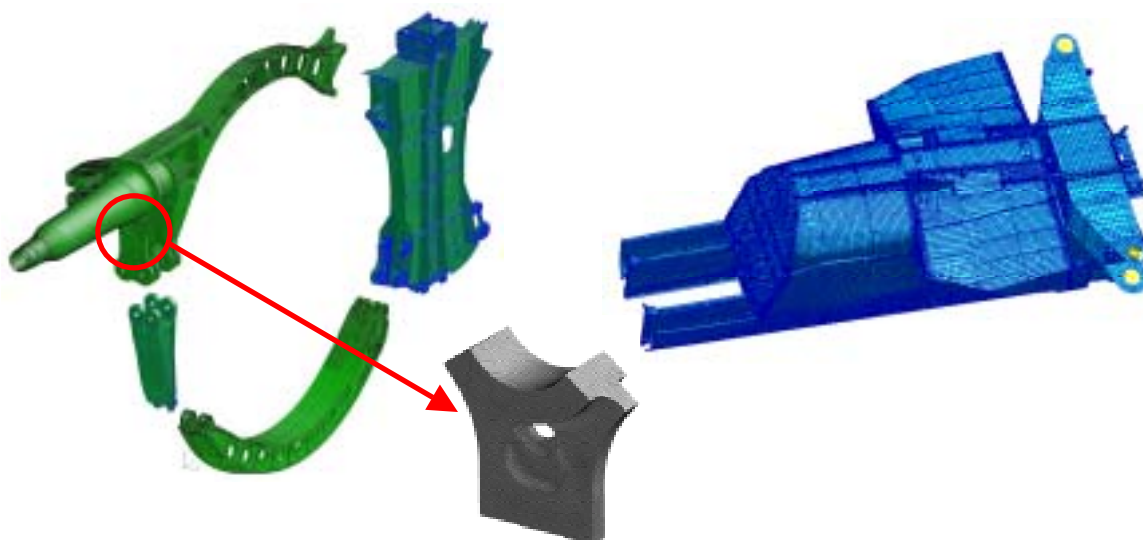
The F-111 FEM is known as the Internal Loads Model (ILM), and one of its primary roles is to provide accurate free body loads for the stress analysis of fine grid FEM's. The ILM is an MSC NASTRAN model with 396,708 elements, 318,318 nodes and approximately 1,870,000 degrees of freedom. A picture showing the main structural elements of the ILM is shown in Figure 1. The results are subsequently used to enable DADTA's to be performed on critical structure of the F-111 airframe. These DADTA results are used to determine inspection intervals, which underpin the structural management philosophy of the fleet by Safety-by-Inspection (SBI).



Figure 1: Major structural components of F-111 Internal Loads Model.

Confidence in the performance of the ILM has been assured by a thorough correlation exercise, which involved a full-scale strain survey of a fleet aircraft. Strain data from over 420 gauges were compared with the ILM strain results under the same (virtual) loading that the real aircraft experienced. Three key fine grid locations were rigorously correlated, these being the Fuselage Station (FS) 770 bulkhead, Over-wing Longerons (OWL) and FS 496 former. The Wing Carry Through Box (WCTB) also received the same level of attention due to its structural significance. These structural components are all manufactured from D6ac steel. Modifications to the ILM at these areas were made as necessary to improve the correlation results.

Internal loads from the correlated ILM have been applied to the FS 770 fine grid FEM (Figure 2), resulting in a new stress equation for DADTA Item (DI) 36. The OEM's original equation produced unacceptably short intervals. On the other hand, the OEM's DI20 (located on the OWL) stress equation has been validated, although in this instance the correlation of the ILM was sufficient without having to use a local fine grid FEM. It is hoped that the positive findings from the DI20 work (representative coupon tests) may remove the requirement to continue with a costly cold-worked hole modification currently being implemented on the fleet. The ILM was also used to construct a sub-model of the forward fuselage tanks (Figure 2). In the fleet, these tanks, manufactured from 7079-T651 aluminium alloy, are susceptible to stress corrosion cracking. Accounting for the many instances of reported cracking, the correlated model demonstrated the high level of redundant strength in the structure, and indicated that compromises to the structural strength of this location at the aircraft's planned withdrawal date are minimal.



*Figure 2: Fine Grid FEM of FS 770 bulkhead showing Super Fine Grid FEM detail of DI36, and sub-model of Forward Fuselage Fuel Tanks.*

#### **8.2.8 Structural integrity assurance for the F-111 outer lower wing skin through a condition assessment program (K. Walker, J. Walker and G. Swanton, DSTO)**

A RAAF F-111C wing undergoing full scale fatigue testing at DSTO failed by fracture from a fatigue crack in February 2002. The failure originated at a taper lok fastener at Aft Auxiliary Spar Station 277.3 (see Figure 1 for the failure location). The fastener is one of a spanwise row connecting the skin and spar. Subsequent investigations revealed numerous cracks at similar holes throughout the wing and also significant cracking in the spars. Failure by fatigue cracking at these holes was not anticipated, and prior to the failure there had been no known instances of this type of cracking in earlier fatigue tests or through service experience. Investigations revealed that the build quality of the wing was very poor, and many of the fasteners did not exhibit sufficient interference to be of any fatigue benefit. Also, the surface finish on many holes was extremely poor with significant gouges and out of round holes present. An investigation of several other wings indicated that the test wing was probably the worst of the cases examined.

The widespread nature of the problem (there are hundreds of fasteners, many with similar stress levels) meant that reliance on safety by inspection for a small number of discrete locations was not possible. However, a targeted semi automated ultrasonic based inspection method is being developed to support management of this issue under a safety by inspection basis. It is hoped that ultimately this will cover the entire lower wing skin, but at present it is limited to regions outboard of bulkhead two (see Figure 1). Linear Elastic Fracture Mechanics (LEFM) based models have been developed [1] to cover these regions. Confidence in these models is high because they have been correlated to the most significant cracks discovered during the fatigue test, such as the one at AASS 225. The fracture surface from the AASS 225 crack is shown at Figure 2, and the correlation between the observed crack growth (measured by fractography) and the modelling is shown in Figure 3.

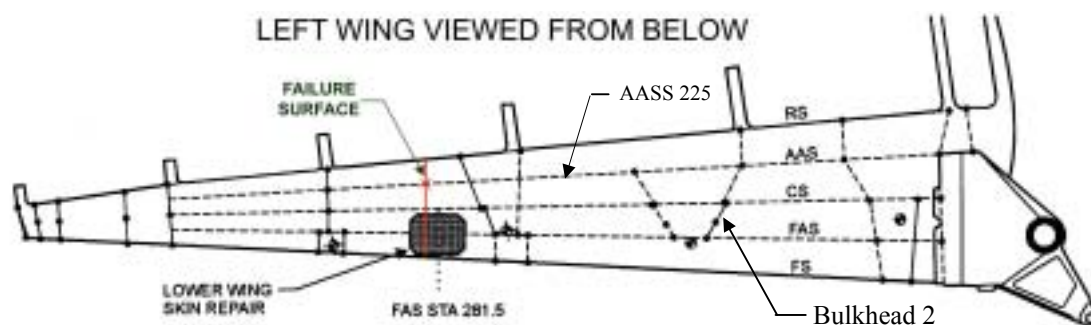


Figure 1. RAAF F-111C fatigue test wing showing failure location at Aft Auxiliary Spar Station (AASS) 277.3. The other spars are the Rear Spar (RS), Centre Spar (CS), Forward Auxiliary Spar (FAS) and the Front Spar (FS). Another significant crack location is at AASS 225.

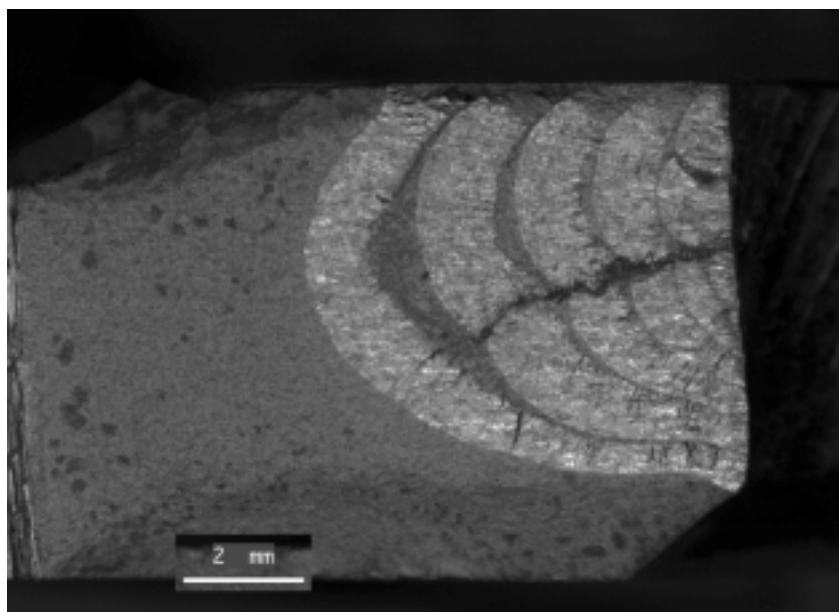


Figure 2. Fracture Surface from the forward side of the hole at AASS 225

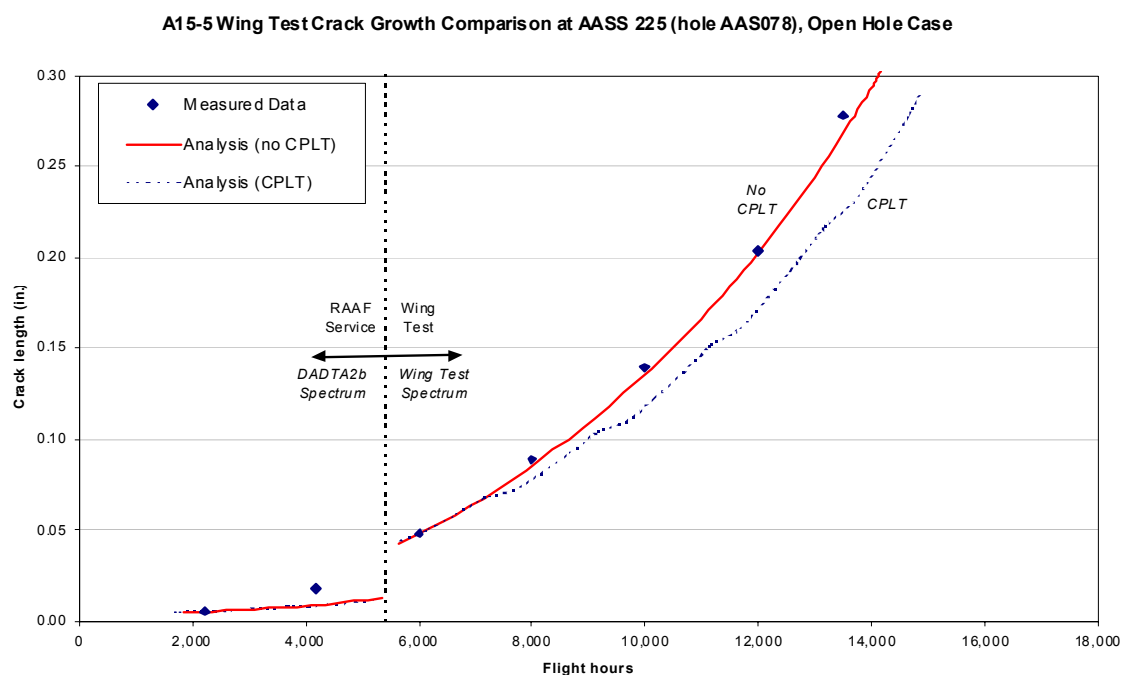


Figure 3. Comparison of experimental and analytical crack growth at AASS 225 (Hole AAS078) for the in-service and fatigue test periods. CPLT refers to Cold Proof Load Testing<sup>3</sup>.

From this it has been possible to determine the size of cracks which will need to be detected to support certain inspection intervals. This is assisting with the development and validation of the semi-automated inspection system. Further work is underway to extend the applicability of the models to locations further inboard on the wing. The inspection process becomes more difficult in the inboard areas due to increased skin thickness, and fewer cracks were detected there in the test so there is limited data to correlate the models. However, coupon test data is being generated to correlate the models. Further full scale wing testing is also underway to hopefully provide an alternative structural integrity management strategy (safe life) for the inner part of the wing in case safety by inspection cannot be implemented.

## References

1. Walker, K. Walker, J., and Swanton, G., "Structural Integrity Assurance for the F-111 Outer Lower Wing Skin through a Condition Assessment Program", DSTO-TR-1608, August 2004.

<sup>3</sup> The CPLT is a periodic proof loading program performed on the F-111 (nominally every 2,000 AFHRS) to confirm the absence of any flaws in the D6ac steel structure above a very small critical size. The aircraft is cooled in a special environmental chamber to -40°C (-40°F), which reduces the fracture toughness (making more brittle) the D6ac steel structure. Starting at rest, load cycles corresponding to -2.4g and +7.33g (at 56° wing sweep angle) and -3.0g and +7.33g (at 26° wing sweep angle) are then applied to the airframe via the wings, horizontal tails and other reaction points, before coming back to rest at zero load. A successful test (i.e. no structural failure) clears that structure for a further period of safe flight.

### 8.2.9 Fatigue Cracking of F-111 FS 496 Nacelle Former (K. Walker, G. Swanton, G. Chen, DSTO, V. Sridhar Aerostructures)

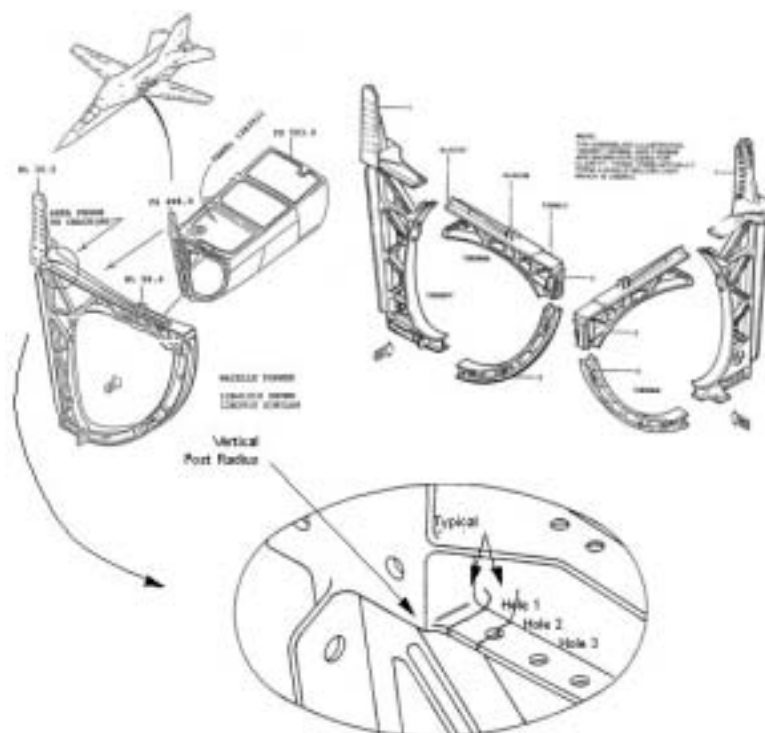


Figure 1: Location of crack prone area on the FS 496 nacelle former

Cracking in the upper inboard region of the high strength D6ac steel FS 496 nacelle former continues to be a major problem for the RAAF (see Figure 1). The cracking is characterised by large compressive loads leading to local yielding at holes and other stress concentrations resulting in significant tensile residual stresses and fatigue. A bathtub fitting type repair was designed by the manufacturer Lockheed Martin several years ago, and it has now been installed on the aft flange are on most of the Australian F-111C fleet (the problem does not affect the F-111G models). Key issues are summarised as follows:

Contrary to previous Lockheed analyses, cracking in the forward flange continues to occur once the repair is installed.

It is also possible that the repair fitting may introduce stress concentrations and therefore new fatigue susceptible locations may be present. Inspection of the aft flange is difficult or impossible with the repair in place.

Aerodynamic engine intake loads have been ignored until now, and these may be significant from a fatigue perspective.

In terms of the intake loads, significant progress has been made. A simplified pseudo compressible fluid theory has been developed and is being correlated against Computational Fluid Dynamics (CFD) data [1-4]. Preliminary results indicate that the stresses at the critical region for an extreme engine stall case are of the order of 15 ksi which is about 8% of the monotonic material yield stress for the D6ac steel material. The intake loads are therefore potentially significant from a fatigue perspective. Work is underway to develop a representative spectrum for the intake load conditions, and this will be included in a fatigue analysis.

Significant work is also in progress to develop the fine grid model mentioned in the last review. This is being correlated to full scale strain survey data for both the with and without repair fitting cases. Revised stress equations and stress spectra will be developed accounting for both the wing/fuselage induced flight loads and the aerodynamic engine intake loads. Elastic plastic fatigue analyses will then be carried out and correlated to fractographic data from service aircraft. Initially however it is planned to evaluate the repair statically to determine if the repair fitting is expected to introduce any new problem areas which would require ongoing inspection.

Fractographic analysis of the fracture surfaces from major cracks at the subject location on an ex-USAF F-111A which was torn down at DSTO has provided vital crack growth information for the unrepaired case. This data will ultimately be compared to analysis results, but in the meantime it is being used directly to assist in management of the problem. The data shows that routine Non Destructive Inspection (NDI) by Magnetic Rubber Inspection (MRI) provides a feasible management strategy for the forward flange cracking, and at the very least should provide a safe operating period for the aft flange once the repair is installed. Work is aimed at providing a sufficient basis to see the fleet out to the Planned Withdrawal Date (PWD) of 2010.

#### References:

1. Chen, G, Walker, K, Swanton G and Hill, S D, "Modelling the F-111 fighter bomber aircraft engine intake loads", Proceedings of ACAM, Australia, Feb, 2005.
2. Chen, G, Walker, K, Swanton G and Hill, S D, "Stress Analysis of Aerodynamically Loaded Structure under Supersonic Conditions", Proceedings of SIF 2004, Australia, September, 2004
3. Chen, G, Walker, K, Swanton G and Hill, S D, "An Envelope Method for Stress Analysis of Aerodynamically Loaded Structure under Subsonic Conditions", Proceedings of SIF 2004, Australia, September, 2004. p32
4. Chen, G., and Walker, K. "Computational fluid dynamic analysis for the F-111 fighter bomber aircraft engine intake", to be presented at the 11<sup>th</sup> Australian International Aerospace Congress, Melbourne Australia 13-17 March 2005.

#### **8.2.10 Fatigue assessment of critical features in the F-111 Wing Pivot Fitting (K. Walker, J. Walker, DSTO)**

The potential for fatigue cracking in the upper plate areas of the high strength D6ac steel Wing Pivot Fitting (WPF) of the F-111 aircraft (see Figure 1) is well known and has led to the development of an optimised reshaping modification (reorted previously). The modification has been demonstrated to significantly reduce the peak stresses and strains at the critical WPF upper plate locations. This is expected to result in increased inspection intervals. An assessment has now been carried out [1] using a combination of analysis and examination of full scale wing damage tolerance testing data. The result is that significantly increased inspection intervals for the modified configuration can be recommended for wings manufactured from New Heat Treat (NHT) material, which applies to the majority of wings now in RAAF service.

An assessment of the existing fleet configuration has also been carried out [2], to resolve concern that the inspection intervals in place were not underpinned by fully validated analysis or test data. The assessment carried out considered analysis, testing of representative coupons, and an investigation of in-service data. In the end, the in-service data was heavily used because it was the most reliable source. The result is that the current inspection regime is difficult to support. However, a detailed examination of the particular circumstances for each individual wing has been recommended to quantify the risk and determine the urgency for the application of the optimised reshaping modification, or revision of inspection interval.

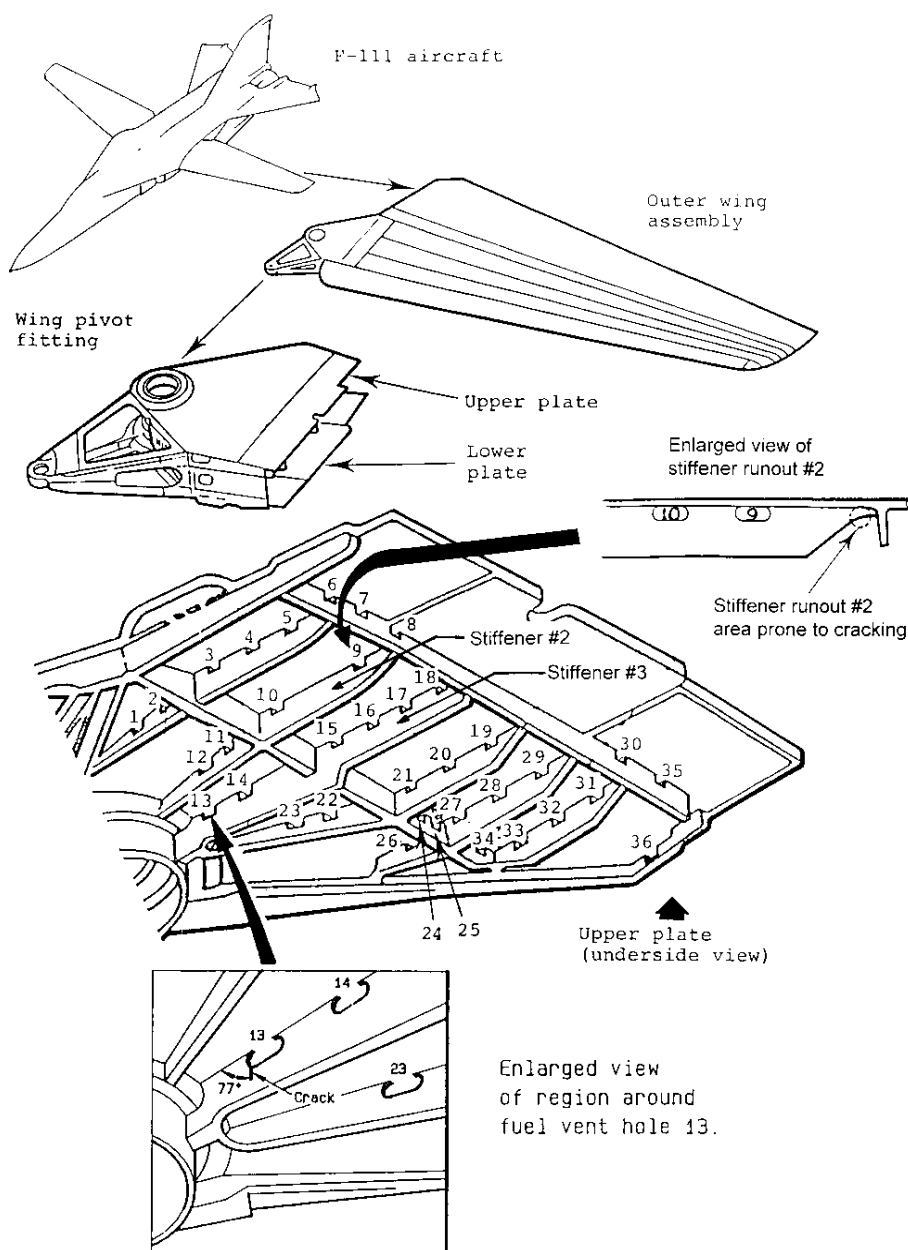


Figure 2: Internal view of the Wing Pivot Fitting (WPF) structure showing Fuel Flow Vent Hole (FFVH) and Stiffener Runout (SRO) features and typical crack locations.

#### References:

1. Walker, K., Weller, S., and Walker, J., "F-111 Wing pivot fitting upper plate critical features fatigue assessment – post wing optimisation modification" DSTO-TR-, in vetting, February 2005
2. Walker, K., Weller, S., and Walker, J., "F-111 Wing pivot fitting upper plate critical features fatigue assessment – pre wing optimisation modification" DSTO-TR-1682, February 2005

### **8.2.11 Development of a predictive tool for the analysis of fatigue crack growth involving notch plasticity (Weiping Hu, DSTO)**

A crack growth analysis program, CGAP, has been developed for the analysis of fatigue crack growth involving notch plasticity [1]. The development work was motivated by the need of an analytical tool to analyse crack growth at critical locations on F-111 aircraft, where notch plasticity occurs due to the periodic application of severe cold proof load sequences. CGAP implements an advanced constitutive model for cyclic plasticity that takes into account of mean stress relaxation and plastic strain ratchetting. The notch root stress is determined using Neuber's rule and the constitutive relation, and the stress distribution ahead of the notch root is calculated using a semi-analytical method based on finite element analyses. The stress intensity factor is computed using a Green's function approach. The analytical crack closure model developed in [2] was adopted to account for the stress ratio and load interaction effects.

CGAP also has a capability for probabilistic crack growth analyses using Monte Carlo methods. CGAP can generate random input values, using four different distribution functions, for several important parameters such initial crack length, the crack growth rate equation and the external load level. It gives output in terms of probabilistic distribution of crack growth lives.

In addition, CGAP can also deal with residual stress fields generated by surface treatment processes such as laser shot peening. Both built-in and user-supplied residual stress distribution may be analysed.

CGAP runs on MS Windows platforms, with a graphical user interface as shown in Figure 1. To provide easy access and consistent use of input information, CGAP has extensive support of database capability in crack configurations, material properties, load profiles, user-defined cracks, and case control. It also allows the run of FASTRAN [2] to tap into its capability in dealing with more crack configurations.

Preliminary analyses of through-cracks emanating from a central hole in a plate subjected to constant amplitude loading as well as spectrum loading has shown encouraging results, as demonstrated in the comparison given in Figure 1 [3].



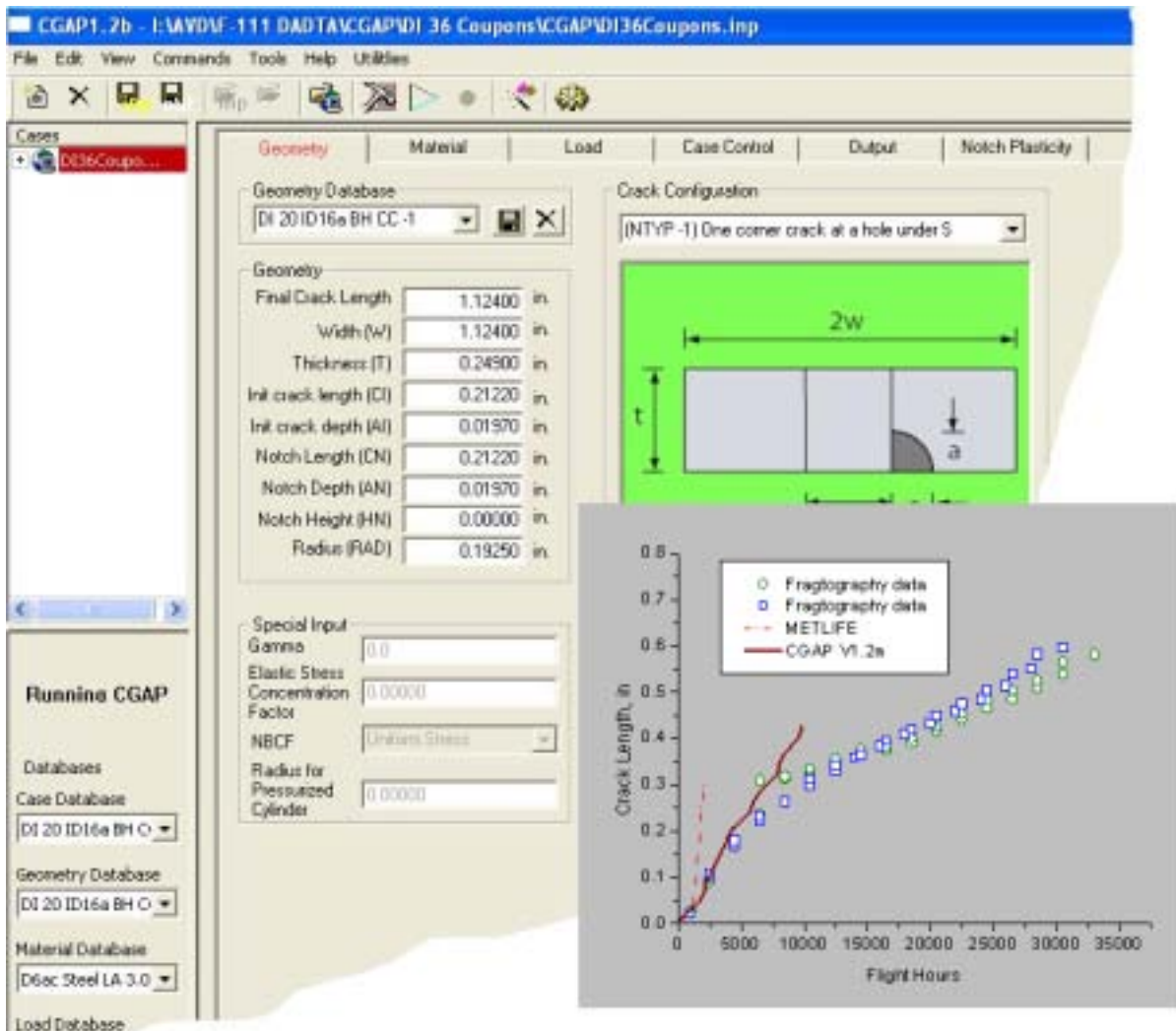


Figure 1 Illustration of the graphical user interface of CGAP, and a comparison of numerical results and experimental data of a coupon representing a component in F-111 aircraft[3].

#### References:

1. Hu, W. and Walker, K.F., *An analysis of fatigue crack growth of a notched aircraft component under compression-dominated spectrum loading*. in *SIF2004 Structural Integrity and Fracture*. 2004. Brisbane, Australia: Australian Fracture Group Inc.
2. Newman, J.C.J., *A crack closure model for predicting fatigue crack growth under aircraft spectrum loading*. ASTP STP 748, 1981: 53.
3. Walker, K., Hu, W., Walker, J., and Ignjatovic, M., *Fatigue crack growth in high strength metallic F-111 aircraft structures involving significant cyclic notch plasticity*. in *AIAC*. 2005. Melbourne, Australia.

### **8.2.12 Support of the ADF F-111 Safety By Inspection Program (Rahul Kashyap and Michael Houston, Aerostructures)**

The structural integrity of the F-111 aircraft is managed primarily by a Safety by Inspection (SBI) basis. As the sole operators of the F-111, the Australian Defence Force (ADF) conducted the F-111 Sole Operator Program (SOP) in order to provide tools, data and infrastructure to support the F-111 in the absence of OEM and USAF input. In this endeavour, the ADF was supported by DSTO, Aerostructures and other agencies. Aerostructures continues to support the F-111 by conducting Durability and Damage Tolerance Analysis (DADTA) and associated activities to obtain inspection intervals for critical F-111 structure so they can be safely and effectively managed.

As an example of the tools produced through the SOP, Aerostructures and DSTO recently completed the correlation of the F-111C Internal Loads Finite Element Model (ILM) against static strain survey data. The ILM provides the ADF with the capability of investigating discrepancies in and refining OEM stress equations to support DADT analyses.

Aerostructures is using SOP outputs to develop strategies for the long term management of key areas on the aircraft. FS770 Bulkhead and FS496 Nacelle Former are two such areas. For the FS770 Bulkhead, there is some evidence to suggest that the Original Equipment Manufacturer (OEM) load and stress equations are overly conservative. The project seeks to develop revised load and stress equations for the FS 770 bulkhead and to perform a revised DADTA on the basis of this new work. The results from this analysis will be employed to provide authoritative advice regarding the ongoing management of the FS770 bulkhead on RAAF F-111 aircraft.

The process being followed for the FS770 study was exercised during an earlier DTA on the FS770 lower lug region (identified as DI 42/43). Loading and stress levels in the region were determined through fine grid finite element analysis derived from the ILM. Lug pin load and lug radius stress spectra were developed and a damage tolerance analysis of the lug bore was performed.

The upper inboard region of the FS496 Nacelle Former has experienced cracking in both United States Air Force (USAF) and ADF F-111 aircraft. The published OEM data used to predict fatigue life for the component showed that no cracking should occur. Aerostructures are developing a strategy for the management of the upper inboard region of the FS496 Nacelle Former. This investigation presents particular challenges as the cracking is driven by residual tensile stress fields created by Cold Proof Load Test (CPLT) loads and so must be analysed using Elastic Plastic Fracture Mechanics (EPFM). DSTO, supported by Aerostructures, is developing a robust F-111 EPFM capability.

The availability of a spectrum representative of ADF F-111 usage presents another challenge to developing an acceptable SBI baseline. In order to address this issue, D20 data recorders have been installed on two RAAF F-111 aircraft to gather flight data. Over the past year Aerostructures have been analysing D20 data and a 500 AFHR spectrum was created by assembling acceptable D20 flights to match F-111C mission data for the period. This mix of D20 flights is considered to provide a more accurate representation of current F-111C fleet usage than the previous baseline spectra, known as DADTA or DADTA2B. However, damage tolerance based sensitivity analyses will be performed at several key locations driven by different loading actions to assess the significance of the spectrum differences.

F-111 wings are moved from aircraft to support maintenance needs or to address specific airworthiness concerns. Consequently, the severity of and variation in usage of each wing must be separately assessed. To assist ASI with the management of wings, especially those approaching life limits (imposed as an interim measure), a relative usage severity analysis on RAAF wings was performed. Along with other techniques, this study utilized statistical methods to identify and gauge characteristic variations between spectra. This characterisation was then used to assist with the comparison of usage severity.

Aerostructures are also supporting DSTO in the conduct of the final major activity of the SOP, the F-111F Wing Economic Life Determination (F-WELD) full-scale fatigue test on a retired F-111F wing. Aerostructures' activities include loads and stress sequence development.

### 8.2.13 Build Quality Assessment of F-111 Wings (C.A. Harding, M.W. Hobson and G.R. Hugo, DSTO)

An F-111C wing A15-5L failed unexpectedly during DSTO full-scale fatigue testing due to a fatigue crack initiated at a fastener hole in the lower wing skin. The failure occurred at a lower number of equivalent flight hours than expected and was largely attributed to very poor build quality of the test wing. In particular, during post-test teardown, a large proportion of the Taper-Lok fasteners were found to have below-specification interference and a significant proportion of the fastener holes were found to have excessive (above specification) surface roughness.

The RAAF F-111 fleet was recovered by replacing F-111C and F-111G wings with ex-USAF F-111F and F-111D model wings. To support the structural integrity management of these wings, DSTO conducted a detailed build quality assessment of the failed fatigue test wing (A15-5L) and a sample of five F-111F and F-111D wings. Wing build quality was assessed by measuring the fastener interference and hole bore surface roughness for a sample comprising more than 300 fasteners holes in the fatigue test wing A15-5L, and a minimum of 60 fastener holes in each of the F- and D-model wings.

The build quality of the test wing A15-5L was confirmed to be very poor. For A15-5L, 47% of fasteners sampled had below-specification interference and 7% of fasteners sampled were loose in the hole (zero interference), see Figure 1. In addition, 34% of fastener holes sampled were measured to have above-specification surface roughness in the hole bore. The data from the F-111F and F-111D wings showed that, on average, the build quality of these wings was significantly better than the test wing A15-5L. However, there was also a statistically significant variation in measured build quality between the F and D wings sampled. In addition, a number of significant manufacturing defects were detected in the F and D model wings during the build quality survey. A statistical analysis was performed to examine the probability that an F or D wing might have a build quality as poor as the failed test wing A15-5L. Unfortunately, it was not possible to conclude, with a high level of statistical confidence, that this probability was negligible, primarily due to the statistically significant variation in measured build quality between the F and D wings sampled.

The overall assessment that the build quality of F-111F and F-111D wings was, on average, better than A15-5L provides a basis for managing the F and D wings as a separate population using the results of a second full-scale fatigue test of an F-111F wing, which is currently in progress, in combination with a management approach for the remaining manufacturing defects believed to be present in the F and D wings.

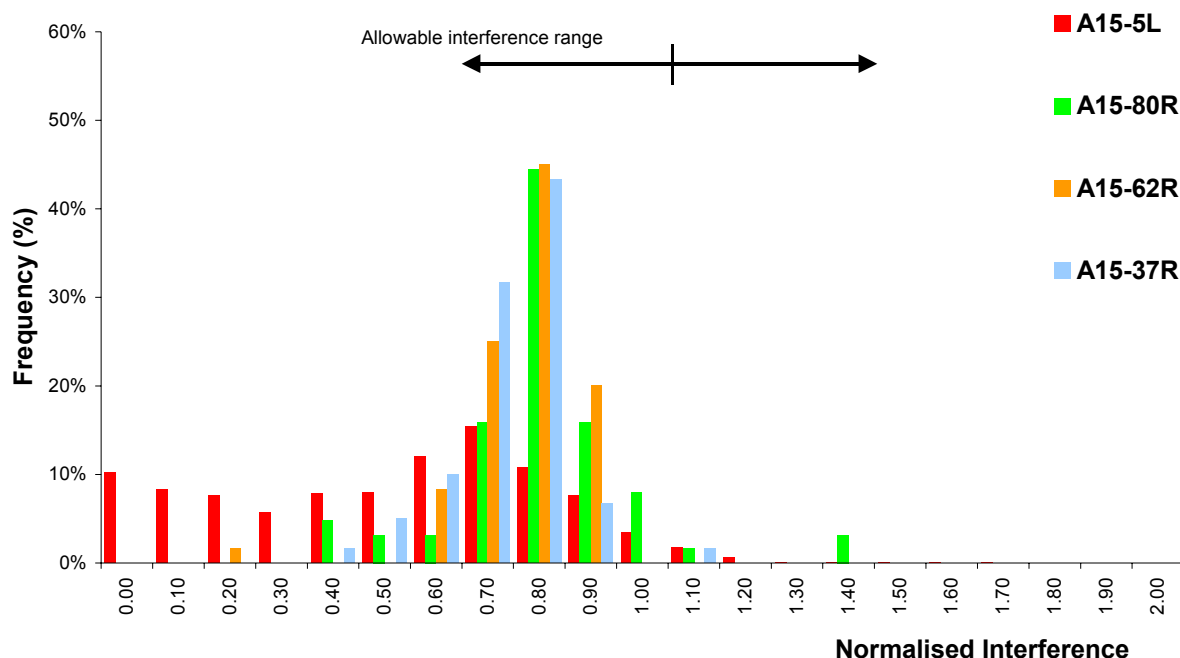


Figure 1 Frequency distribution of fastener interference for the failed F-111C fatigue-test wing A15-5L compared to three F-111F wings (A15-80R, A15-62R and A15-37R). Interference values are normalised by dividing by the nominal interference level, so that a normalised interference of 1 corresponds to the nominal (blue-print) interference level. The allowable range of normalised interference is from 0.6 to 1.4.

#### **8.2.14 Automated Ultrasonic Inspection for Cracks in F-111 Wing Planks (G. Hugo, C. Harding, S. Bowles, H. Morton, DSTO, G. Craven, D. Ward, J. Duncombe, RAAF NDTSL)**

Following the failure of an F-111C wing during full-scale fatigue testing by DSTO, RAAF have identified a requirement to nondestructively inspect up to 500 Taper-Lok fastener holes in the lower skin of each F-111 wing for possible fatigue cracks. DSTO and RAAF Non-Destructive Testing Standards Laboratory (NDTSL) are currently developing automated ultrasonic inspection procedures to perform the required inspections using 45 degree angle-beam shear wave ultrasonic testing (UT), Figure 2. The SAIC Ultra Image International Ultraspect-MP was selected to implement the automated inspections following a detailed evaluation of available automated NDT systems.

Two characteristics of this inspection problem present unusual challenges, compared to previous applications of automated NDT for crack detection in wing skins:

- (i) a very large variation in skin thickness, from 6 to 30mm, over the regions of the wing requiring inspection, combined with substructure features such as spar web stiffeners which must be accurately interpreted, and
- (ii) the fact that it is practically impossible to remove and replace individual lower skin Taper-Lok fasteners, to confirm by bolt-hole eddy-current inspection any indications from the automated UT, without removing the entire upper wing skin for access.

Given the inconsistent build quality demonstrated for F-111 wings, some rate of possible defect indications from the automated UT is expected, due to occasional mechanical damage within the fastener holes. In the regions of the lower wing skin less than 13 mm thickness, possible defect indications from the automated UT will be managed by a program of targeted supplementary inspections using low-frequency eddy current, to ensure that any cracks present do not grow to an unsafe size during further service. In thicker regions of the wing skin, the sizes of suspected defect indications, as measured from the automated UT data, will be used to assess the ongoing serviceability of wings, supported by recurring automated UT to detect any growth of suspected defect indications during further service.

The automated UT procedures are currently being applied to an F-111F wing undergoing full-scale fatigue testing at DSTO. Comparison of the UT results with the final teardown of the wing will provide valuable data on the limitations of the automated UT procedures for detection of real fatigue cracks.



Figure 2 Automated ultrasonic inspection of Taper-Lok fastener holes in an F-111C wing using the SAIC Ultraspect-MP system.

### 8.2.15 F-111 Strake failures (G. Redmond, DGTA)

The following provides one example from the many forensic activities undertaken at RAAF base Amberley: RAAF have had recent failures of F111 strakes - the lower fins at the rear. The strakes stabilise the aircraft during high speed (G) turns, and are effectively a static extension of the stabs.

The failures were interesting because of the low loading; the cracks grew to about 18 inches in a total of 24 inches section length before the strakes fell off. There was an interesting combination of fatigue and tearing/ductile fracture along the lengths. Two failures had almost exactly the same fracture patterns on the surface. One failed after fleetwide inspection (STI) because the (16 inches long) crack was missed, in part because it is geometrically hard to access the inner radius (high re-entrant angle due to proximity with fuselage). DGTA developed a very quick and effective before flight test –“ lean into the leading edge using all of your weight” - if it deflects - it is probably cracked. A simple, but reliable method because of the very long critical crack size (about 18 inches).

Figure 1 shows position of the strake – the fin on bottom side of rear fuselage. Figure 2 shows a failed strake next to a good one. Figure 3 shows two failures - failure occurred by fatigue of the aluminium mounting plate member, from the front working backwards. Note the similarity of the two failures about 18 inches in a total length of 24 inches was cracked, although there were smaller fatigue cracks in the "overload" region, around the side of the section. Figure 4 shows visual detail of typical fatigue region near front - fatigue cracks start on the upper radius and work there way down the length and through the section thickness. Figure 5, SEM striations on fracture surface - vibrational loading with occasional large load (i.e. high G turn). Unfortunately, there is no information on the time frame of G turns so it is difficult to obtain the rate of growth - although we can conclude that the 18 inch cracks have probably been growing since new (after an "incubation" period). Figure 6 shows a smaller fatigue crack in "overload" zone at rear.



*Figure 1: Position of strake - fin on bottom side of rear fuselage*





*Figure 2: Failed strake next to a good one.*



*Figure 3: Two failures.*



*Figure 4: Detail of typical fatigue region.*

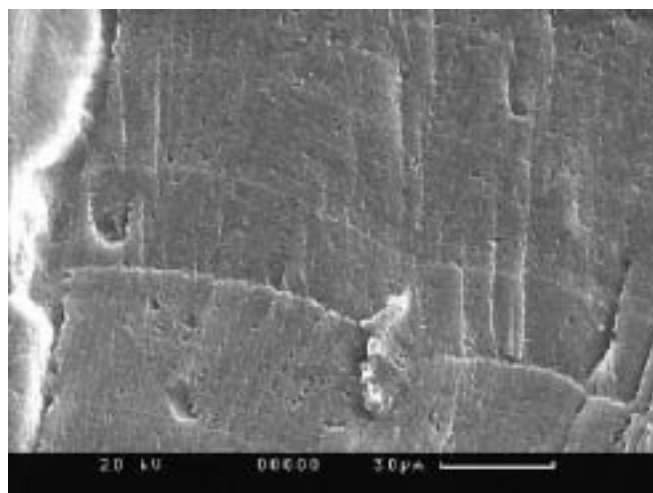


*Figure 5: SEM striations on fracture surface.*



*Figure 6: Fatigue crack in "overload" zone.*

#### **8.2.16 Extended Testing of a P-3 Empennage at DSTO, Melbourne (P Jackson, DSTO)**

As part of Australia's contribution to the international P-3 Orion aircraft Service Life Assessment Program (P-3 SLAP), DSTO undertook the full scale fatigue test of the empennage section of the aircraft. The test cycling phase commenced in January 2002 and was completed, along with residual strength testing and a post-test teardown, in July 2004. The test article consisted of the fin, tailplane and aft fuselage from a retired airframe. Loads were applied via a total of 27 hydraulic actuators, to a 15,000 flight hour load spectrum that represented one lifetime of aircraft usage to a USN 'severe' spectra. Cycling was applied for two lifetimes, at which point little fatigue damage was observed in the primary structure. In order to explore the possibility of providing additional test clearance for life extension, and to provide a test basis for DTA based inspection locations and intervals, further testing at augmented load levels was then commenced (Reference 1). Transport aircraft fin and tailplane loads during normal operations are generally much lower (perhaps as much as 50%) than the static design limit load cases that generally include abnormal events such as engine-out. This results in low in-service stresses, which in turn require either a long testing time or significantly augmented loads in order to provide typical fatigue failures. Fortunately these same low stresses allow the loads to be raised significantly before unrepresentative local residual stresses can give misleading effects. The load factor finally applied was 1.6, with clipping at 1.1 times the maximum unfactored loads for the fin and 1.5 times the maximum unfactored loads for the tailplane. Under the augmented load sequence a major failure was generated in primary structural at the root of the fin. Cycling of the tailplane then continued, including the insertion of saw cuts, and further fatigue cracks were generated after another 15,000 hours. The test concluded with residual strength testing to a number of limit load cases and a full teardown. Coupon testing supported the interpretation of the test findings back to in-service load levels and the test failure locations and times enabled fleet management actions to be developed.



*Fig 1. Jackson P. & Cardrick A. W., "The challenge of Conducting a Meaningful Full Scale Fatigue Test on a Transport Aircraft Empennage", ICAF 2003, Lucerne, Switzerland, May 2003.*

#### **8.2.17 P3 Orion Flap Track (G. Redmond, DGTA)**

DGTA investigated the failure of a P-3C Orion flap track. Figures 1 and 2 show the position of the flap tracks on the Orion aircraft (Flap Track Station 174 on the port side). The picture was taken while the aircraft was grounded in Hawaii where the complete separation of the flap track was noticed.

There is a history of problems with cadmium plating of these tracks (it appeared that bright coating had been applied, which despite baking, can result in the hydrogen not getting out). DGTA assessed the situation about the cadmium at the time and decided that the brightening was not too bad and that the tracks were not subjected to a constant tensile stress anyway. Also, we had had no failures of the track...ever.

The immediate concern with the Hawaii incident was - was this hydrogen embrittlement after all? Figure 3 shows where the cracking is on the track and Figure 4 the detail. The fracture certainly looked very brittle. Figure 4 however was sent later on from Hawaii and the very smooth front during crack propagation suggested that it might be fatigue and not hydrogen embrittlement.

On getting the fracture into the lab, it was found that it was not fatigue either (a least most of it), but stress corrosion cracking (Figure 5). There was a little bit of fatigue before final overload (Figure 6 upper and lower lugs). The smooth transition on the surface was due to two periods of SCC. That the track had SCC present at the last overhaul was evident from cadmium and paint on the sides of the fracture face (Figure 7). Metallography confirmed that the mechanism was SCC (Figure 8).





*Figure 1: Flap track*



*Figure 2:*



*Figure 3:*

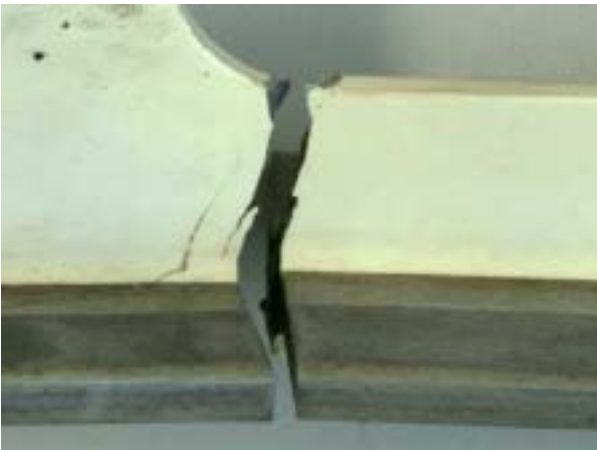


*Figure 4: Optical view of fracture*

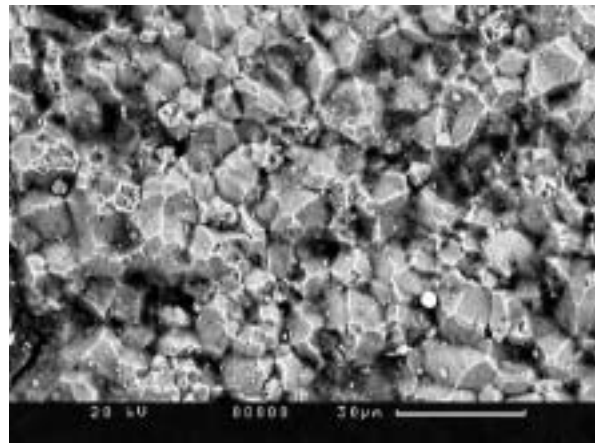


*Figure 5: SEM examination of surface*

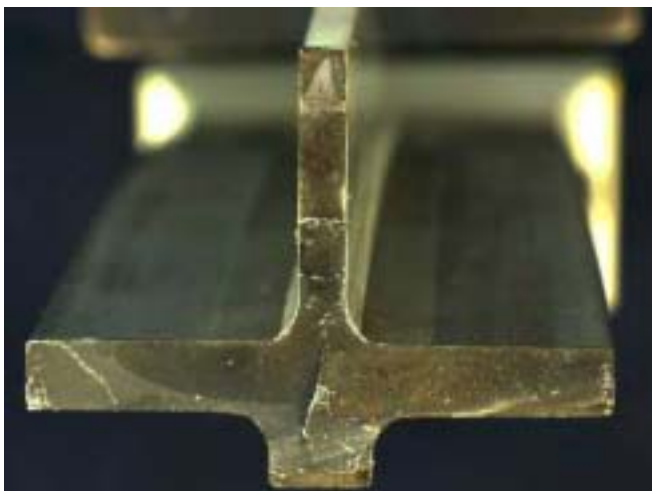


Figure 6: Fracture surface



Figure 7:

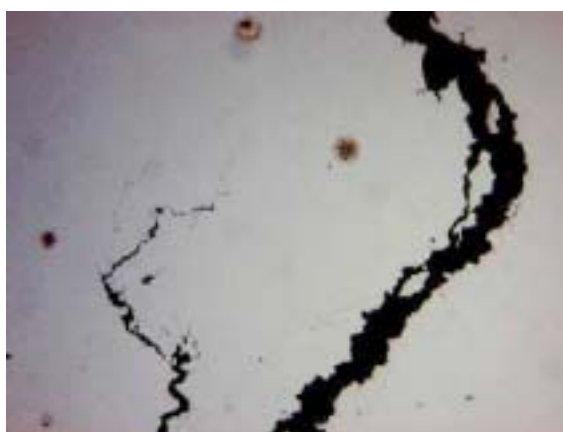


Figure 8: Metallographic section, showing SCC nature of cracking.

#### 8.2.18 C130J Structural Life (L. Meadows, R. Ogden, DSTO)

The Royal Australian Air Force (RAAF) C-130J-30 Hercules fleet was introduced to Commonwealth service in September 1999. Subsequently the FAA certification basis, achieved by LM Aero for the 382J, (civil variant) was considered inappropriate for the structural certification of the RAAF C-130J-30 fleet. This was due primarily to differences in the intended military operational role and environment.

From an Aircraft Structural Integrity (ASI) management perspective the Commonwealth is currently focused on resolution of the outstanding structural certification issues, and establishment of mature data and system infrastructure to support ongoing management of structural integrity. Ongoing key activities aimed at addressing these issues are as follows:

##### 8.2.18.1 Collaborative Wing Fatigue Test

The RAAF has entered into a collaborative arrangement with the UK Ministry of Defence (MoD) to conduct a C-130J full-scale WFT in the UK. Testing is due to commence in late 2006 and is intended to provide substantiation of the 30,000 hr/30 year Life Of Type (LOT) durability requirement.

### 8.2.18.2 SBI Program

In the absence of WFT results the RAAF is implementing a mature Safety By Inspection (SBI) program based on Damage Tolerance Analysis conducted by Lockheed Martin Aeronautical Systems (LM Aero). This accurately accounts for mature, representative RAAF usage.

### 8.2.18.3 Structural Health Monitoring

In support of the collaborative WFT program the Defence Science and Technology Organisation (DSTO) is developing a system for processing and managing fleet C-130J-30 Structural Health Monitoring System (SHMS) data, (i.e. the OEM supplied usage monitoring system). The DSTO developed system, comprising software and database elements will be utilised primarily to characterise RAAF usage for consideration in the upcoming WFT. The database and an example mission profile plot are shown in Figure 1.

### 8.2.18.4 Individual Aircraft Tracking

The RAAF has implemented an Individual Aircraft Tracking (IAT) system to monitor usage, calculate severity factors and evaluate inspection intervals for the C-130J-30 fleet with respect to the baseline SBI program, (i.e. DTA). The requirement for this interim system is driven by the uncertified status of the OEM supplied SHMS.

### 8.2.18.5 Operational Loads Measurement

The RAAF is in the final stages of acquiring and installing an operational load measurement (OLM) system in at least one RAAF C-130J-30 aircraft. The OLM, designed by Marshall Aerospace (UK) is required in order to gather loads data for RAAF contribution to, and interpretation of, the collaborative C-130J WFT, see Figure 2.

### 8.2.18.6 Environmental Degradation Management

Finally the RAAF is engaging in the development of an environmental degradation management philosophy and establishment of an environmental degradation assessment capability.

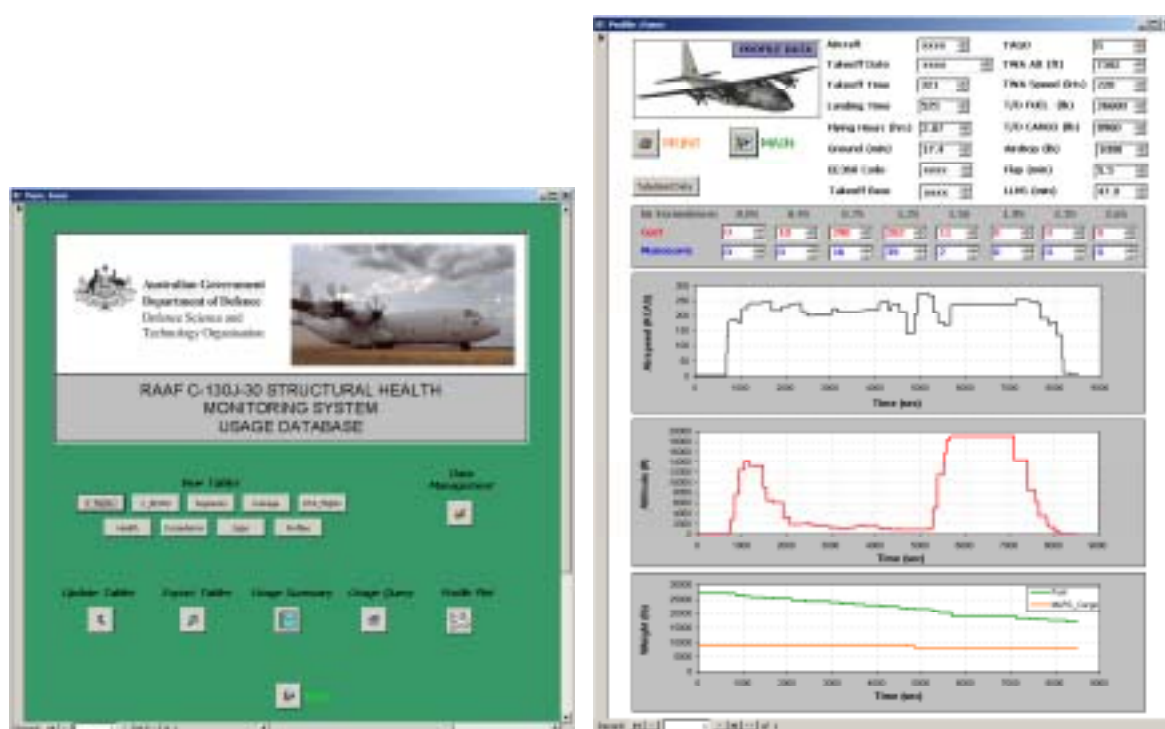


Figure 1: DSTO C-130J-30 Fleet Usage Database

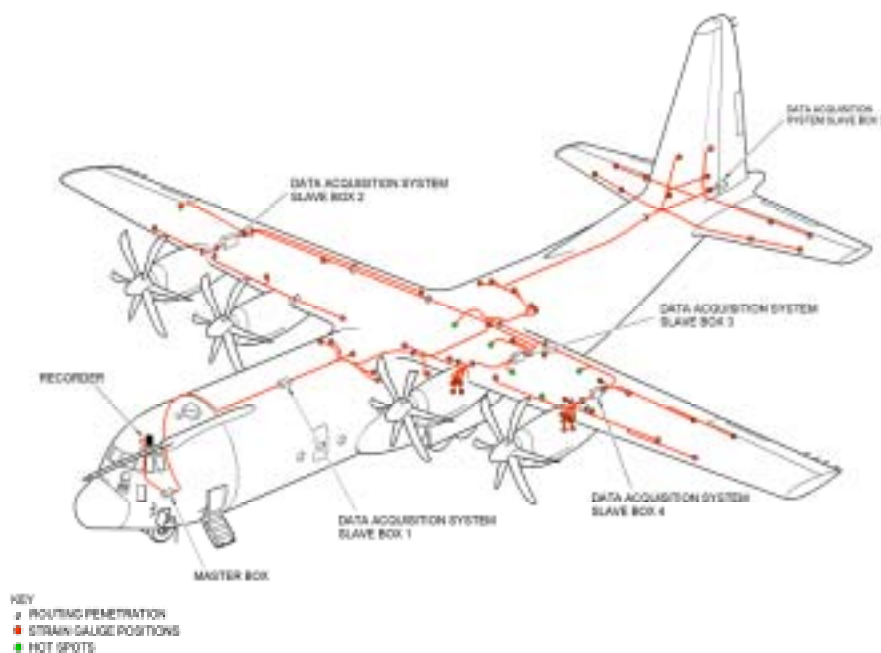


Figure 2: RAAF - Marshall Aerospace OLM Installation

#### 8.2.19 LIF Fatigue Test (T. Bussell, DSTO)

In 1997, the RAAF formalised a contract for the delivery of 33 Hawk Mk.127 aircraft, to satisfy the requirement for a new Lead-In Fighter (LIF) aircraft. Under the terms of the contract, 12 aircraft were produced at Brough in the United Kingdom, with the other 21 manufactured in Brough and assembled at a purpose built BAE SYSTEMS facility at Williamtown, New South Wales. The first UK-built Hawk Mk.127 made its maiden flight in December 1999, with the first Australian-built aircraft following just five months later.

In comparison with the T Mk 1, the Hawk Mk.127 is approximately: 600 mm longer and 20% heavier (1% weight increase equates to approx 4% reduction in life). DSTO had been asked to conduct an assessment to determine whether a full-scale fatigue test of the aircraft was required. Fatigue tests on earlier models of the Hawk had been conducted but the DSTO analysis determined that new tests were essential to provide specific information on RAAF operational usage of the Australian version of the aircraft, therefore minimising the possibility of fatigue-related accidents, and potentially increasing the operational life of the RAAF fleet.

Once the decision had been made to proceed with a comprehensive fatigue test, DSTO and BAE SYSTEMS entered a commercial business agreement to conduct the test in Australia. Personnel from both organisations are involved in the test, as are several Australian contractors with a range of backgrounds and expertise.

The Hawk Mk.127 fleet has been operational since 2000, under an interim flight clearance that allows for such activity prior to full-scale testing. However, once testing begins, the test team will reach 15000 Equivalent Flying Hours (EFH) (which equates to approximately 3000 actual safe flying hours) before the operational aircraft get to that point. This is considered a requirement in ensuring the safe operation of the fleet. The tests involve loads, based on both computational modelling and instrumentation from actual flights, being applied to the test article. The full-scale fatigue test is expected to continue until 2012, eight years before the fleet's proposed withdrawal date. The test at Fishermans Bend is being complemented by a tailplane (buffet) test in the UK by BAE SYSTEMS.

Design and construction of the test rig has been underway since May 2002. Based in a new test laboratory at DSTO's Fishermans Bend site, it is an 8-metre high, three-level test rig designed by BAE SYSTEMS with DSTO input. Key features include:

- a 1<sup>st</sup> level platform raised 2.0 metres off the ground to allow sufficient headroom and systems installation within the rig footprint;
- additional floor area on all levels surrounding the fatigue article to allow ergonomic work practices and equipment distribution;
- a removable top deck that allows for the installation and removal of the fatigue article as required.

The main control system was developed by MTS Systems Corporation, USA, while DSTO provided some background intellectual property to enhance the functionality of the system. The system applies and monitors loads to the test article from 84 hydraulic and 6 pneumatic channels simultaneously. It also includes a fully integrated 1200 channel data acquisition system. The MTS systems have been provided through Australian Calibrating Services (ACS).

The hydraulic actuators have been designed and manufactured by Moog Australia, while the valve packs, or Controlled Abort Manifolds, which form part of a fully independent controlled abort unload system, have also produced by MOOG Australia, though based on an earlier DSTO design. The associated unload controllers have been developed jointly by Moog and MTS. The rig is scheduled to be fully operational by September 2005, with expected completion in late 2012., followed by RST and teardown., completed project 2014.

### **8.2.20 Helicopter Structural Integrity - Flight Data Recorder (FDR) Trials (Chris Knight, DSTO)**

Since the late 1990's, the entire Australian Army Black Hawk fleet has been fitted with Flight Data Recorders (FDR). While the primary purpose of the FDR is to provide investigators with information about an accident or incident, previous DSTO work has identified the FDR as a possible source of data for usage monitoring. [1], [2], [3], [4]

Usage monitoring is undertaken to identify how aircraft within a fleet are being used and to compare that against the assumptions made when the aircraft was designed. This information helps aircraft operators to improve the structural integrity management of their aircraft fleets and hence enhance safety.

Currently, usage monitoring is completed by aircrew filling in a standard form after each flight. These forms contain information such as flight time, numbers of landings and rotor starts, and occurrences of extreme manoeuvres.

To quantify the potential benefits of usage monitoring via an FDR, DSTO's Air Vehicles Division conducted a trial using 6 Black Hawks from a training squadron. During the trial, FDR data were downloaded and processed in conjunction with the standard forms.

The analysis of collected data helped to identify several problems related to data retrieval, reliability of the data stream and other data-fusion issues associated with automated data-recording equipment. Also, comparisons between the manual data and the FDR data allowed the fidelity of the manual data to be assessed. Ultimately, though, the trial quantified the benefits of utilising existing sources of automated data gathering, such as the FDR, as part of regular maintenance procedures.

Since most planned maintenance actions are based on flight times, significant savings in aircraft direct operating costs should occur if logged flight hours are greater than those measured automatically. Alternatively, if the aircraft hours and operations are being under-reported then there are airworthiness issues to address.

Trial data has been downloaded since December 2003 and is expected to continue to February 2005. Across the 8 aircraft involved in the trial approximately 1300 flight hours have been acquired and compared. Preliminary results indicate that although most parameters are accurately recorded, some conditions, principally "Number of Landings", are being significantly under-recorded. Of special note is the high correlation between the pilot's and FDR records of flight hours.

#### **References:**

- 1 Knight, C.G., "Mid-Term Review of DSTO Flight Data Recorder Trial", *DSTO Melbourne*, July 2004.
- 2 King, C.N. and Knight, C.G., "S-70A-9 Black Hawk Usage Monitoring by Utilising Output from the Flight Data Recorder", DSTO Report DSTO-TR-143, May 2003.
- 3 Knight, C.G., "FDR's as HUMS: A Report on Data Issues, Including the Accuracy of Manually Entered Data", Proceedings of the Eleventh Australian International Aerospace Congress, Melbourne, 13-17 March 2005
- 4 Dore, C. and Knight, C.G., "Flight Data Recorder Information Retrieval Trial", Proceedings of the Eleventh Australian International Aerospace Congress, Melbourne, 13-17 March 2005

### 8.2.21 Automatic Synthesis of Transfer Functions to Predict Helicopter Dynamic Component Loads from Fixed System Parameters (Luther Krake, DSTO)

The rotor and its attachments contain most of the fatigue-critical structural components in a helicopter; however, quantifying the loads in these components requires slip rings or rotating telemetry systems that currently lack the reliability and maintainability needed for everyday fleet usage. An alternative is to use transfer functions to predict the loads in dynamic components from loads (and other parameters) measured on the airframe. HSI has recently commenced an investigation into the automatic synthesis of transfer functions to predict helicopter dynamic component loads from measured airframe loads. Traditionally, such transfer functions have been derived from mathematical models of the rotor system; however, owing to the complexities involved, this approach has had limited success. Our approach will instead attempt to generate transfer functions automatically using Genetic Programming (GP) – a domain-independent problem-solving approach in which computer programs are evolved to solve problems. The GP algorithm will use Black Hawk helicopter data obtained during the joint USAF/ADF flight loads measurement program, which was conducted in 2000 and reported in previous ICAF reviews.

To date, the focus of this project has been on filtering GP input data parameters using Fast Fourier Transform (FFT) and cross-correlation analyses. The goal here is to select only those input parameters that are likely to contribute something unique to the GP algorithm. The final choice about which input parameters to include in the transfer functions will, of course, be left up to the GP algorithm.

This approach complements the work done in previous years [1], [2], and [3], which was based on a more traditional mathematical modelling approach.

#### References

- 1 Polanco, F. G., Estimation of Structural Component Loads in Helicopters: A Review of Current Methodologies, DSTO Technical Note, *DSTO-TN-0239*, December 1999.
- 2 Polanco, F. G., Development of a Stress Transfer Function for an Idealised Helicopter, DSTO Research Report, *DSTO-RR-0171*, March 2000.
- 3 Polanco, F. G., Determining Beam Bending Distribution Using Dynamic Information, DSTO Research Report, *DSTO-RR-0226*, January 2002.

## 8.3 FATIGUE OF CIVIL AIRCRAFT

### 8.3.1 Piper Brave - New Long Life Spar (Juergen Moews, Aerostructures)

The Piper Brave PA-36 is a crop dusting aircraft whose spar is required to be replaced every 4100 flying hours in its current design. Spar replacement is currently with the same design part, which means it will again require replacement in another 4100 hours.

Brave Aviation and Aerostructures are designing a new spar with a design life in excess of 20,000 hours. The design will be Type Certified for the Piper Brave aircraft - called a Supplemental Type Certificate - by CASA for Australian aircraft.

The FAA is closely following the process in Australia to enable an FAA Supplemental Type Certificate to also be obtained for the US Piper Brave aircraft.

Fatigue Spectrum Considerations: For the fatigue analysis of the new spar, a loading spectrum had to be established and little information was available in the public domain about the usage severity during special service operations like crop dusting and fire fighting.

As a baseline, information from the FAA document AFS-120-73-2 'Fatigue Evaluation of Wing and Associated Structure on Small Airplanes' (1973) was used. For gust and manoeuvre load spectra, updated information from the 'General Aviation Aircraft-Normal Acceleration Data Analysis and Collection Project DOT/FAA/CT-91/20' (1993) was utilised. To account for severity, the mean spectrum plus one standard deviation was applied as suggested by the FAA. Additionally a pilot survey was performed which revealed that short Ground Air Ground cycle durations of 15 to 40 minutes had to be taken into account.



Using a final spectrum developed with the above process, fatigue life analyses of the blueprint and redesigned spar were performed using the FAA methodology for wing and associated structure on small aircraft. The method was shown to deliver conservative results when comparing analytical safe lives with published test demonstrated safe lives for the blueprint design.

Future work will include a ground strain survey to confirm analytical stress levels. In addition, Aerostructures' Maxlife Flight Data Recorder will be installed in at least one aircraft to verify the spectrum used in the fatigue analysis.

### 8.3.2 The 'Damage Tolerance' of Civil Aircraft (S. Swift, CASA)

Since last ICAF, four Australian events have raised questions about 'damage tolerance'.

#### 8.3.2.1 Is 'damage tolerance' only good for some damage?

In 2003, an Australian airline found a 30-inch crack in the rear fuselage of one of its Boeing 747-400s. The fuselage had lost so much bending strength it could have failed at any time.

It could have failed before the crack was 'obvious'. Sealant hid the crack and stopped a leak. So, for this damage, there was no 'fail safety'. When designing and approving the 747-400, to FAR 25 (Amendment 9), neither Boeing nor the FAA anticipated it.

It could have failed before the crack was 'detectable'. So, for this damage, there was no 'damage tolerance'. When developing and approving the SID (Supplemental Inspection Document), to FAA Advisory Circular 91-56, neither Boeing nor the FAA anticipated it.

It could have failed if a sharp-eyed mechanic had not seen the crack amid thousands of square feet of frames and stringers (like trying to find a needle in a haystack) at a 6-yearly check. The 747 would not have survived until the next one.

It could have failed because of a common maintenance error. See Figure A. The current evidence suggests half the world's airliners (and not just Boeings) could be scratched to varying degrees. Some could be unaffected by it. Some could be unsafe. Some could be unrepairable.

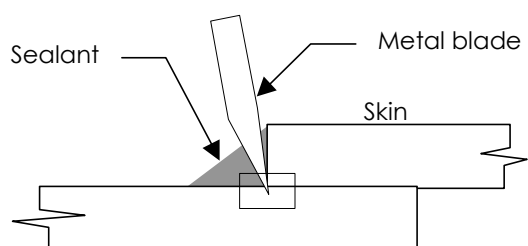


*Figure A: To save time, some painters improperly use a metal blade instead of a plastic scraper to remove sealant from skin joints. The scratch cracks, as shown at right. The Australian 747 was an extreme case; someone penetrated half the thickness with some kind of power tool.*

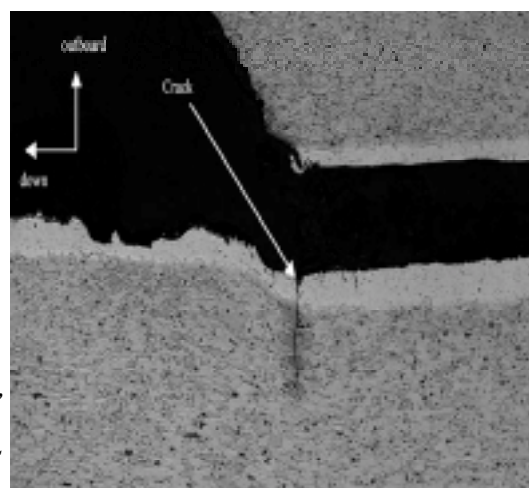


*Figure A. Skin scratches and cracks.*

The Civil Aviation Safety Authority (CASA) does not criticise the airline: they did not do the last repaint. CASA commends them: they found the crack. CASA does not criticise Boeing or the FAA: no one else would have anticipated this mode of failure. CASA commends them: they responded quickly and competently.

What can we learn from this? Should we consider damage like this in our ‘damage tolerance’ analyses? If we apply FAR 25.571 (the civil rule for ‘damage tolerance’), is not the damage ‘accidental’? Could it not happen in ‘manufacturing’ or any time ‘throughout the operational life of the airplane’? Could it not ‘contribute to a catastrophic failure’? Is it not a ‘probable ... mode of ... accidental damage’?

So, the rule seems to say we *should* consider accidental damage like this in our ‘damage tolerance’ analyses. It says we should consider *all* ‘probable...damage’ (not only the ubiquitous 0.050 inch corner crack). Is that we want? If not, perhaps we should make the rules clearer, to better define what damage our designs and maintenance programs *should* anticipate, and what damage is better addressed by better training and processes for manufacture and maintenance.

### 8.3.2.2 Is ‘damage tolerance’ only good for some errors?

In 1999, in the United States, a Cessna 402C crashed when the wing spar failed by fatigue. The FAA ordered fleet wide inspections. But, in 2005, the wing spar failed on another one. This one was luckier. The pilot managed to land it by using full aileron to correct for the twisting, wobbling wing. Again, the FAA ordered inspections.



Figure B: A Cessna 402C

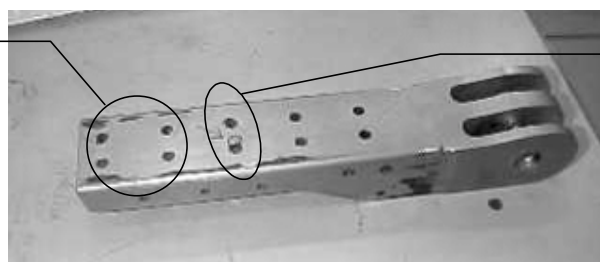
*Neither time did CASA follow suit.*

There was no need. In Australia, owners must replace or strap their wing spars before they get old enough to develop the cracks that now concern the FAA. Are there lessons for damage tolerance?

CASA’s ‘safe lives’ come from a fatigue analysis Cessna did in 1978. They chose and analysed five sites. Then, in 1999 (before either the crash or the close call just mentioned), they did a ‘damage tolerance’ analysis. This time, with finite elements, more tests and more service experience, they chose the same five sites.

Neither of the wing spars broke at any of the five sites Cessna predicted. This is common in aviation. If so, which fatigue management strategy is more forgiving: ‘damage tolerance’ or ‘safe life’? If, by ‘damage tolerance’, we mean inspections, how often have we inspected the wrong holes? In 2002, that nearly happened in Australia. See Figure C.

*The damage-tolerance-based maintenance program said to inspect these holes (using eddy currents).*



*Luckily, the inspector went further and found a crack in one of these holes!*

Figure C: This fitting held the wings on a small airliner. It wouldn’t have for much longer!

If, by ‘safe life’, we mean retirement, we sometimes get the *life* right, even if we got the *site* wrong. If we retire the whole part, it doesn’t matter. Safe life’s forgiving serendipity has protected Australian Cessna 402Cs twice now.



### 8.3.2.3 Is 'damage tolerance' only good for some aircraft?

Australia's safety rules generally require owners to follow the manufacturer's maintenance program (even though indirectly in places). However, in December 2004, CASA told hundreds of Cessna owners they did not have to follow the maintenance based on 'damage tolerance'. The affected Cessnas are twins that seat 6 to 10. Some are pressurised. Some are among the oldest in the world.

Australia was following the United States, where the Cessnas were designed and built. In 1999, the FAA proposed to require 'damage tolerance' for Cessnas (and Pipers, Beechcraft and other little airliners). But, by 2005, the FAA had changed its mind. The 'Final Rule' on 'Aging Airplane Safety' only requires 'damage tolerance' for aircraft that seat 30 or more. For smaller aircraft, the rule says 'the FAA has determined that imposing damage-tolerance-based inspections and procedures...would impose an undue economic burden *with little increase in safety benefits*' (see the United States *Federal Register*, Volume 70, No. 21, Wednesday, February 2, 2005, page 5529).

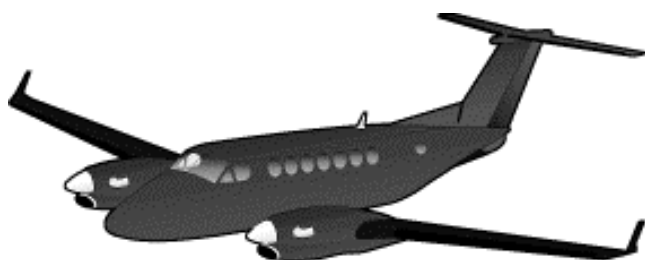


*Figure D: Is 'damage tolerance' for aircraft like these 'an undue economic burden with little increase in safety benefits', as the FAA said in 2005?*

Why would the FAA think 'damage tolerance' is only cost-effective for large aircraft, but not small? Is the problem one of regulation, application or education?

### 8.3.2.4 Is 'damage tolerance' only good for some people?

The principles of managing structural integrity (especially 'damage tolerance') are poorly understood outside its clique of specialists. For safety, there needs to be greater awareness among managers and maintainers, pilots and politicians, and repairers and regulators. Insufficient management awareness contributed to the safety lapse, then business collapse, of Ansett Australia in 2001. That is why the Australian Transport Safety Bureau (ATSB) is funding development of a training package for managers and others. For similar reasons, CASA is developing one for its management and inspectorate (ex-mechanics). There will be more about these at the next ICAF meeting.



*Figure E: Even airline managers need to know the basics of structural integrity. After all, they are the ones who allocate resources and make the big decisions that affect how well it is managed.*

## 8.4 FATIGUE-RELATED RESEARCH PROGRAMS

### 8.4.1 In situ Structural Health Monitoring of an Impact Damaged F/A-18 Horizontal Stabilator (A.P. Walley, N. Rajic, DSTO).

DSTO has been conducting preliminary experimental work addressing the practical efficacy of an acousto-ultrasonic *in situ* structural health monitoring system for a full-scale aircraft structure. The system comprises a network of piezoelectric elements autonomously controlled by a new device developed by DSTO and CPE Systems, called the Acousto-Ultrasonic Structural health monitoring Array Module or AUSAM. Work is described that demonstrates the capacity of this system to detect the presence of damage in the composite skin of an F/A-18 horizontal stabilator, introduced by a controlled impact event. Overall, the AUSAM system exhibited good reliability and robustness, even under a mechanically and electrically noisy environment. The trial has however underscored the need for further effort in clarifying the importance of piezo-transducer degradation as a source of diagnostic uncertainty, and in improving system immunity to electrical noise

Features: Single Board – approx 100mm long - controlling 2 piezo actuators & 4 piezo sensors; the amplifiers can be placed in close proximity to the piezo sensor elements.

Example –trial on F/A-18 stabilator: Conduct a frequency sweep to determine sweet spots (strong signal with minimal noise). 45kHz, 100k, 150k, 200k, 300k

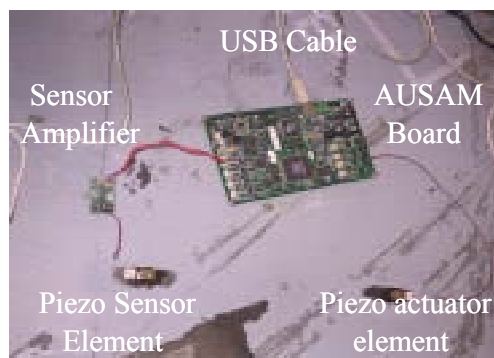
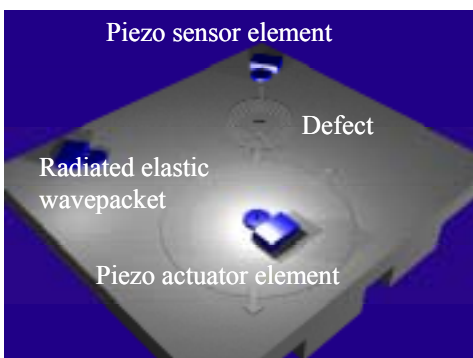
Excitation was a Modulated Tone Burst (MTB) with 5 cycles.

Conduct a structure characterisation (pre-impact).

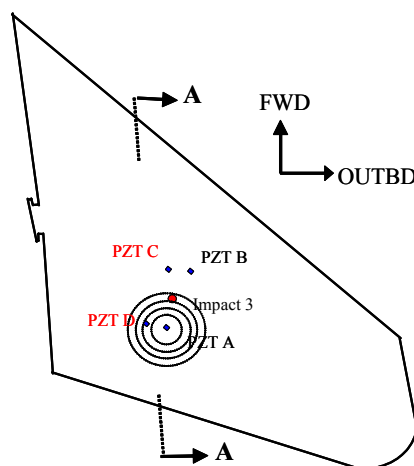
Record structure characterisation after damage (post impact).

Active mode test program was conducted using the Acousto-Ultrasonic SHM Array Module

The results demonstrated the capacity of the AUSAM system to detect probable impact damage growth due to loading. The system also exhibited good reliability and robustness in electrically and mechanically noisy environments.



*AUSAM on the F/A-18 Horizontal Stabilator*



#### 8.4.2 Use of Sonic Thermography as a Non-destructive evaluation technique (Kelly A. Tsoi and Nik Rajic, DSTO)

The rapid rate of advancement in materials and manufacturing technologies ensures an ongoing requirement for improved non-destructive evaluation (NDE) techniques. A strong impetus already exists in relation to the inspection of tightly closed cracks in metallic components and kissing bonds in composite structures, which are often an insuperable problem using conventional NDE methodologies.

Sonic thermography is an emerging technique which to date has shown good prospect for difficult inspection problems like tightly closed cracks in metallic structures and kissing bonds in composite repairs. The technique uses elastic waves injected with an acoustic horn operating typically at either 20 or 40 kHz, to induce lateral motion at the surfaces of cracks or delamination defects. This lateral motion induces frictional heating and in turn a thermal indication, which can often be detected with thermal imaging equipment [1].

A sonic thermographic facility has been developed by DSTO for the detection of defects in a series of specimens relating to the F-111C aircraft including (i) disbonding in a composite repaired lower wing skin section from a failed wing (see Figure 1), (ii) the detection of cracks beneath a composite bonded repaired aluminium honeycomb sandwich panel (Figures 2 and 3) and (iii) loose interference-fit fasteners in the context of the F-111C wing [2].

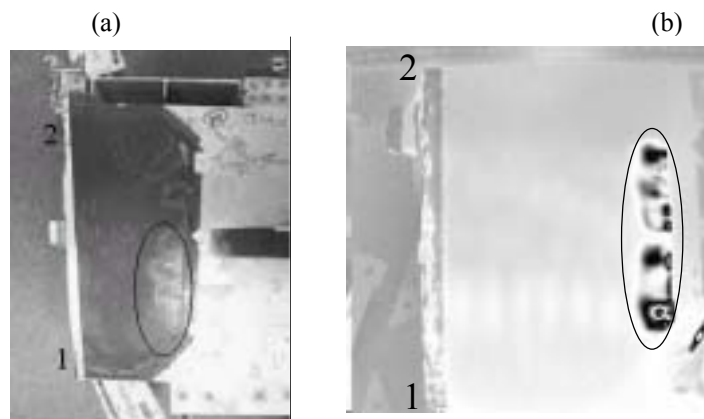


Figure 1 (a) Photograph of the LWS section, indicating region of interest. (b) Raw sonic thermograph showing darkened regions indicating elevated heat production and possible disbands.

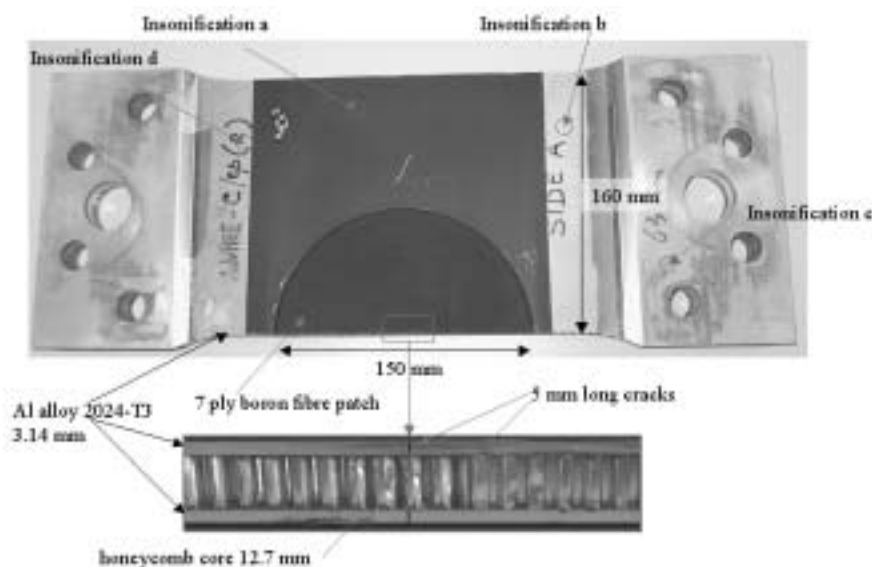


Figure 2: Photograph of the boron epoxy patched honeycomb panel showing the dimensions and insonification points

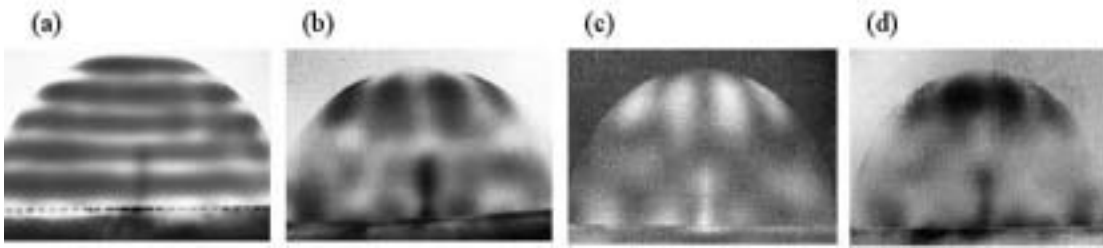


Figure 3. Sonic thermographs of boron epoxy patched honeycomb panel insonified at four locations (a, b, c and d) corresponding to Figure 2. The vertical indication corresponds to the crack in the Al 2024-T3 panel beneath the composite patch.

Research has also been undertaken to determine the effect of insonification on the growth rate of cracks in aluminium alloy specimens during mechanical tensile testing. The efficacy of the technique in detecting cracks has been addressed as has the influence of the specimen thickness on crack detectability [3].

#### References:

- [1] "Sonic thermography as a NDE technique", Kelly A. Tsoi and Nik Rajic, DSTO technical note, DSTO-TN-0584, October 2004.
- [2] "Sonic thermography- a destructive or non destructive evaluation technique?", Kelly A. Tsoi and Nik Rajic, *Advances in Applied Mechanics*, Proceedings of the Fourth Australasian Congress on Applied Mechanics, Xie, Y.M., Mouritz, A.P., Afaghi Khatibi, A., Gardiner, C. and Chiu, W.K. (Eds.), pp. 631-636, 2005.
- [3] "Non destructive evaluation of F-111 aircraft components using sonic thermography", Kelly A. Tsoi and Nik Rajic, *Advances in Applied Mechanics*, Proceedings of the Fourth Australasian Congress on Applied Mechanics, Xie, Y.M., Mouritz, A.P., Afaghi Khatibi, A., Gardiner, C. and Chiu, W.K. (Eds.), pp. 649-655, 2005.

### 8.4.3 Aircraft Forensic Engineering – Investigations (N Athinotis, DSTO)

The following sections contain examples of investigations undertaken in the last two years:

#### 8.4.3.1 Aircraft Engine Compressor Turbine Blade Failure

While the pilot of an RAAF PC-9A aircraft was carrying out touch and go manoeuvres, a loud bang accompanied by flames emanating from the exhaust stubs occurred on take-off after the fifth touch and go at approximately 20 feet off the ground. The flight was aborted and the aircraft landed without further incident. The investigation by the DSTO found that a perforated airfoil of a Compressor Turbine (CT) vane resulted in a CT blade being hit by vane material during the break-up of the perforated airfoil resulting in crack initiation leading to fatigue cracking and subsequent failure of the blade. The damage to the CT vane was consistent with rapid oxidation due to overheating of the vane. In addition, deleterious phases were observed which most likely formed as a result of prolonged exposure at elevated temperatures. The investigation revealed external cracking and both thinning and cracking of the internal surfaces of other vanes. While the external cracking was most likely caused by thermal cycles (i.e. thermal fatigue), the internal cracking was mostly due to preferential grain boundary oxidation and possibly thermal fatigue. The fatigue cracking associated with the blade propagated to approximately 51% of the blade cross-sectional area over numerous flights. Vibration analysis on ex-service CT blades found that it was unlikely that the blades were in a resonant mode as a consequence of the pulse of air emanating from the perforated airfoil. Furthermore, it was also considered unlikely that a fatigue crack driven by a forced aerodynamic excitation (i.e. once per revolution) due to disruption of the gas flow passing through the perforated airfoil would take multiple flights to reach a critical crack size. Whilst it was possible that the CT blade may have been mistuned, dimensionally and/or through fitment, mistuning induced cracking would have affected any mistuned blade and was not the result of a once per revolution frequency excitation. No evidence was found to indicate that a defect(s) in the microstructure, or weakness in the casting, led to the initiation of the cracking in the CT blade. However, the origin of the crack (i.e. suction side and two-thirds from the leading corner) was not at a location that was usually expected from cracking from a blade fir tree, i.e. at the corners. It was considered likely that the blade may have been hit by vane material during the break-up of the perforated airfoil consequently resulting in crack initiation and subsequent failure of the blade.

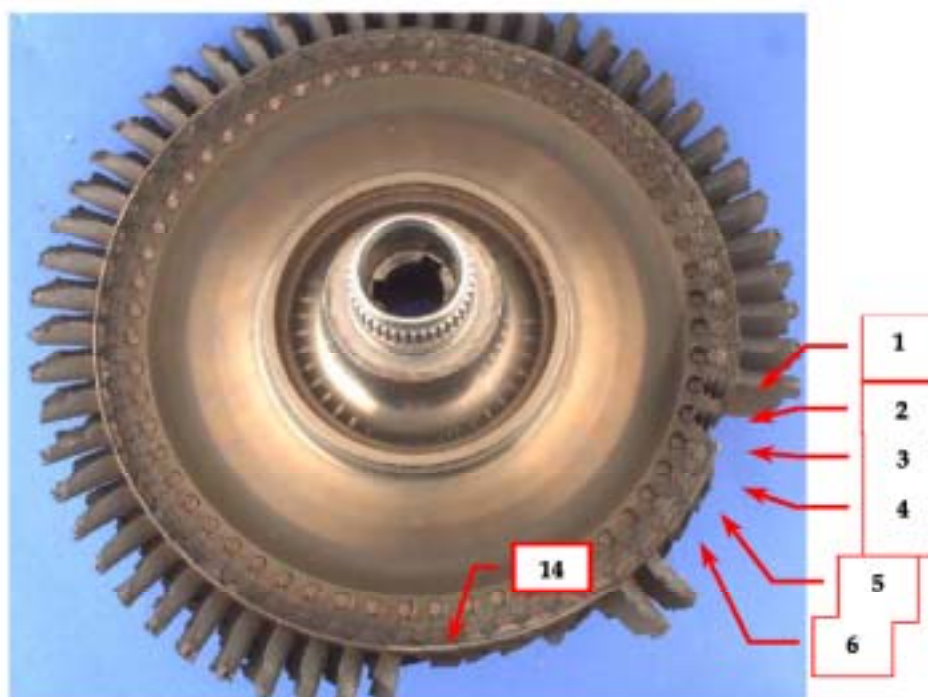


Figure 1. Photograph of the CT turbine disk assembly as received. Blade 1 (containing the primary fracture surface) and Blade 2 were removed by P&WC. DSTO labelled the blades from 1 to 59 in the clockwise direction



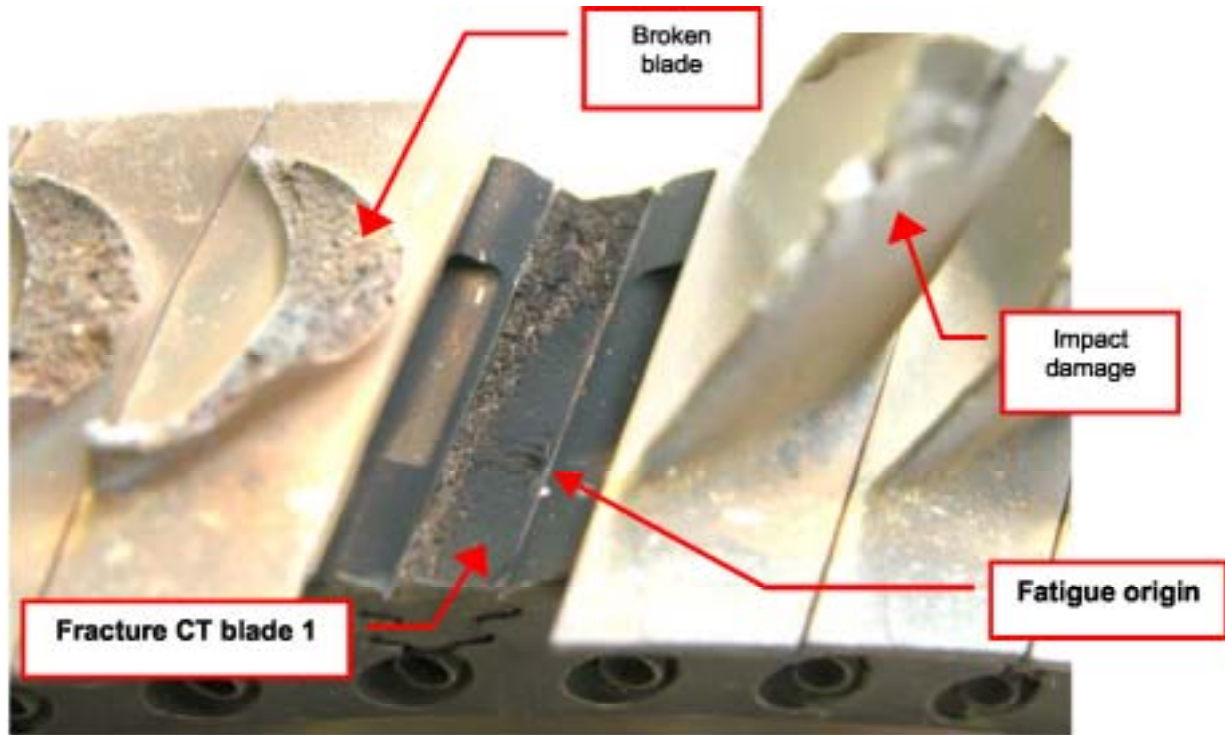


Figure 2. Photograph of the subject CT turbine blade assembly showing the fracture surface and the fatigue crack origin (Labelled) on CT blade 1. Also note that the remnant of the trailing edge of the adjacent CT blade was bent in the direction of impact (labelled).

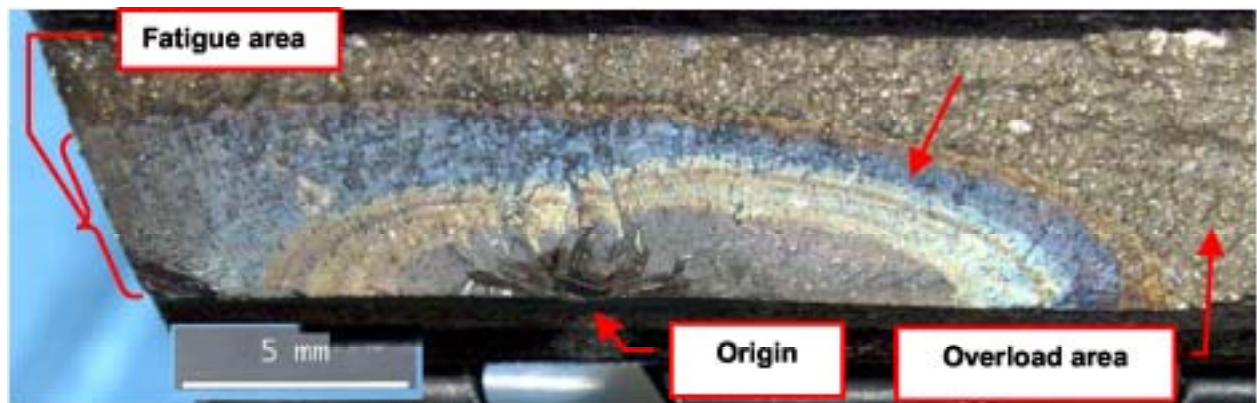


Figure 3. Photograph of the fracture surface of CT blade. Note the concentric rings produced by differing thicknesses of the oxide due to exposure time. The fatigue crack propagation is from bottom to top. Note banding of the fracture surface (example arrowed). The bands are caused by changes in the oxide layer due to variations in the service conditions and/or exposure time; this indicated that the fatigue crack propagated in numerous engine cycles

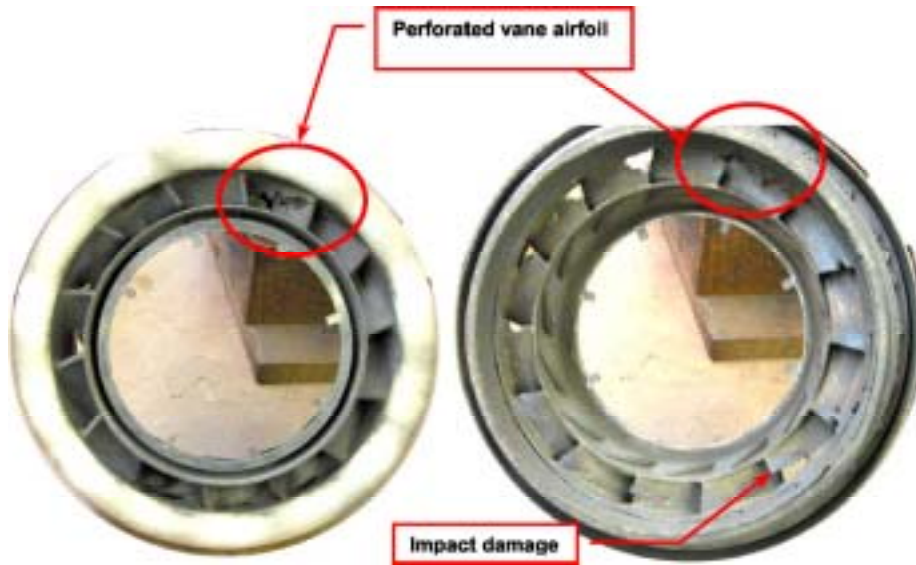


Figure 4. Photographs of the CT stator from both the leading (left) and trailing (right) sides. Severe impact and wear damage is observed at the trailing side (right). Also note the perforation of CT vane (circled). A higher magnification view of the perforated airfoil is shown in Figure 5 and 6.

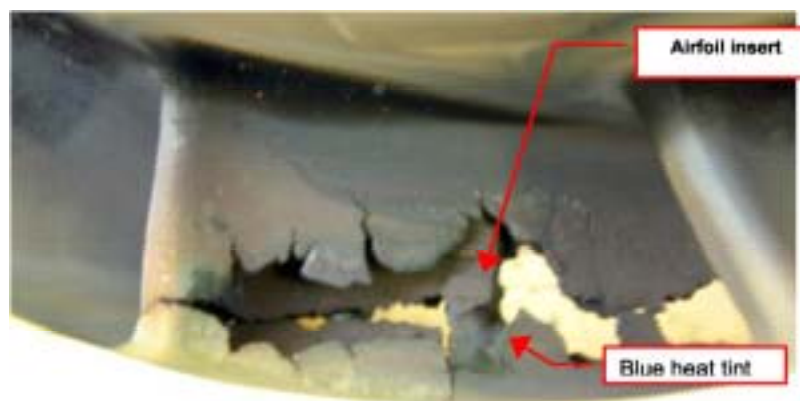


Figure 5. Photograph of the leading side of the perforated airfoil of CT vane 10 (Circled area in Figure 2). Note the rounded edges and the jagged cracking. Heat tinting of the surface is also observed (labelled).

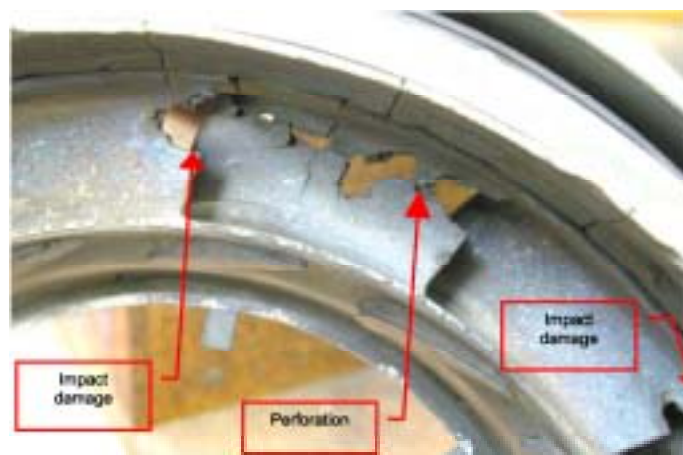
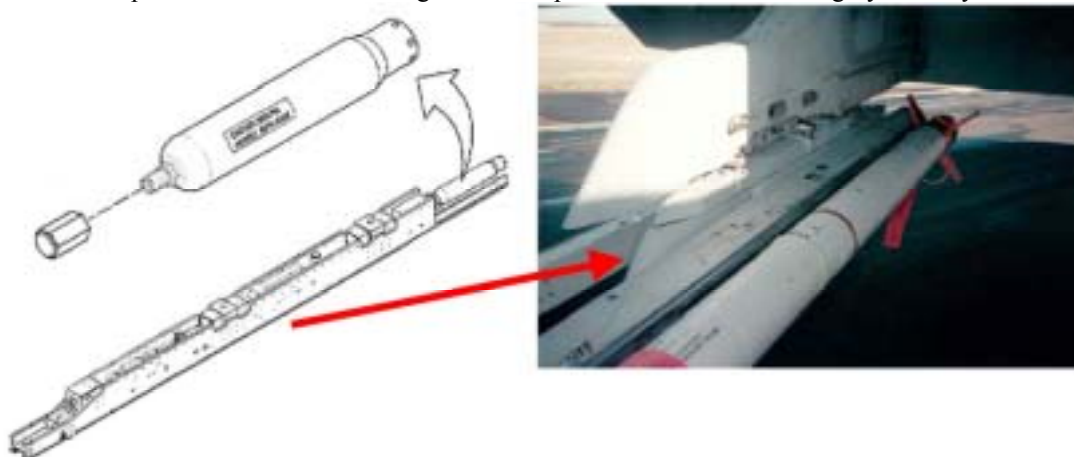


Figure 6. Photograph of the trailing side of the perforated airfoil of CT vane 10 (Circled area in Figure 4). Evident impact damage sustained on the adjacent vanes during the departure of the CT blades is also labelled.



#### 8.4.3.2 LAU-127 Guided Missile Launcher Nitrogen Receivers Corrosion

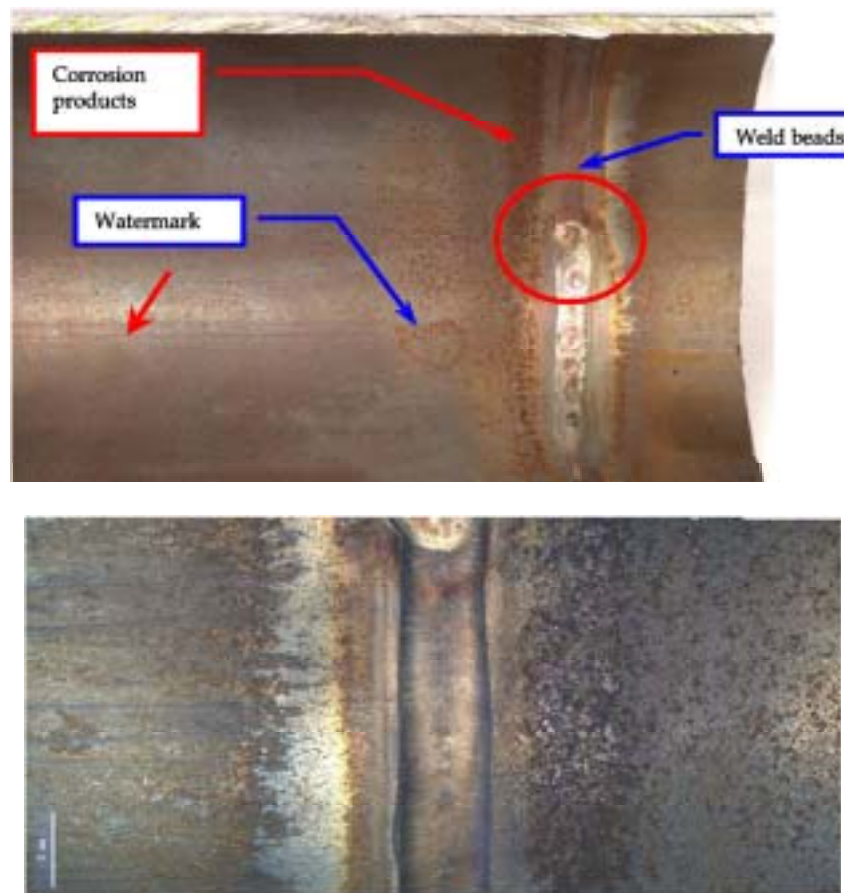
DSTO investigated the cause of corrosion found during an acceptance inspection/service of the cylinders, on the internal and external surfaces of two new LAU-127 Guided Missile Launcher Nitrogen Receivers. The investigation found that a manufacturing defect, which resulted in the formation of deleterious phases (i.e. pearlite layer) on both the internal and external surfaces of the material comprising the cylinders was the main contributing factor for the formation of the corrosion and cracking. These deleterious phases resulted in a material surface layer with lower strength, lower corrosion resistance and passivity, which consequently led to corrosion and cracking when the cylinders were exposed to an otherwise mild corrosive environment. The investigation concluded that the cylinders failed to satisfy the requirements specified by the Original Equipment manufacturer regarding corrosion resistance and surface condition (e.g. cracks or corrosion free surfaces), and that the presence of these defects might have compromised the structural integrity of the cylinders.



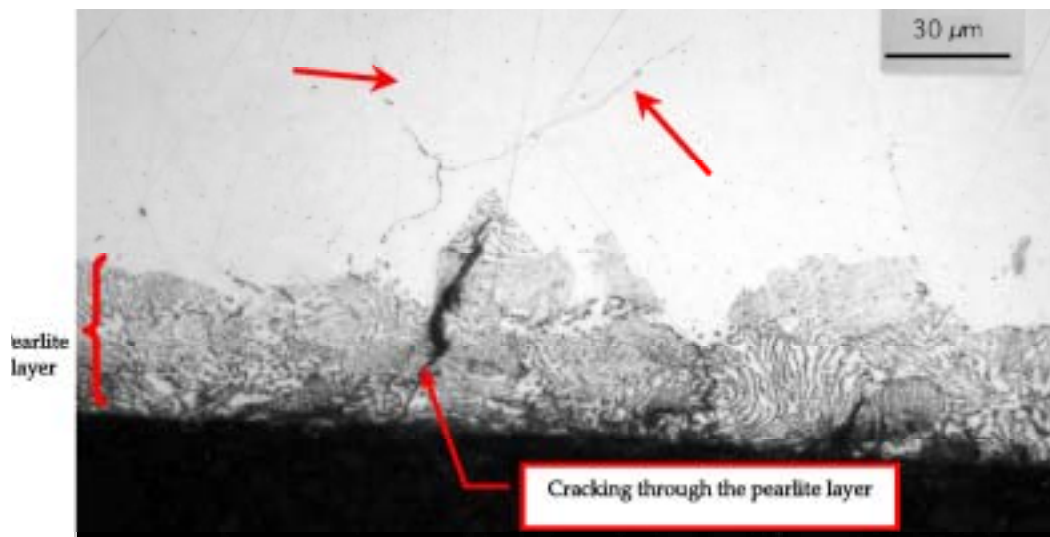
Left. Diagram showing the location of Nitrogen Receivers in the LAU-127 Guided Missile Launcher. Right. Photograph of the underwing position of the F/A-18 LAU-127 Guided Missile Launcher.



(Top) Photograph of a subject cylinder showing a large area of cracking (circled area). (Bottom left) An enlarged view of the cracking showing a network of circumferential cracks. (Bottom right) Note the corrosion products (i. e. 'rust stain') inside and in the vicinity of the cracks (arrowed).



Photograph of a section of the internal surface of a subject cylinder (Top) and a higher magnification view (bottom) of the weld beads (circled). Note the large concentration of brown corrosion deposits and the dark grey colouration of the background surface. Plug scores (i.e. longitudinal score marks) are also noted (examples arrowed). Also note that the amount of surface corrosion observed on the HAZ.



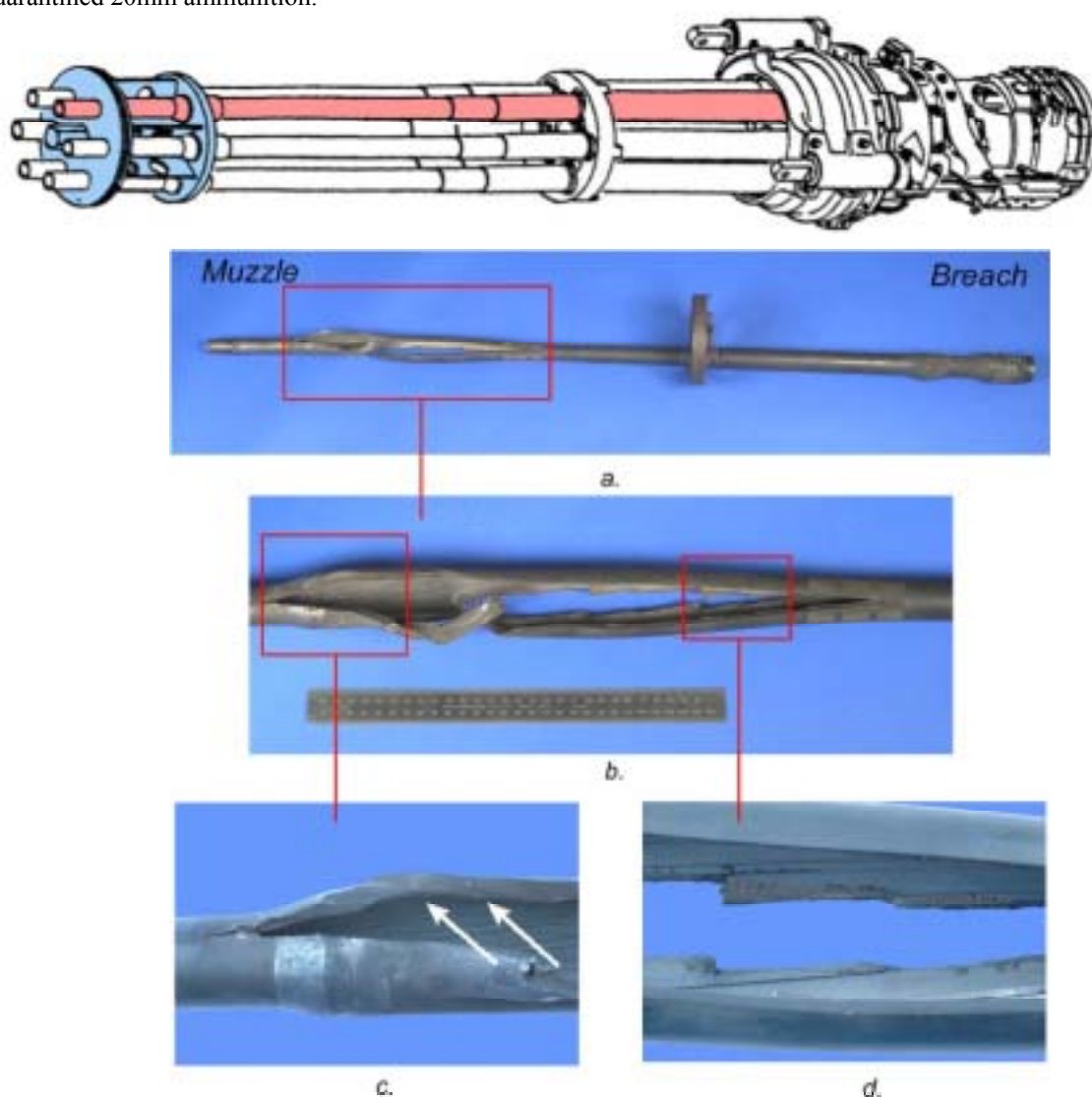
Electrolytic etching of metallographic specimens revealed the presence of a pearlite layer at the areas where corrosion and/or cracking were observed. Cracking through the pearlite layer is evident. Intergranular hairline cracking along the austenitic grains is also observed (examples arrowed).

### 8.4.3.3 Aircraft Rotary Cannon Failure

During a live firing training exercise, one of the barrels of the onboard 20mm M61A1 rotary cannon of an RAAF F/A-18 aircraft failed catastrophically. The barrel failure resulted in significant damage to the cannon system and other areas of the aircraft including the blast diffuser, muzzle clamp, aircraft structure surrounding the cannon, and the radar and radome. The cannon failure resulted in the suspension of all RAAF F/18 live-fire training exercises and the quarantine of several hundred thousand rounds of M61A1 20mm ammunition until the root cause of the problem could be determined.

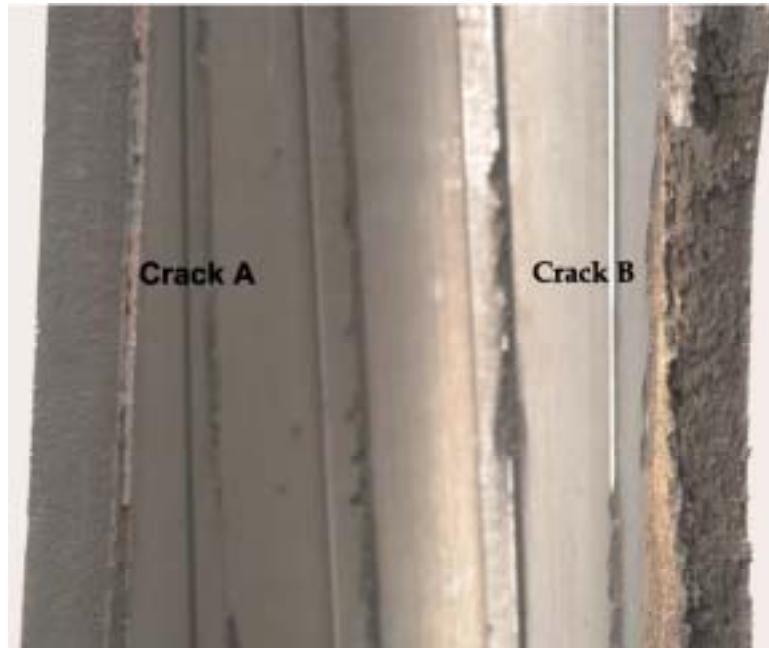
DSTO examination of the failed barrel from the gun system revealed that a large manufacturing defect was present prior to installation in the aircraft. The presence of the defect caused failure of the barrel after only relatively few rounds had been fired. The defect extended longitudinally penetrating from the outer surface of the barrel and was present from manufacture. Crack progression from the defect was rapid resulting in catastrophic rupture of the barrel.

Non-destructive inspection procedures were recommended to search for defects and cracking in M61A1 cannon barrels. No further defects were found in the fleet, which allowed resumption of live-fire training and commissioning of the quarantined 20mm ammunition.



Photograph (a) shows the defective cannon barrel as received by the DSTO. Photographs (b), (c) and (d) show higher magnification images of the damaged region of the barrel and parts of the fracture surfaces. Longitudinal cracks in the barrel were located approximately 200mm aft of the muzzle, and extended for approximately a further

420mm toward the breech. Note 'smearing' witness marks on parts of the fracture surface [white arrows in photograph (c)], probably caused by projectile penetrating the barrel wall.



Macro-photograph of part of the fracture surface from the ruptured barrel. Two different regions of fracture associated with the failure are identified and labelled (Crack A) and (Crack B). Crack A is associated with a pre-existing defect within the barrel and Crack B is associated with rapid overload.

#### **8.4.4 The effect of pitting corrosion on the position of aircraft structural failures (B.R. Crawford, C. Loader and P.K. Sharp, DSTO)**

##### *8.4.4.1 Background*

Corrosion has been shown over the last decade to significantly reduce the structural integrity of aircraft as they age. Previous work at DSTO has shown that pitting and exfoliation corrosion are particularly deleterious to aircraft structural integrity. In addition to reducing fatigue endurance, pitting also increases the surface area of the component over which fatigue failures can occur. Recent work has focussed on developing a Monte-Carlo model of this phenomenon, which has been labelled 'corrosion criticality'. This model concentrates on the effect of the pit spatial density and position on the endurance of a fatigue coupon designed to mimic a simple aircraft component. The study's results show that pitting increases the area of the coupon over which failures can occur.

##### *8.4.4.2 Introduction*

The structural integrity of aircraft is based upon design practices in which the fatigue critical sections of components are identified either during design or as part of a teardown after full-scale fatigue testing, with the aim of preventing fatigue failures within the design life of the aircraft type. Pitting corrosion, however, creates damaged regions which are not necessarily located in the nominally fatigue critical regions. In-service experience has shown that fatigue cracks initiated from corroded regions can grow to failure within the aircraft's design life [Cole et al., 1997]. This greatly complicates the inspection of aircraft by enlarging the surface area of the aircraft that must be examined to ensure continued structural integrity.

The practices described above work because it is reasonable to assume that the size of intrinsic defects, such as constituent and second phase particles, is approximately the same throughout the structure of an aircraft. This means, as a consequence of the definition of  $\Delta K$  and the nature of fatigue crack growth, that only the location of the defect, which controls the stress and, therefore, stress intensity factor, will have an effect. However, the introduction of corrosion into the structure changes this by introducing a set of defects with a completely different and significantly larger size distribution. As a consequence both the defect's size and position become critical. This means that a large defect, such as a corrosion pit, in a low stress region may reduce fatigue life to the same extent as a small defect in a high stress region. This causes the number of critical regions in an aircraft to increase, potentially enlarging the area of an aircraft's structure requiring inspection. This behaviour has been observed in research conducted at DSTO [Mills et al., 2002; Sharp, 2003]

#### 8.4.4.3 Experimental details and results

##### 8.4.4.3.1 Development of corrosion protocol

The experimental work concentrated on the development of a realistic corrosion pitting distribution for input to the criticality model. The underlying corrosion protocol was developed by swabbing four coupons of 60 mm by 10 mm dimensions with a 3.5wt% aqueous solution of NaCl. These coupons were ground to a 1200 grit finish using silicon carbide paper prior to corrosion to activate the material's surface. The coupons were then placed in a high humidity (RH > 80%) environment for periods of 1, 2, 4, 7 and 14 days to allow corrosion pits to develop. At the end of these times the coupons were removed from the high humidity environment and washed with ethanol to remove the corroding solution. The coupons were then serially sectioned. The surface of each coupon was divided into 9 regions of equal area. Serial sectioning was used to identify the largest pit in each of these regions. Successive 10  $\mu\text{m}$  slices of material were removed until all evidence of pitting in a region had disappeared. These depth data were then used to determine an extreme value distribution for largest pit size. Given that this sectioning was conducted on coupons corroded for several different durations this allowed a relationship between deepest pit size and corrosion period to be established. Largest pit size was used in favour of mean pit size as, given an equal stress, the largest defect will typically initiate the fatigue crack that leads to final fracture.

##### 8.4.4.3.2 Maximum pit size distribution

Pit size distributions obtained for seven and fourteen days exposure are shown in Figure 1 as probability and cumulative density functions. These distributions were calculated using an extreme value statistics approach based on the exponential distribution [Castillo, 1988]. Extreme value statistics greatly reduce the number of observations required to obtain a size distribution. Figure 1 shows the predicted largest pit size distribution based on a corrosion strike 2 mm wide and 196 mm long. Examination of parts (a) and (b) of this figure shows that the median pit size increased with increasing exposure time. Note also that the size range of the distribution also increased.

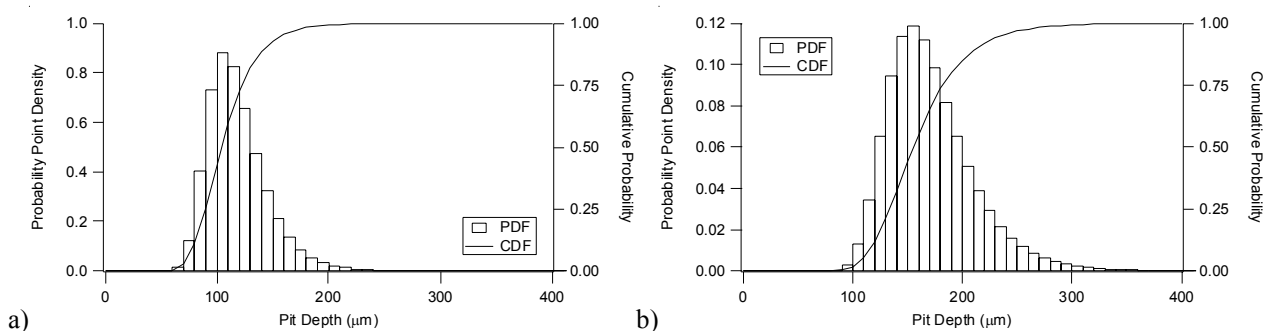


Figure 1: Point (PDF) and Cumulative Density Functions (CDF) of maximum pit depth in 7010-T7651 after (a) 7 days and (b) 14 days exposure in humid air. Distributions were calculated using the exponential distribution function.



#### 8.4.4.4 Modelling Details and results

The structure and algorithm of the criticality model are illustrated in Figure 2. Note that the model is based on the Monte Carlo method which has been implemented without any variance reduction techniques. The purpose of the model is to simulate the effect of pitting corrosion on the spread of fatigue failures along the surface of a simple fatigue coupon. Corrosion is assumed to occur as “corrosion strikes” which are regions in which pitting corrosion has occurred. In practice such corrosion strikes typically occur due to the failure of the paint system covering the region of a component that has corroded.

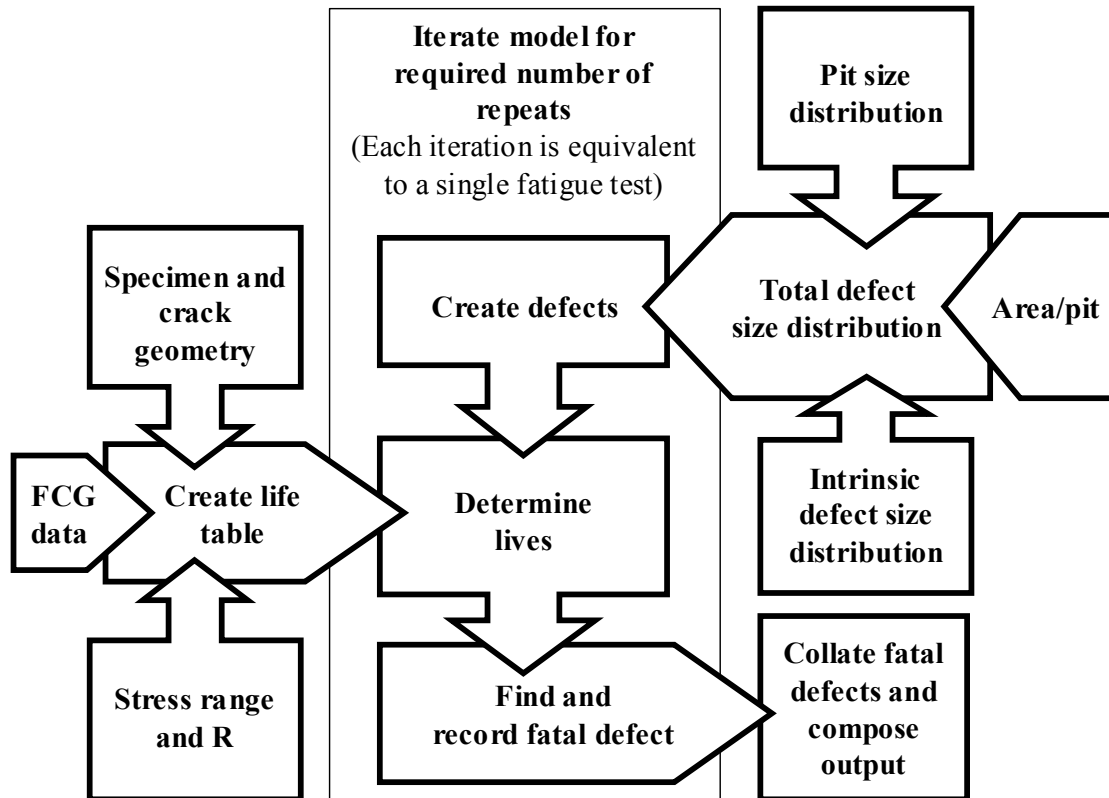


Figure 2: Structure of criticality model showing the model's various inputs and the underlying algorithm.

To simulate pitting corrosion the model requires inputs detailing the material properties of the material, the applied loading and the size of both the intrinsic defects and the pits in the material. These inputs are:

- **Coupon geometry:** Expressed in terms of a finite element solution of the stress along the longitudinal axis of symmetry of the coupon to which a polynomial equation was fitted. This allowed the stress at any position along the coupon to be estimated as a function of distance from the middle of the gauge-section. The coupon design is shown in Figure3(a).
- **Fatigue crack growth data:** The fatigue crack growth data [Crawford et al., 2004] were used to create a lookup table of fatigue lives as a function of defect size (expressed as defect radius in microns) and applied maximum stress (in MPa). Fatigue lives above  $3.5 \times 10^6$  cycles were considered to be infinite. A load ratio ( $R$ ) of 0.1 and a semi-circular crack shape was assumed. The AFGROW fatigue life modelling program was used to create this table [Harter, 2003b; c] using the program's COM interface [Harter, 2003a].
- **Maximum Stress range:** This fell within the range of stresses allowed by the underlying fatigue crack growth data. The upper value of maximum stress used was always less than the material's yield stress.
- **Pit size distribution:** This was obtained experimentally by serial sectioning of corroded surfaces of as-machined 7010-T7651. The pit size distribution is illustrated in Figure 1. The 7-day pit size distribution was used in this paper. It was assumed that there was no size difference between a corrosion pit and the fatigue crack producing an equivalent life.
- **Corrosion strike length:** This is the length of the corroded region on each coupon. This increases the number of pits on the coupon but does not change the linear density of pits. Note that there is a stress gradient along the corrosion strike.

- **Corrosion strike width:** This is the width of the corroded region on each coupon. Increasing the width of the corrosion strike increases the linear density of pits and the total number of pits. Given that the stress is effectively constant across a corrosion strike this should only affect the spread of fatigue failures.
- **Corrosion strike centre:** This is the centre of the corroded region, which represents the position of the corrosion strike on the coupon's surface. This position can either be allowed to vary randomly along the coupon's gauge length (within a selected range) or can be set to a specific value (such as in the centre of the coupon's gauge section).
- **Area per pit:** defines the area in which the largest pit is being estimated. That is, if the area per pit is  $20 \text{ mm}^2$  then the pit size distribution (which is defined by an exponential distribution function) will return the distribution of largest pits in this area. It also determines the number of pits on a coupon as a percentage of the total defects within the corrosion area.
- **Intrinsic defect size distribution:** This is the size distribution of the intrinsic defects, which was determined by microscopic examination of polished sections of the material. It was assumed that the intrinsic defect size and equivalent fatigue crack size were identical.

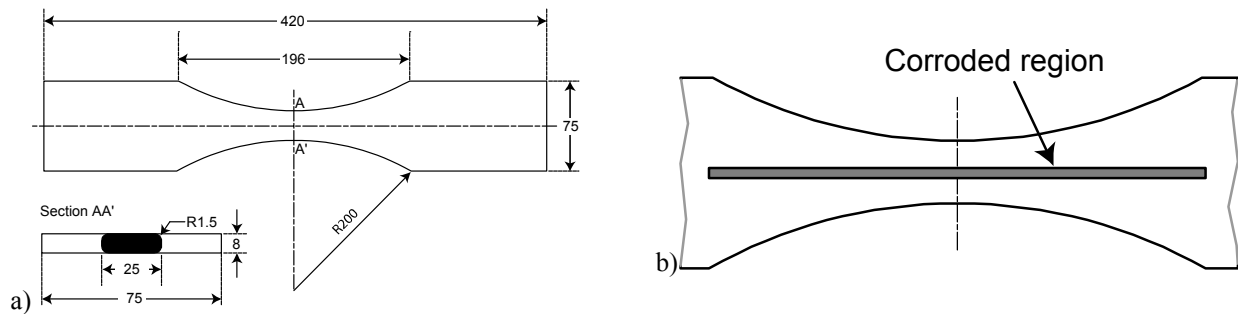


Figure 3: (a) Coupon geometry (b) position of corrosion region

These inputs are used to simulate a corroded fatigue coupon (Figure 3(a)) using the following algorithm. Defects on the coupon's surface are generated using cumulative particle size histograms (e.g. Figure 1) using the inverse transformation method [Ayyub and McCuen, 1995] while defect position is randomised uniformly along the coupon's gauge. Defect sizes within the corrosion strike are simulated using a combined (pit and intrinsic defects) size histogram. Those outside the corrosion strike use only the intrinsic defects size distribution. The size and position of the resultant defects and pits are then compared with a lookup table of fatigue life as a function of these inputs. The defect with the shortest life is selected as being the "fatal" defect and its size and position recorded. The model then repeats this process for the required number of iterations. The model's output is a scatter graph showing the relation between pit size and failure location.

#### 8.4.4.5 Model Results

##### 8.4.4.5.1 Effect of corrosion strike length

The model was run using the parameters listed in Table 1. The fatigue limit was selected to eliminate spurious runouts due to the lack of data in the lower end of the fatigue crack growth curve collected for the material.

Table 1: Model parameters used to evaluate the effect of corrosion strike size.

$\sigma_{\max}$ (MPa)	R	Area per pit ( $\text{mm}^2$ )	Strike width (mm)	Strike length (mm)	Defect density ( $\text{mm}^{-2}$ )	Fatigue limit (cycles)	Repeats
380	0.1	20	5	0, 10, 50, 100	30	290,000	5000

Figure 4 shows the results for corrosion strike lengths of 0 (no-corrosion), 10 mm, 50 mm and 100 mm. It also shows the domain in which a fatigue failure is possible at the loading and runout conditions listed in Table 1. Part (a) of this figure shows the case where there is no corrosion. Therefore, fatigue failures will be due to intrinsic particles, which due to their small size can only fail within the central high stress region (see the normalised stress profile in Figure 4(a)). This produces the observed narrow distribution of failures. Note also that this distribution of failures is far narrower than those that are theoretically possible.



The introduction of relatively short corrosion strikes (10 mm long) positioned randomly along the gauge length (see Figure 4(b)) increases the spread of fatigue failures to  $\pm 60$  mm. Once a small corrosion strike is introduced to the coupon there is a good chance that this strike will (a) contain a large corrosion pit and (b) that this pit will be located outside the region of the coupon where intrinsic failures occur. Further increases in the corrosion strike length (see Figure 4(c) and (d)), however, cause the fatigue critical region to contract again. This occurs because of the increased probability of a large defect occurring in the coupon's central, high stress region. This is particularly apparent in the case of a 100 mm long corrosion strike (Figure 4(d)). Despite this, failures can still occur at large distances from the high stress region, as shown by the outlier in Figure 4(d). The probability of these, however, is extremely low due to the typically high density of pits in the high stress region.

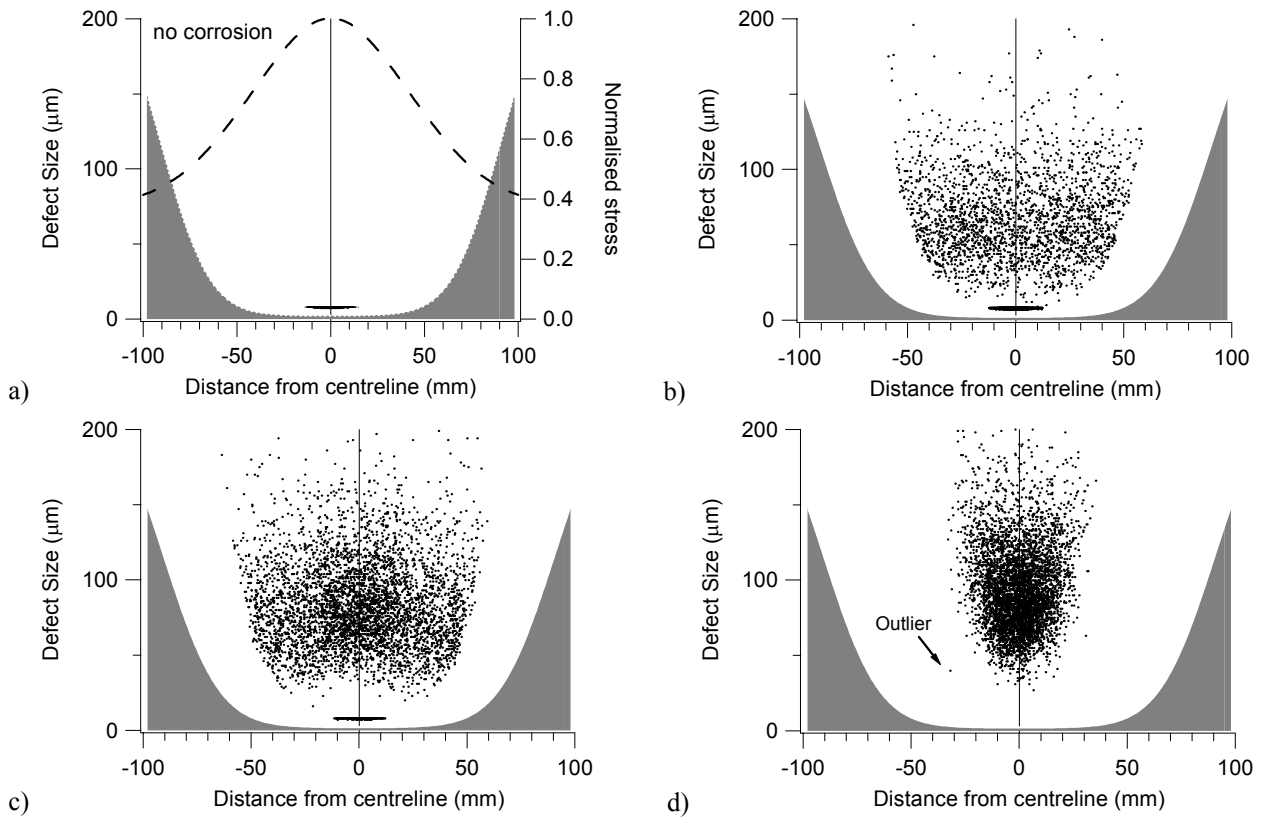


Figure 4: Scatter graphs showing distribution of failures due to fatigue cracks initiated from intrinsic particles and pits with pit strike lengths of (a) 0 mm (no corrosion), (b) 10 mm, (c) 50 mm and (d) 100 mm. The pit strikes were all 5 mm wide and the area per pit was 20 mm<sup>2</sup>. The shaded region in each graph is the domain in which a fatigue failure is not possible at the applied maximum stress (380 MPa) and fatigue limit (290,000 cycles). Note that this domain is the same for all cases shown in this figure. The dashed line in part (a) is the longitudinal stress in the coupon normalised by its maximum value at the coupon's centre.

#### 8.4.4.5.2 Effect of corrosion strike width

Having investigated the effects of corrosion length, DSTO studied the effect of corrosion area width which controls the lineal density of pits on the coupon. Pit lineal density was defined as the number of pits per unit length along the coupon's gauge length. It is controlled by the exponential pit size distribution described above and the width of the corrosion region. At a corrosion region length of 196 mm and given the pit size distribution in Figure 1, a 0.1 mm wide corrosion region will produce one pit of fatigue critical size per coupon (i.e. iteration of the Monte Carlo model).

Figure 5(a) shows the effect of a single corrosion pit on the spread of fatigue failures. The spread of failures is far wider than for an uncorroded sample (cf. Figure 4(a)) in which only intrinsic defects are present. Increasing the width of the corrosion area to 1 mm, which gives an average of 10 corrosion pits per coupon, however, decreases the spread of fatigue failures. For example, a corrosion pit of 100  $\mu\text{m}$  size located  $\pm 50$  mm from the coupon's middle can cause failure at a corrosion area width of 0.1 mm but is very unlikely to cause failure at a corrosion area width of 1 mm. This is because the increased number of pits per coupon means that there is likely to be a pit of shorter life towards the middle of the coupon.

This narrowing of the spread of fatigue failures is caused by interaction of the increased number of pits per coupon due to an increase in corrosion area width with the change in stress with distance from the coupon's middle (see Figure 4(a)). Removal of the stress gradient would eliminate this effect but only because the position of fatigue failures would become completely independent of corrosion. That is, the introduction of corrosion into a constant stress structure would only decrease its life and would not affect the position of failures. Further increases in corrosion area width as shown in Figure 5(c) and (d) further concentrate failures in the coupon's high stress region.

Note that an increased corrosion area width also eliminates failures due to intrinsic defects and increases the minimum size of a critical defect. This is due to the increased number of pits on the coupon increasing the likelihood of a pit with a shorter life being at a similar distance from the coupon's centre. This is the same mechanism that narrows the spread of failures with increased corrosion area width. Failures from intrinsic defects are eliminated simply because the intrinsic defects in this simulation are smaller than the pits.

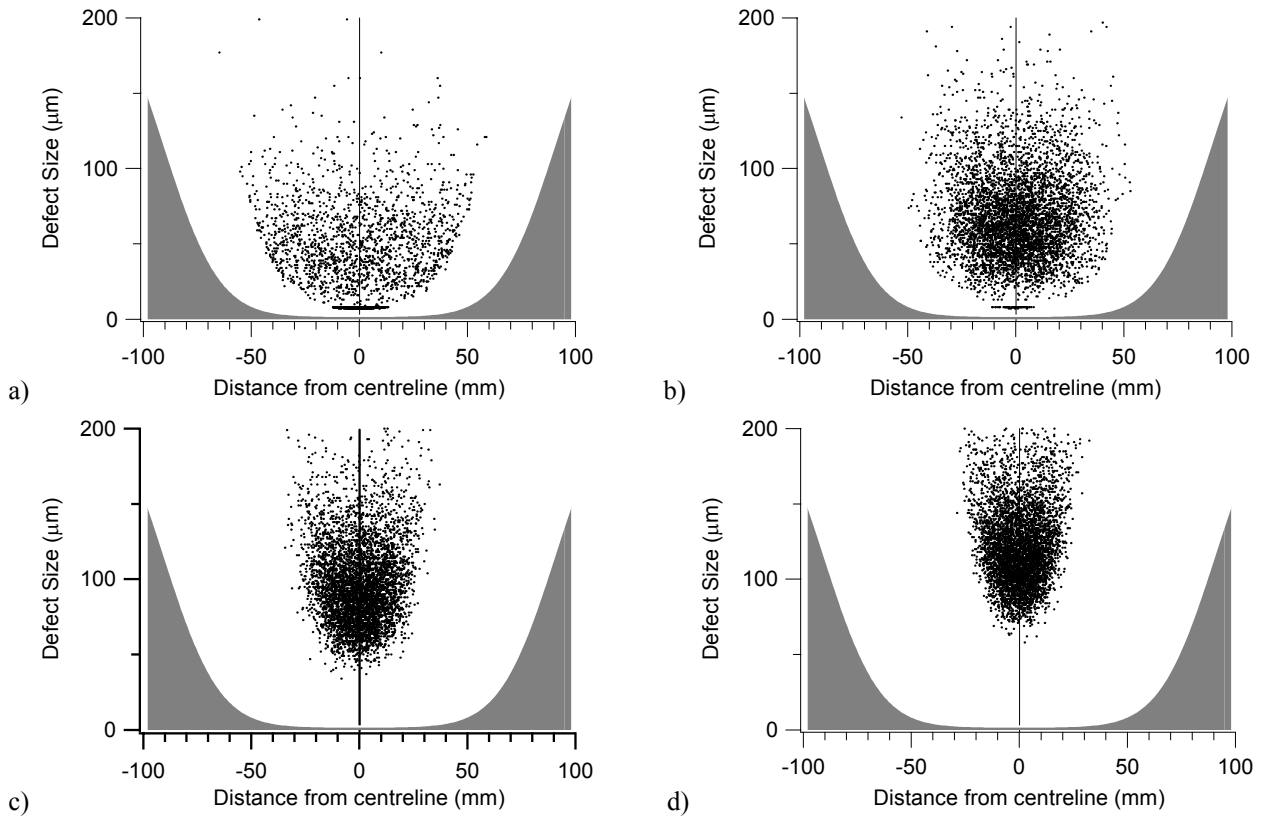


Figure 5: Scatter graphs showing distribution of failures due to fatigue cracks initiated from intrinsic particles and pits with corrosion strike widths of (a) 0.1 mm, (b) 1 mm, (c) 5 mm and (d) 20 mm. Corrosion strike length is 196 mm in all cases. The shaded region in each graph is the domain in which a fatigue failure is not possible at the applied maximum stress (380 MPa) and fatigue limit (290,000 cycles). Note that this domain is the same for all cases shown in this figure.

#### 8.4.4.5.3 Frequency of pitting failures as a function of fixed corrosion strike position

In the previous two sections the position of the corrosion strike was allowed to vary randomly. While this allows the effect of corrosion strike size to be modelled a comparison with experimental results is impractical because of the large number of iterations in the model (5000) and the difficulty of creating “random” corrosion strikes. For these reasons the model’s prediction of the proportion of failures due to pitting and intrinsic defects was studied as a function of the position of a deliberately placed corrosion strike.

The corrosion strike was set to a length of 10 mm a width of 5 mm and the position was varied along the coupon’s gauge length. Figure 6 shows the output of the model under these conditions. The number of failures due to pitting increases as the corrosion strike placement approaches the centre of the coupon, but intrinsic defect failures always occur, as there exists a small chance that no corrosion pits will occur on any given coupon. The model determines the combined distribution of defects within a corrosion strike, which takes into account the probability of occurrence. A defect is assigned a position and if this falls into the corrosion strike, it is assigned a defect size based on the combined distribution. There are a large number of defects with each having only a small probability of its defect size coming from the pitted distribution. With a large number of runs, occasionally none of the defects will result in pitting. As the corrosion strike moves away from the centre, the chance of having no defects large enough to cause failure occurring within the corrosion strike increases. Intrinsic failures however, continue to occur. Such a prediction can be tested experimentally though the number of repeat coupons will clearly be several orders of magnitude less. Coupons are currently being prepared to perform such an experimental comparison.

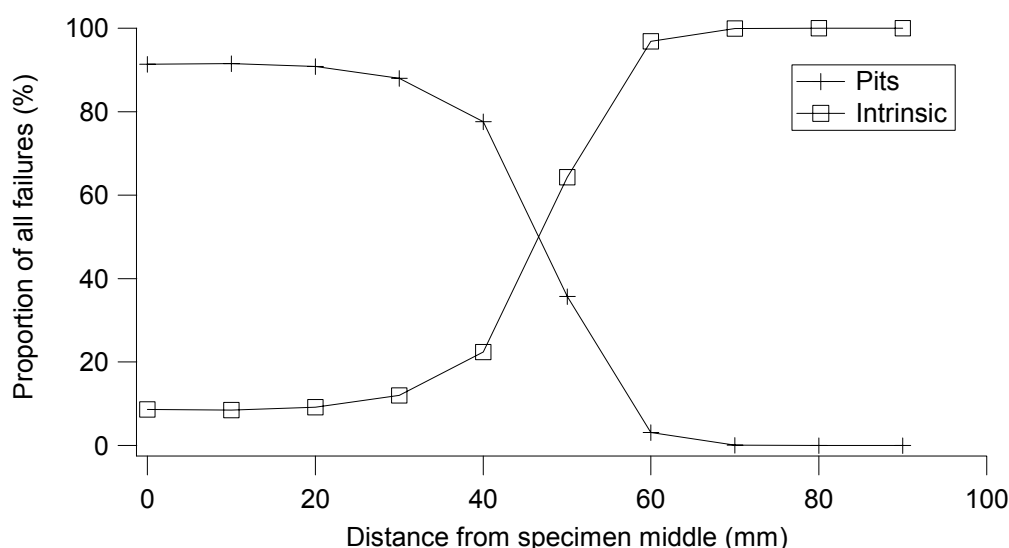


Figure 6: Proportion of failures due to intrinsic defects and pits.

#### 8.4.4.6 Conclusions and further work

This paper represents the second phase of research being conducted at DSTO into modelling the effect of pitting corrosion on the spread of fatigue critical regions in aircraft structural components. In the process of doing this several simplifying assumptions have been made. One of these was to assume that a surface defect acts as a crack of the same size. Despite these assumptions, a range of useful observations has been made.

As shown by this model, corrosion criticality has implications for the management of the structural integrity of aircraft. The spread of fatigue critical regions due to pitting corrosion means that those regions of aircraft, which were considered to be safe by design, may not actually be safe once corroded.

There are at least two scenarios to be considered. In the first, the corrosion of low stress regions of a fatigue critical component means that the area of that component requiring inspection will need to be increased if safe operation is to be ensured. This increases the cost of maintenance and, consequently, the cost of fleet operations. The second scenario is where the corrosion of a durability component (i.e. a component that is designed with a fatigue life far in excess of the aircraft) may cause it to fail during the life of the aircraft. Such a failure could prevent the safe operation of the aircraft and may lead to expensive repairs.

The model is yet to be experimentally validated. It is planned to conduct a series of fatigue tests on coupons that have been selectively corroded to determine if the effects observed in the results of this model are observed under experimental conditions. A direct test of the spread of failures shown in this paper (see Figure 4 and Figure 5) is not possible due to the large number of repeats that would be required.

#### Acknowledgements

The authors would like to thank Claude Urbani of CSIRO for the FEA model used in this work.

#### References

- Ayyub, B. M. and McCuen, R. H., Simulation-Based Reliability Methods. *Probabilistic Structural Mechanics Handbook*. C. Sundararajan. New York, Chapman and Hall: 745 (1995).
- Castillo, E., *Extreme Value Theory in Engineering*. San Diego, Academic Press (1988).
- Cole, G. K., Clark, G. and Sharp, P. K., The implications of corrosion with respect to aircraft structural integrity. Melbourne, DSTO: 120 (1997).
- Crawford, B. R., Loader, C., Ward, A. R., Urbani, C., Bache, M. R., Spence, S. H., Hay, D. G., Evans, W. J., Clark, G. and Stonham, A. J., "The EIFS distribution for anodised and corroded 7010-T7651 under constant amplitude loading." *Fatigue and Fracture of Engineering Materials and Structures Submitted for publication* (2004).
- Harter, J., AFGROW COM Server Manual, USAF WPAFB. **2003** (2003a).
- Harter, J., AFGROW Program, USAF WPAFB. **2003** (2003b).
- Harter, J., AFGROW User's Guide, USAF WPAFB. **2003** (2003c).
- Metropolis, N. and Ulam, S., "The Monte Carlo Method." *Journal of the American Statistical Association* **44**: 335-341 (1949).
- Mills, T., Sharp, P. K. and Loader, C., The Incorporation of Pitting Corrosion Damage into F-111 Fatigue Life Modelling. Melbourne, DSTO: 178 (2002).
- Sharp, P. K., ECS Modelling of 7050 Aluminium Alloy Corrosion Pitting and its Implications for Aircraft Structural Integrity. Melbourne, DSTO (2003).

#### 8.4.5 Shape optimisation of holes for multiple-peak stress minimisation (W. Waldman and M. Heller, DSTO)

Further work has been undertaken at DSTO in the development of an iterative FEA-based method which simultaneously minimises the tangential stresses on multiple segments around the boundary holes in loaded plates, [1]. This is an extension of work reported in the last review, considering more complex geometries including holes in 3D plates.

This has been focused primarily on rework shape optimisation for airframe life extension, but is also highly relevant to initial design of cut-outs. Typically it is desirable to minimise all stress peaks around the hole boundary, because the most fatigue critical location may not be the one with the highest tensile peak. For example, different hole-boundary segments can have different residual stresses or probabilities of detection of cracks (i.e. a bigger crack size may be required for reliable detection of cracking at a secondary location).

In the present work the automated approach is demonstrated by both 2D and 3D numerical examples, each of which includes significant geometric constraints. It is shown that the separate tensile and compressive stress segments around the hole boundary converge to constant stress regions of different values, when the optimal shape is achieved. The optimal hole shapes produce significant reductions in peak stress for all regions around the hole boundary, as compared to typical non-optimal circular holes.

A sample analysis is given below. **Figure 1a** shows a loaded plate containing an initial slotted hole of aspect ratio of  $h:w = 3:1$  (with  $h = 6r$ ) and which is inclined at  $\theta = 16^\circ$  to the vertical. The optimal hole was constrained by a bounding constraint line also inclined at  $\theta = 16^\circ$ , and is shown in **Figure 1b**. A comparison of corresponding stress is given in **Figure 1c**, where it can be seen that the peak stresses have been significantly reduced and rendered uniform in each of the four regions.

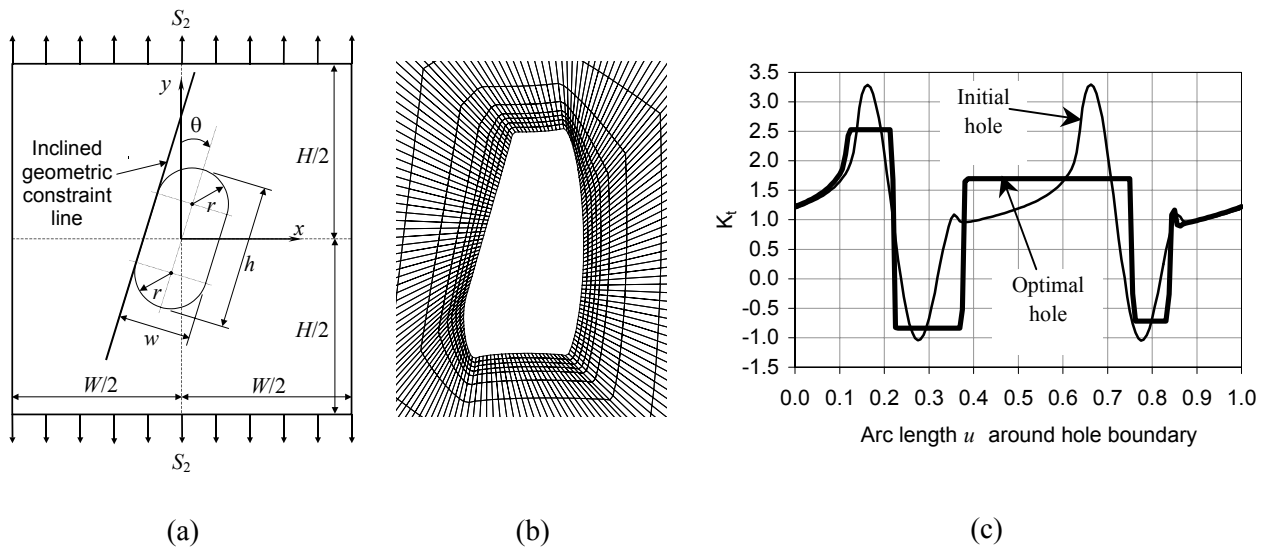


Figure 1. Optimisation of geometrically constraint slotted hole in uniaxially loaded rectangular plate: (a) geometry and loading, (b) optimal shape, and (c) comparison of stress results around hole boundary.

#### 8.4.6 Risk and Reliability Assessment Methods (K. Watters and P. White, DSTO)

A risk analysis has been carried out on an F-111 wing. The C-model wings on the Australian F-111 fleet have been replaced during the last 2 years with ex-USAF D and F-model wings. This was because a previous full-scale fatigue test had shown the C-model wings to have insufficient life for the RAAF requirement. It was anticipated that the D and F-model wings would have longer life and this is being demonstrated currently by another full-scale fatigue test. However, pending the result of that test, it was decided to get an estimate of the likely extra life by performing a comparative risk assessment of the new and old wings.

The key factor in the fatigue of the wings is the build quality of the lower skin-to-spar fastener holes. The determining parameters of build quality were the surface roughness and interference level of the holes. The build quality parameters of the C-model test wing were measured and related to the crack starting flaw size and growth at the holes. This database was obtained from an extensive teardown inspection of the test wing and fractographic analysis of the cracks. The build quality statistics of the replacement D and F-model wings were obtained by taking 5 wings from the fleet and removing 60 fasteners from each one to determine roughness and interference. These build quality statistics of the replacement wings could then be combined with the relationships to crack initiation and growth established from the C-model wing teardown to establish the life of the replacement wings.

A Monte Carlo approach was used to simulate wings matching the build quality statistics of the replacement wings, and the lives of the simulated wings were calculated by a simple log-linear model of crack growth from a starting flaw. The analysis was limited by the inability to show a good correlation between the build quality roughness parameter and the starting flaw size. However, the effect of interference on crack growth rate was able to be modelled and demonstrated some life increase for the replacement wings.

#### 8.4.7 Shape optimisation for life extension of holes in lower wing stiffeners in P-3C Aircraft (R. Evans, R. Braemar and M. Heller)

Fatigue life extension enhancements to maintain aircraft availability may be required for some circular holes in lower wing skin stiffeners of P-3C Orion aircraft, in service with the RAAF. One option is to rework the holes to precise optimal shapes to minimise the peak stresses, thereby increasing the fatigue life.

In this investigation, optimal rework hole shapes for the critical region have been determined, [2]. DSTO computer codes are utilised in conjunction with commercial finite element software. Full three-dimensional analyses are conducted (see **Figure 2**) and it is found that the optimal holes can provide a peak stress reduction of 40%, as compared to the initial holes.

Typical stress distributions around the optimal hole boundaries and the corresponding shapes are shown in **Figure 3a** and **3b** respectively. If the optimal shapes were implemented, they are expected to lead to a more than sufficient life extension via reduced crack growth rates, to meet any likely planned P-3C aircraft withdrawal date requirement.

At this stage the 2:1 aspect ratio optimal hole is recommended for further investigation. Work currently underway involves a demonstration of efficient *in situ* manufacturing, to provide the RAAF with a practical and cost effective repair option.

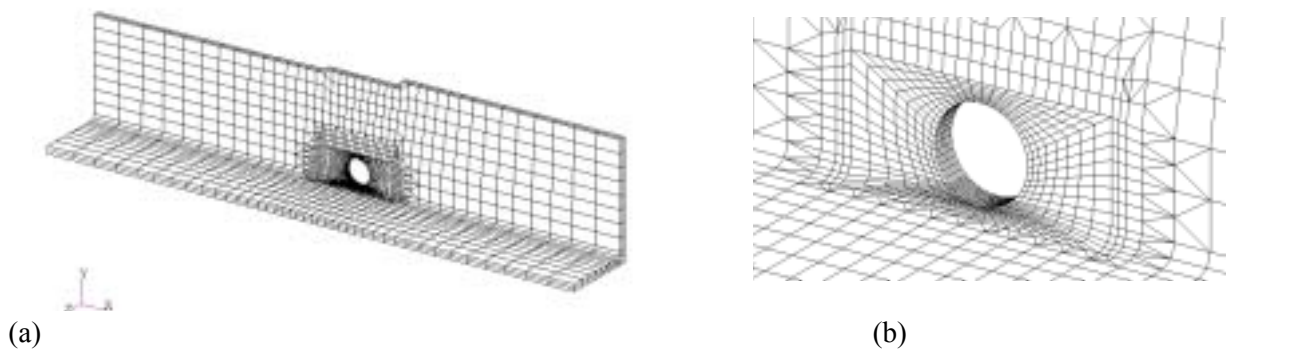


**Figure 2.** Typical finite element model for initial circular hole: (a) overall, (b) local detail around hole.

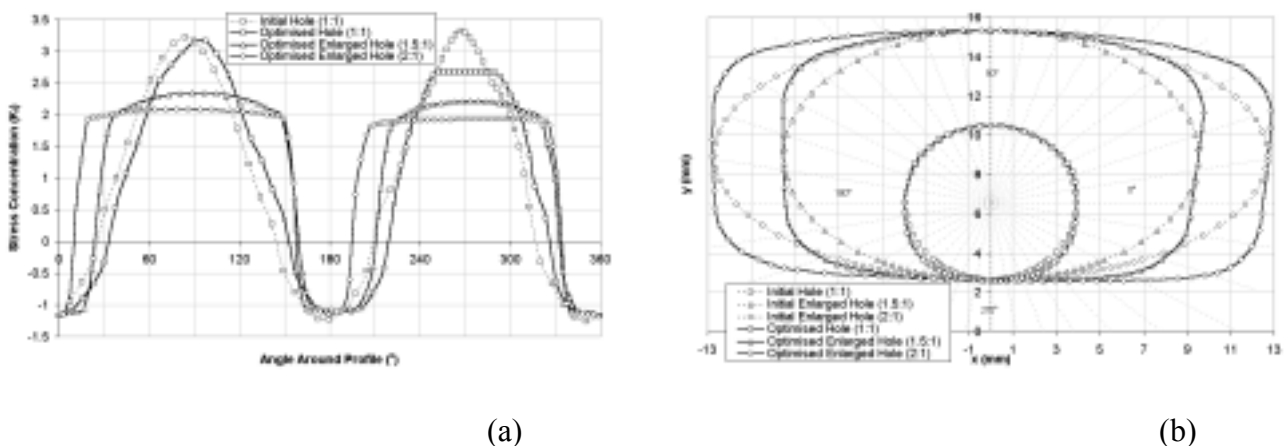


**Figure 3.** Comparison of initial circular hole and standard optimal holes for various aspect ratios, (a)  $K_t$  around hole boundary, (b) hole shapes.

#### 8.4.8 Computational shape optimization with stress robustness constraints (*R. Braemar, M. McDonald, and M. Heller, DSTO*)

An important aspect to consider when determining optimal shapes for airframe stress concentrators is the robustness of the shape to varying conditions. Conditions that can vary include: magnitude and orientation of in-service loads; manufacture tolerances; build quality; and numerical modelling approximations and errors. For a typical scenario where a shape is optimised using an idealized set of nominal conditions it can be expected that any perturbation from these nominal conditions is likely to result in undesirable sub-optimal performance, increasing the peak stress.

Earlier DSTO research was undertaken using 2D FE modelling [3], to determine optimal hole shapes, which are robust to variations in the direction of the remote loading (analogous to manufacture misalignment of the rework). Recently, that prior work has been continued and extended to produce optimal shapes allowing for the 3D effect of through thickness stress variation, [4].

The work has also been extended to allow for the minimisation of multiple stress peaks around the hole boundary, optimised for with single or multiple load cases. Sample results are given below. **Figure 4** shows the local FE model for 3D robustness optimisation analysis where the initial hole in is in a uniaxially loaded plate. The 3D model was initially optimised with a non-robust analysis using a axial load applied at  $0^\circ$  and then with a robust analysis where the load was varied incrementally from  $-5^\circ$  to  $+5^\circ$ .

The profiles and stresses resulting from this analysis are shown in **Figure 5**. The non-robust model experiences an increase in the peak  $K_t$  from 1.83 to 2.27 upon application of the  $\alpha = 5^\circ$  loading, while the robust case had a consistent peak  $K_t$  of 1.94 (for any angle in the design range from  $-5^\circ$  to  $+5^\circ$ ). For all test cases considered the key result is that, unlike standard optimisation based on a fixed load condition, the robust method renders the peak stress minimal and constant over a range of load orientations. This is important for practical application of shape optimisation methods, as there will always be some degree of variability in the dominant load direction.

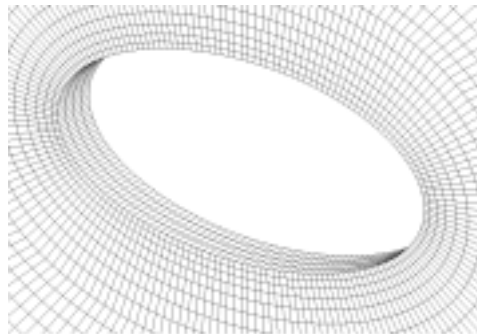


**Figure 4.** Local detail of FE model for 3D robustness optimisation analysis, for initial hole in a large uniaxially loaded plate.

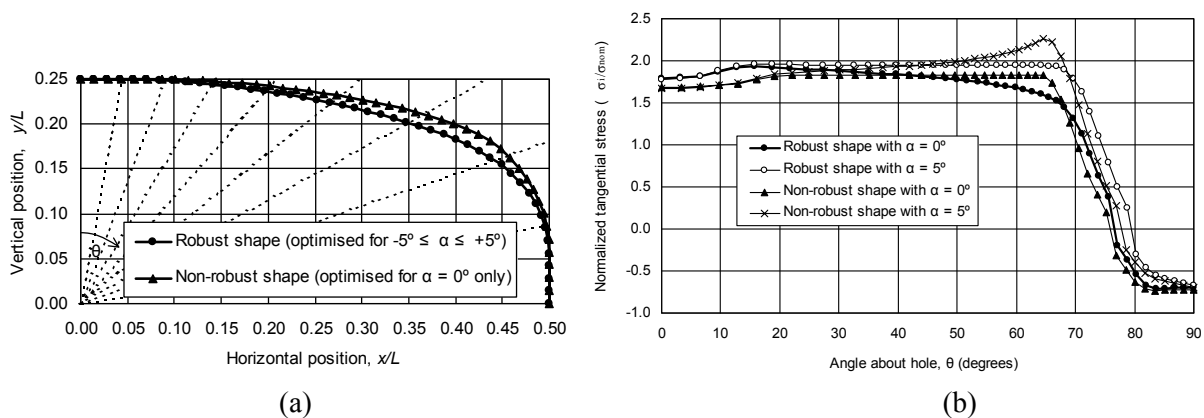


**Figure 5.** Robust stress minimization results using quarter symmetry, showing: (a) optimal hole shapes; (b) stress distributions about the hole boundaries for both robust and non-robust 3D cases when the load angle is at the nominal orientation of  $\alpha = 0^\circ$  and  $\alpha = 5^\circ$ .



#### 8.4.9 Stress analysis of near optimal surface notches in 3D plates (R. Wescott, B. Semple, and M. Heller, DSTO)

DSTO [5] have developed a method of using 2D optimal notch shapes to create near optimal surface notches with various depth and aspect ratios in uniaxially loaded 3D plates. Axisymmetric and elongated surface notches are created by rotating 2D optimal notch shapes about two types of fixed axes, a major reason being to enable the surface notches to be manufactured by elementary methods. **Figure 6** shows the notation for the bounding shape of the typical surface notches. Stresses in the surface notches are determined using 3D finite element analyses. Axisymmetric notches show small reductions in local peak stress relative to spherical notches with the same bounding dimensions. Local peak stresses in elongated notches are reduced by up to 26 % relative to comparable spherical notches. In damage removal applications a significant advantage of both near-optimal notch types, over spherical notches, is that they allow more material to be extracted for the same in-plane notch size, and maximum notch depth. **Figure 7** shows a comparison of stresses for spherical and near optimal axisymmetric notches. Reference [5] presents transferable normalised co-ordinates for plates of various notch depths.

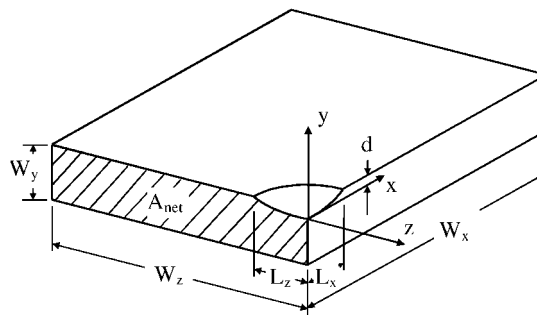


**Figure 6:** Geometry of plate and notation used for surface notches, using quarter symmetry.

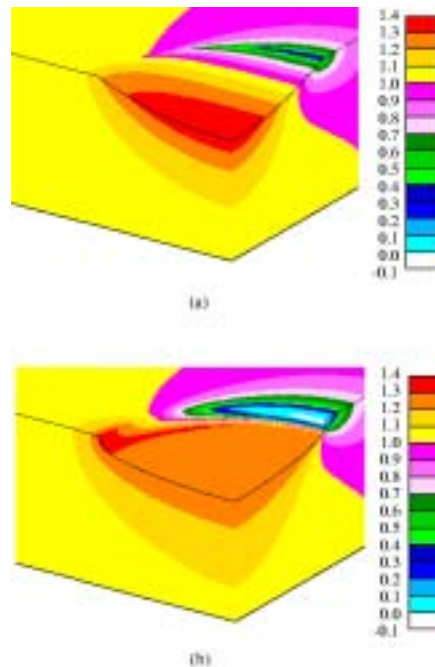


**Figure 7:** Normalised maximum principal stress for surface notches (quarter symmetry) with  $L_x/d=5$  and  $W_y/d=5$  (a) spherical and (b) nominal axisymmetric.

## References

1. Waldman, W. and Heller, M. (2005): Shape optimisation of holes for multi-peak stress minimisation. *Proceedings of the 4<sup>th</sup> Australasian Congress on Applied Mechanics*, Y.M. Xie, A. P Mouritz, A. Afahi Khatibi, C. Gardiner, W.K Chiu (editors), 14-16 February, Melbourne, Australia, pp. 189 –195.
2. Evans, R., Braemar, R., and Heller, M. (2005): P-3C Aircraft life extension via shape optimisation of holes in lower wing skin stiffeners. *Proceedings of the 4<sup>th</sup> Australasian Congress on Applied Mechanics*, Y. M. Xie, A. P Mouritz, A. Afahi Khatibi, C. Gardiner, W.K Chiu (editors), 14-16 February, Melbourne, Australia, pp. 801 –806.
3. McDonald, M., and Heller, M., (2004) ‘Robust shape optimisation of notches for fatigue life extension, *Journal of Structural and Multidisciplinary Optimisation*, **28**, pp. 55-68.
4. Braemar, R., McDonald, M., and Heller, M. (2005): Computational shape optimisation with stress robustness constraints. *Proceedings of the 4<sup>th</sup> Australasian Congress on Applied Mechanics*, Y. M. Xie, A. P Mouritz, A. Afahi Khatibi, C. Gardiner, W.K Chiu (editors), 14-16 February, Melbourne, Australia, pp. 673-678.
5. Wescott, R., Semple, B., and Heller, M. (2005): Stress analysis of near optimal surface notches in 3D Plates’, *Accepted for publication in Journal of Mechanical Design - ASME*.

#### **8.4.10 Effects of Corrosion Prevention Compounds on the Fatigue Life of a Typical Transport Aircraft Skin Splice (S. Russo, Bob. Clark<sup>a</sup>, P. Nolan<sup>a</sup>, B.R.W. Hinton, K. Shankar<sup>a</sup>, DSTO, <sup>a</sup>School of Aerospace and Mechanical Engineering, ADFA, Canberra, Australia)**

A collaborative program between DSTO and the Australian Defence Force Academy (ADFA) investigated a typical joint on the B737 Airborne Early Warning and Control (AEWAC) aircraft which has a history of corrosion/fatigue problems, and where CPCs potentially could be used to prevent corrosion from occurring. The specimen was manufactured from 2024-T3 alcad material and consisted of a lap splice representative of a joint on the forward fuselage of the aircraft. Load characteristics in fatigue testing were similar to those produced by pressurisation stresses at this location.

Fatigue tests indicated that the introduction of a CPC to the faying surfaces of the lap-joint specimens resulted in a reduction in fatigue life of over 50% at a load of 86MPa. This reduction was evident under both dry and humid conditions. The location of the fatigue crack initiation sites (FCIS) was also effected by the presence of a CPC. The introduction of the CPC to the faying surface resulted in a shift of the FCIS from the faying surface to within the bore or edge of the countersink hole and towards the minimum net section of the specimen. In contrast, the majority of specimens tested in the absence of a CPC contained FCIS at the faying surface remote from the minimum net section.

Fractographic examination of the specimens tested in dry conditions without the application of a CPC following failure revealed the presence of fretting damage surrounding the fatigue crack initiation sites. There was minimal fretting damage on specimens tested with CPCs. In the majority of cases, the cause of fatigue cracks was associated with fretting corrosion. Scanning Electron Microscopy also revealed the existence of fretting corrosion product on the fracture surface of specimens that had been treated with a CPC. This was not the case for specimen tested in the absence of a CPC. Holographic interferometry analysis revealed that the fatigue crack initiation and propagation times were reduced by the application of a CPC.

The reduction in fatigue life due to the application of CPC is thought to be associated with a number of factors including a change in the proportion of load transferred through the joint by friction and the transportation of fretting debris to the crack tip.

Further testing has commenced on examining the effect of corrosion on the fatigue characteristics of the joint and whether the application of a CPC to the corroded joint will be beneficial.

#### 8.4.11 Fractographic study of 7xxx Aluminium alloys (P. White, DSTO)

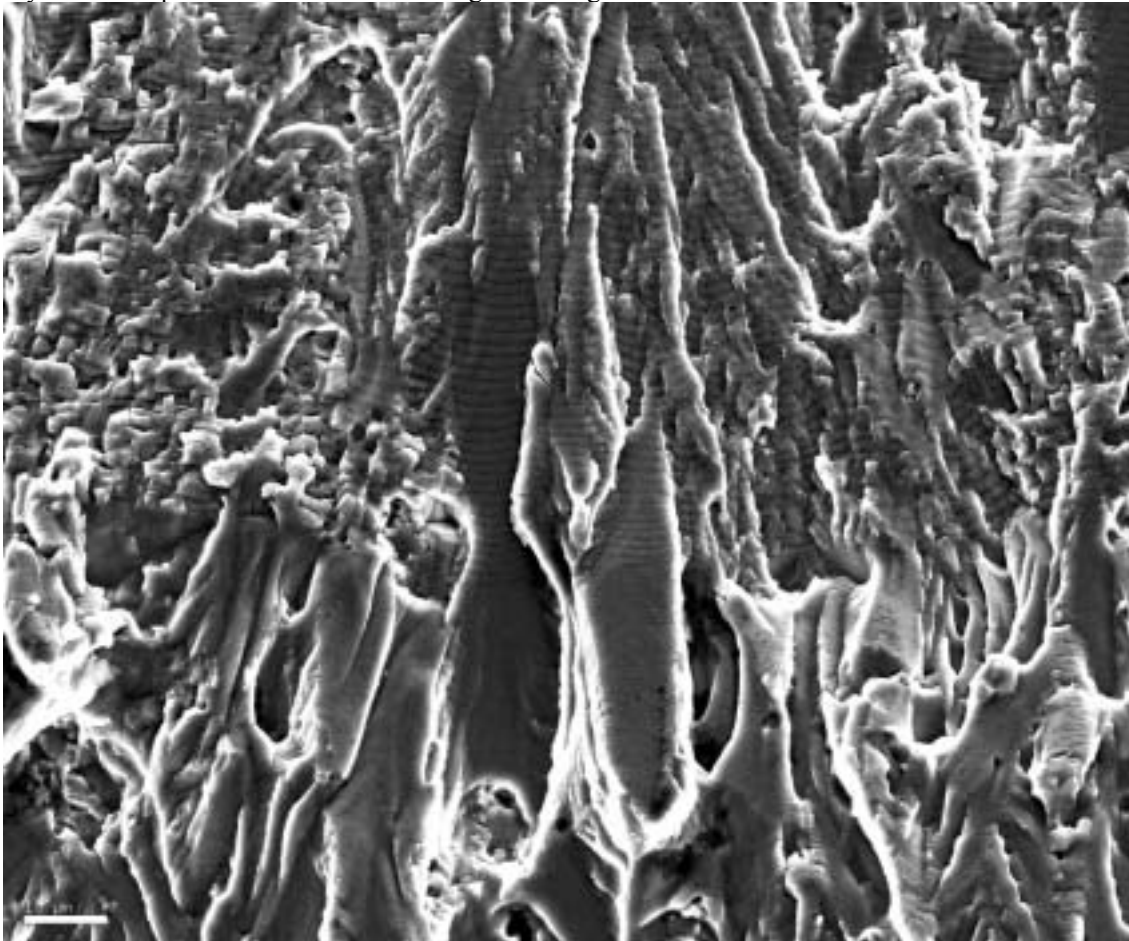
Initial study of the fractography of a series of aircraft aluminium specimens is focussed on developing a better understanding of the factors which control crack growth in these alloys.

In a series using constant amplitude loading with varying levels of compression we can see a number of interesting features.

The first few slides show a surface produced by a single repeated flight with a large ground air ground (GAG) cycle typical of a transport aircraft – this cycle produces distinct markings. Constant amplitude marker bands were inserted between each 500 flights. In the first slide the material is 7075 T6, 3mm thick sheet; in the rest, the material is 7050 T7451 Plate.

##### Slide 1.

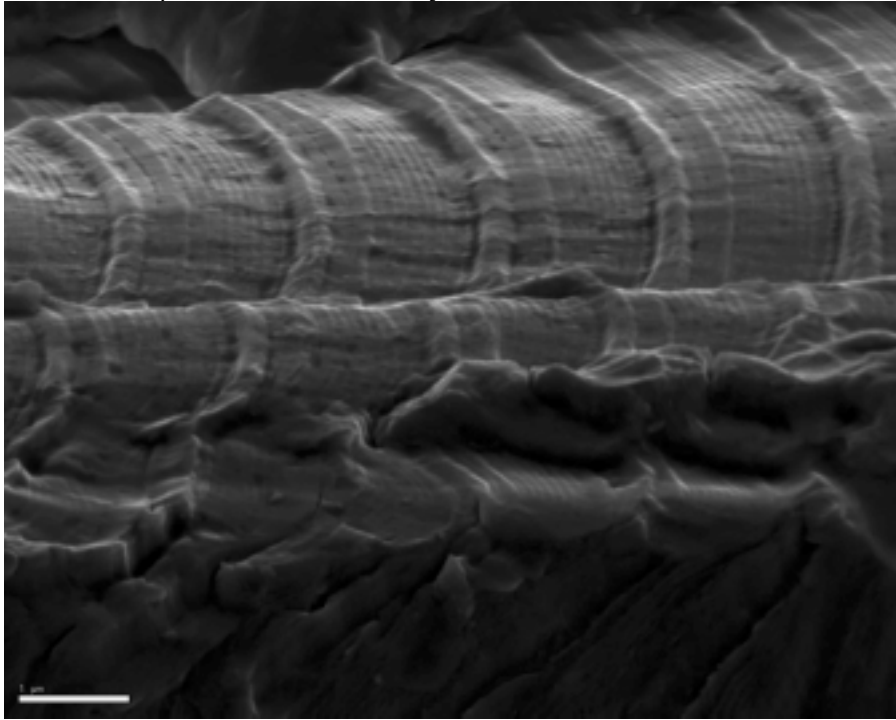
The crack is growing from top to bottom. A constant amplitude marker band shows the difference in growth between flight loading and constant amplitude. The flight loading produces a rougher but shallower surface compared with the CA surface in which the surface is smoother but with deeper holes/chasms. It is thought that this is because the large compression in the GAG cycle causes fissures which leading to break up of the surface. This keeps the flight loading in essentially a constant plane whereas the CA loading can diverge with numerous crack fronts.



*Slide 1*

**Slide 2.** (Same sequence as Slide 1, but in 7050-T7451 plate)

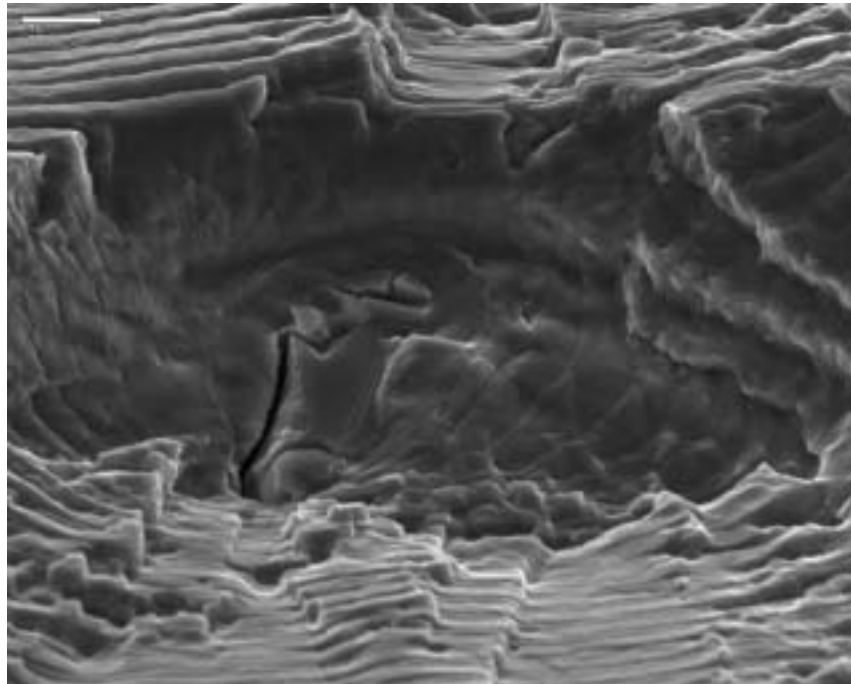
This shows the flight loading effect on the fracture surface in profile. Clearly seen is the large slip occurring between each flight as a result of the compression from the GAG cycle.



*Slide 2*

**Slide 3.**

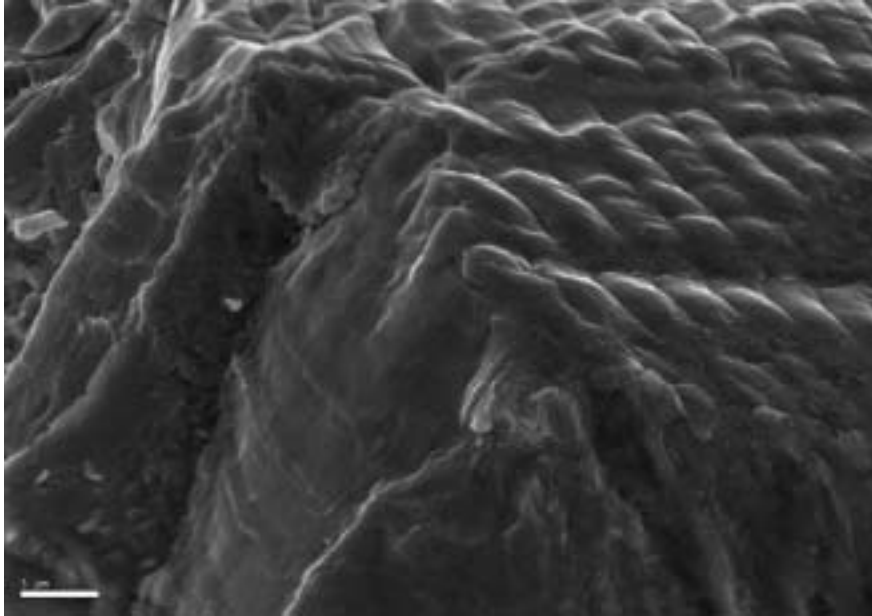
In this instance, a segment has been pulled away when it interacts with an inclusion, revealing the depth of the formed striations/flights. The slip bands and fissures caused link up in a smooth fashion between the flights and those at different orientations around the inclusion.



*Slide 3*

**Slide 4**

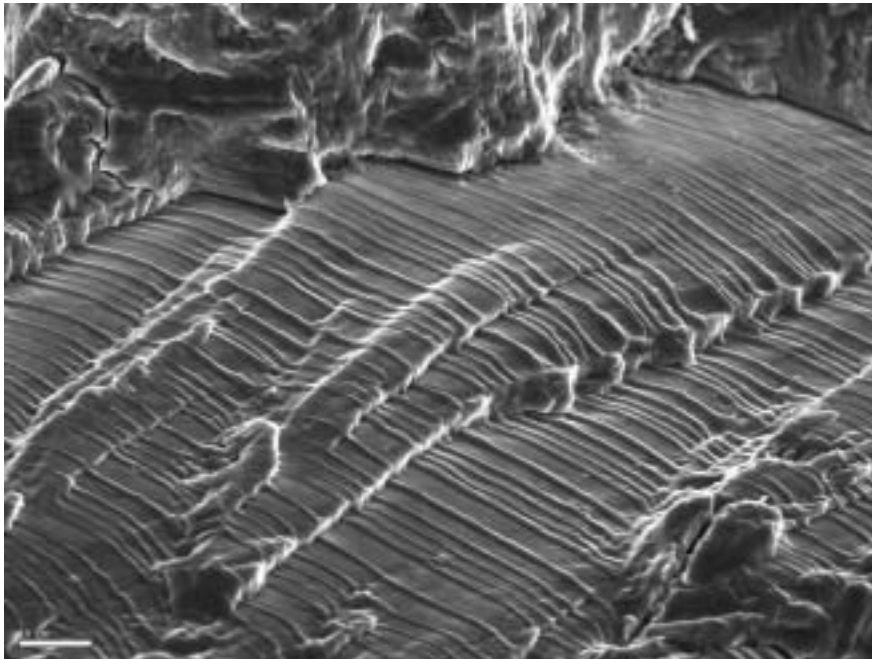
The GAG cycle produces fissures which lead to cracks which subsequently grow during the remaining loads in the flight. There is a high correlation between the growth in the fissures between flights and the growth down the fissures. This ensures the crack front remains coherent and does not fragment into many independent cracks.



*Slide 4*

**Slide 5**

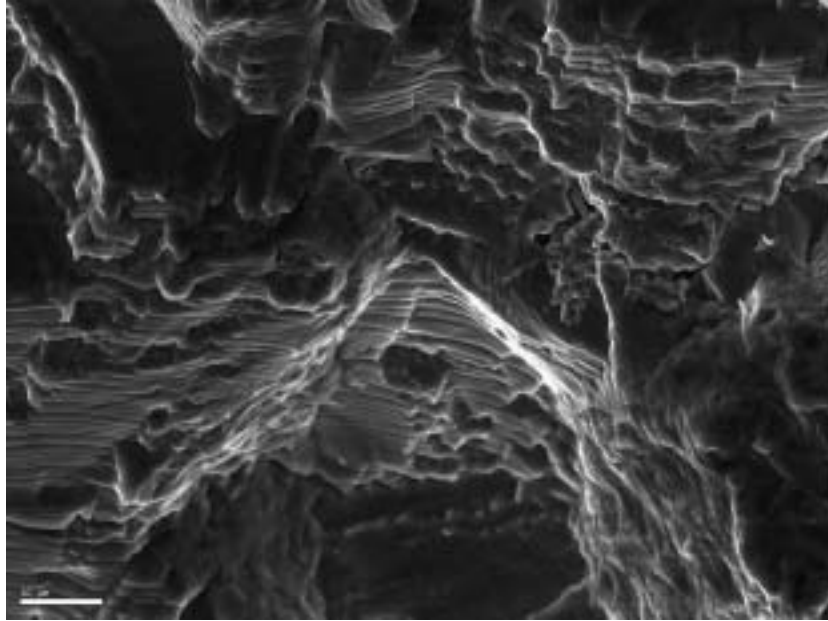
This shows the results of a simple constant amplitude sequence interspersed with large compression loads. The maximum stress is constant for the entire sequence. This shows the ridges produced as a result of the large compression cycle. The surface on the opposite half has a dent and fissure where the ridge occurs. The larger ridges correspond with more intense fissures.



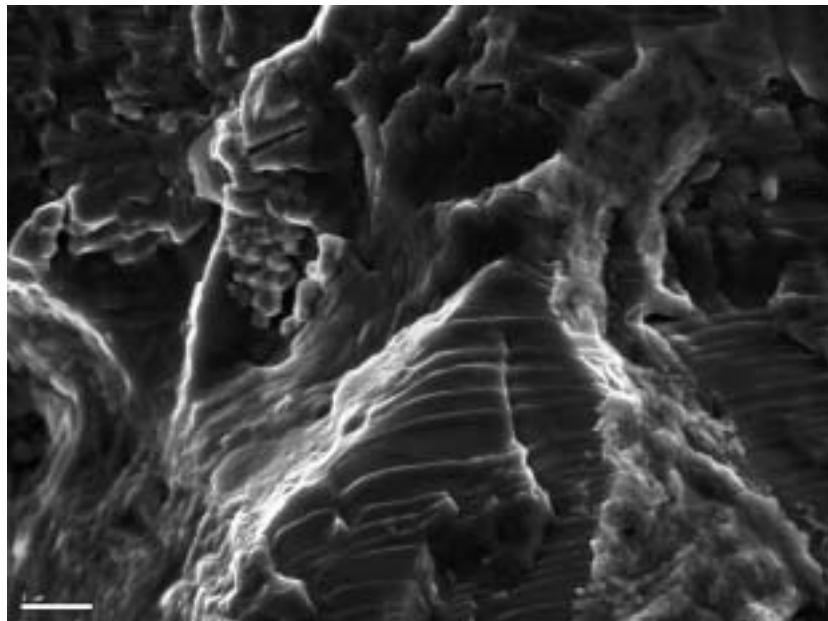
*Slide 5*

**Slides 6 and 7**

Shows matching pairs of each half of the coupon. Dents occur on one half match to ridges on the other half.



**Slide 6**



**Slide 7**

#### 8.4.12 Comparative Vacuum Monitoring (CVM™) A tool for Structural Health Monitoring of aircraft (D P Barton, Structural Monitoring Systems Ltd, Australia)

The Comparative Vacuum Monitoring (CVM™) technology is able to detect flaws in metals and composites by monitoring the stability of a vacuum level in a confined volume. The confined volume can be produced in the structure under test, or by applying a sensor with micro-channels on its surface to contain the vacuum. Structural Monitoring Systems Ltd is currently working with both Airbus and Boeing to validate the technology for use on aircraft.

The company's integral CVM™ lap joint sensors (Figure 1) have been used by Airbus during qualification tests of GLARE®, a lightweight aluminium, glass and epoxy laminate, and provided vital information on the performance characteristics. The accuracy of information provided in real time by the CVM™ sensors on crack initiation from the rivet holes within the lap joints has not been achieved before (Figure 2). A substantial proportion of the new A380, officially rolled out in January 2005, is constructed of the GLARE® material.

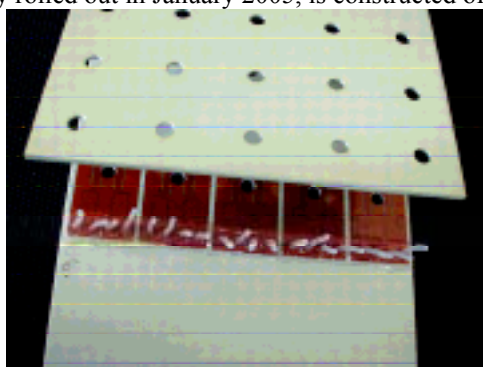


*Figure 1. Standard lap-joint test coupon configuration (from 1.)*

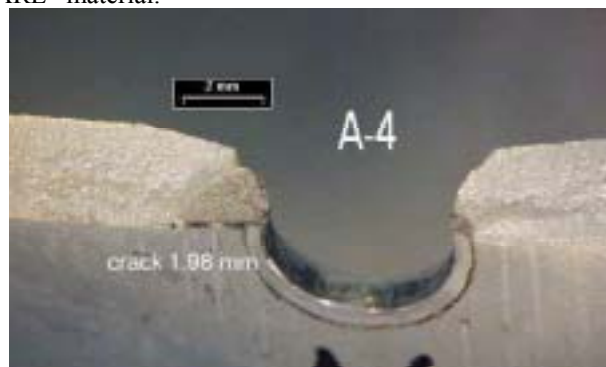


*Figure 2. Fracture surface of test coupon once following crack detection (from 1.)*

SMS is working with Airbus<sup>1</sup> and divisions of EADS<sup>2</sup> in a series of benchmarking and environmental robustness and durability trials of the CVM™ surface sensors. These trials are designed to test the limitations of CVM™ sensors and their ability to meet the requirements for crack detection whilst surviving in harsh aviation environments. The CVM™ technology is being used in a number of laboratory coupon, component and full scale fatigue test programs within the two organisations.



*Figure 3. Surface sensor on a concave curve test coupon (from 1.)*



*Figure 4. TANGO barrel test facility (from 1.)*



SMS has commenced a program with Boeing, Airline Operators and the FAA to have the CVM™ technology entered into the NDI Standard Practices Manual (SPM) for Boeing Commercial Airplanes. Once published in the Boeing SPM, the technology will be available for use by operators of Boeing Commercial Airplanes on their aircraft. Sensors have been flying in the tail cone (Figure 5) and baggage compartment of a commercial DC-9 aircraft for over a year as a precursor to this program.



**Figure 5.** Surface sensors installed in the tail cone of a commercial DC-9 aircraft.

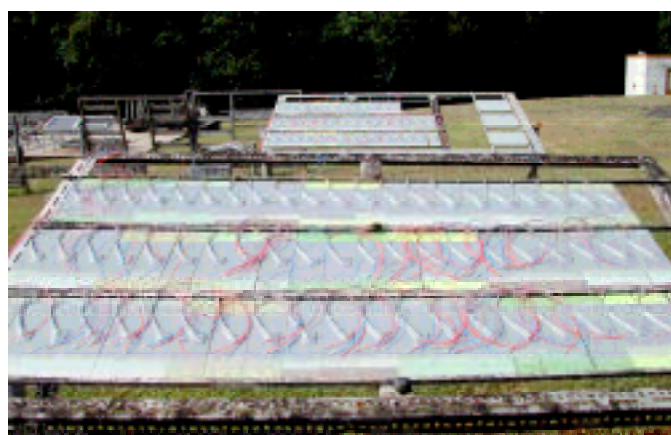


**Figure 6.** Specimens in long term environmental trial on exposure racks in coastal, tropical environment (courtesy of DSTO)

The company is working closely with the Australian Defence Science and Technology Organisation (DSTO) on a two year intensive environmental durability trial of CVM™ surface sensors involving in excess of 250 test coupons. This trial will significantly extend the knowledge of the robustness and functionality of the sensors after exposure to temperature cycling, contamination and hot/wet conditions (Figure 6.). The cooperation with the Australian Defence Force extends to a trial program on RAAF P-3 Orion maritime patrol aircraft and a commercial program on the Army's Blackhawk helicopters.



**Figure 7.** Sensor used to monitor crack growth in the US Navy H-53 helicopter

SMS is working with a number of other military fleet operators to validate the technology for use on their fleets of aircraft. CVM™ sensors (Figure 7) have successfully detected consecutive crack growth three times over a two year period on a US Navy H-53 helicopter based at Patuxent River Naval Base. The SMS UK operation is working with the UK Ministry of Defence for trial and commercial programs on military aircraft.

<sup>1</sup> Stehmeier, H. and Speckmann, H. (2004) Comparative Vacuum Monitoring (CVM), Monitoring of fatigue cracking in aircraft structures, Proceedings 2<sup>nd</sup> European Workshop on Structural Health Monitoring, Munich, Germany.

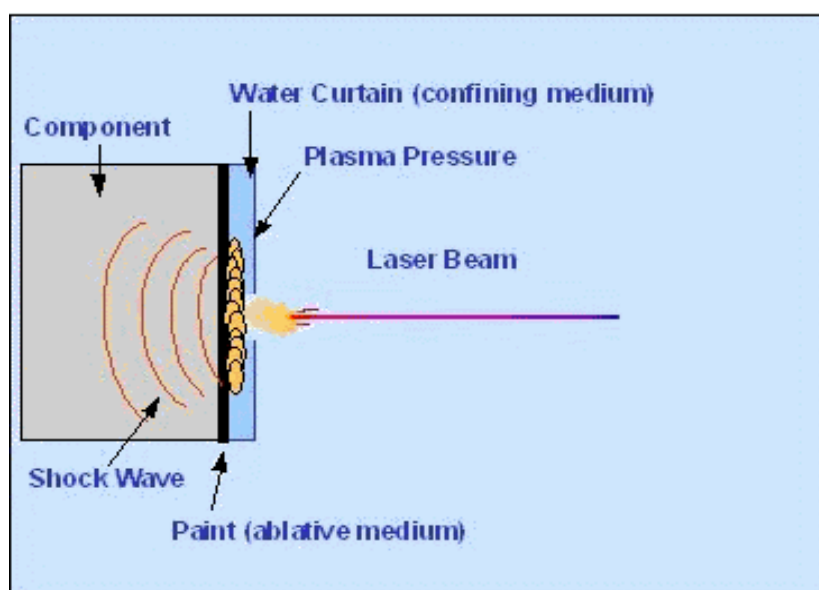
<sup>2</sup> Petitjean, B., Simonet, D., Choffy, J-P. and Barut, S. (2004) SHM technology benchmark for damage detection, Proceedings 2<sup>nd</sup> European Workshop on Structural Health Monitoring, Munich, Germany.

### 8.4.13 Laser Shock Peening of Aluminium alloys (Q Liu, DSTO)

#### Background

Laser shock peening (LSP) technology is a new and promising surface treatment method. Research work shows that this technology can greatly improve the fatigue life of a material or a component. However, DSTO provided a report in ICAF 2003 of work which identified a potential issue which could result in LSP failing to achieve the expected life extension result. This was associated with high laser power densities causing internal cracking in the specimens. The following represents an update on the initial work.

Laser shock peening or processing (LSP) has a number of advantages over conventional shot peening techniques. It can create a deeper residual compressive stress - up to 1.5 mm in the case of Al alloys whereas the conventional impact method only provides about 250  $\mu\text{m}$  deep below the treated surface. In addition, there is very little or no modification on the original surface profile. Even very thin sections can be laser processed without deformation of the part, and in some component geometries which feature small holes and small slots, it is very difficult for conventional technology such as shot peening or cold expansion to be used due to limited accessibility, whereas LSP can easily reach these areas by using an optical fibre as a delivery system. In addition, the laser radiation is highly controllable and the process is readily amenable to automation. Therefore, it is expected that LSP technology will become an important method for increasing fatigue life in developing modern aircraft, and repairing and maintaining “aging” aircraft. LSP has been successfully applied to increase performance of materials and structures by increasing fatigue life, reducing fretting fatigue, enhancing resistance to corrosion and increasing foreign object damage resistance etc.



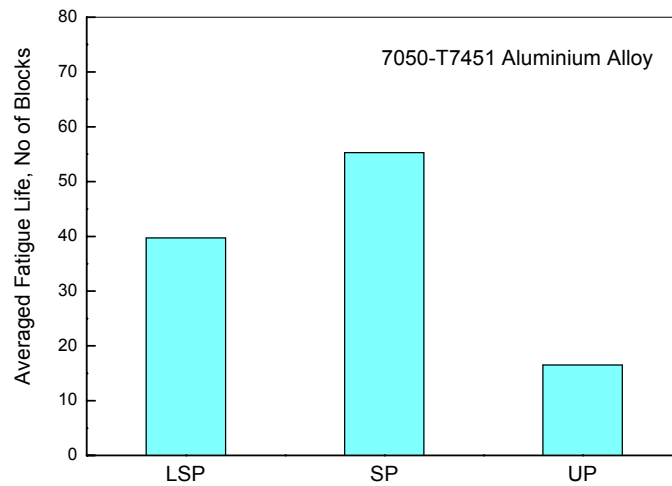
Schematic of Laser Shock Peening Process

DSTO experiments designed to identify any technological risks associated with use of LSP in fatigue-critical aluminium aircraft structure revealed that, as is common with all life extension processing, there are some circumstances where problems might arise, preventing achievement of full life extension.

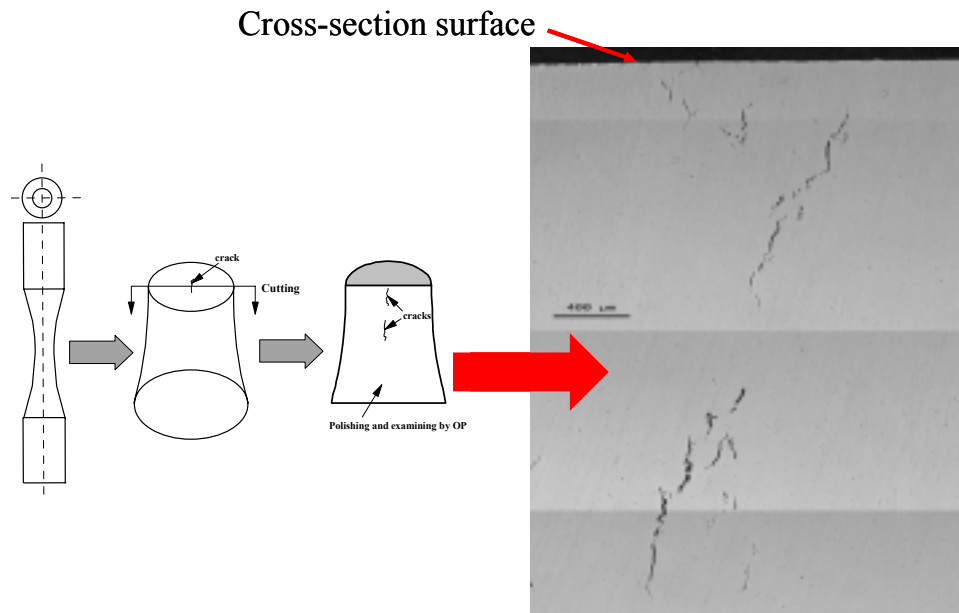
#### Summary of Results

DSTO tested 7050-T7451 aluminium alloy specimens, which were treated by laser shock peening (LSP). In this initial investigation on laser shock peening, the usual large life extension was not observed; the averaged LSP fatigue life was lower than those from traditional glass bead peening at the same applied peak stress. An example is shown in Fig.1, where the applied peak stress was 390 MPa.

Metallurgical examination revealed that large cracks existed inside the specimen, and was associated with the failure crack.

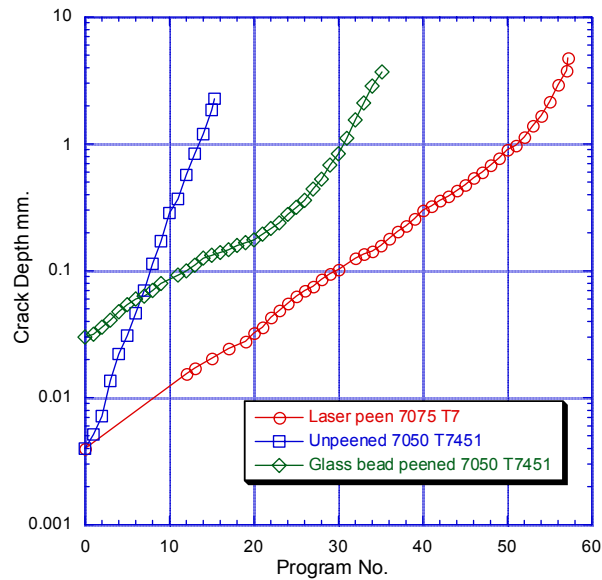


**Figure 1:** Comparison of fatigue life of LSP (laser shock peened), SP (glass bead peened) and UP (unpeened) 7050 specimens under spectrum loading at the applied stress of 390MPa



**Figure 2:** Internal cracking in specimen revealed by sectioning

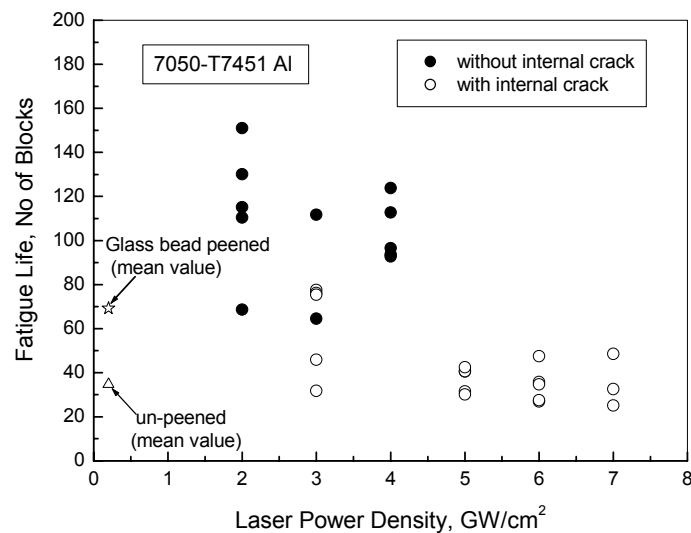
In cases where no internal cracking occurred during LSP, the experimental results (Fig. 3) demonstrated the effectiveness of LSP, with lower growth rates for cracks over a wide range of crack depths.



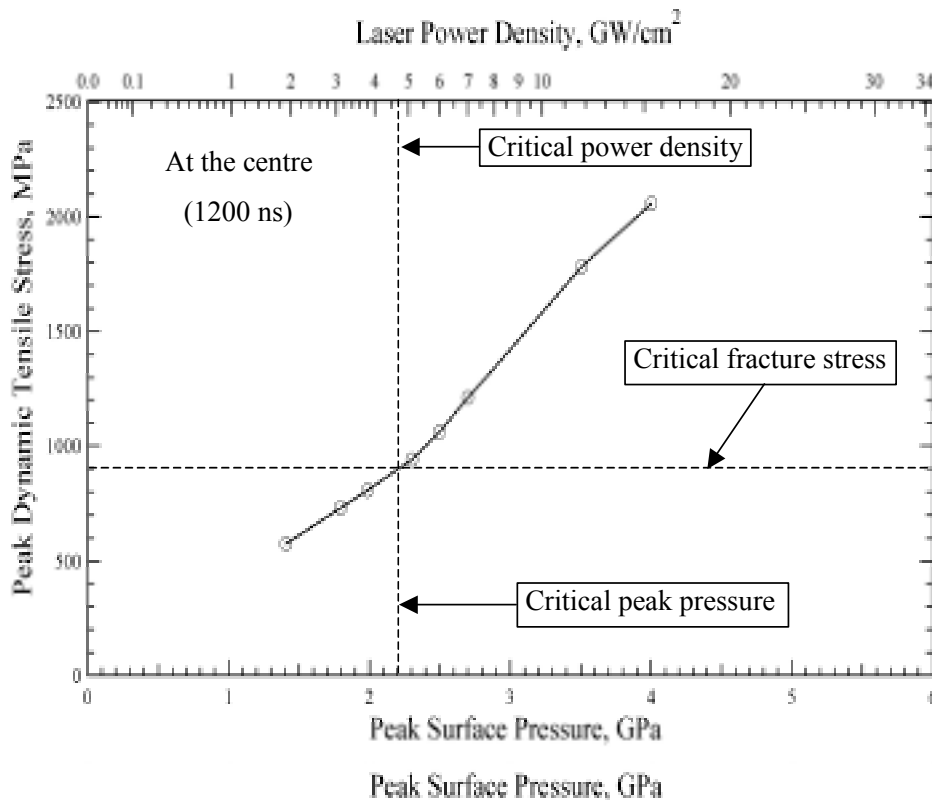
**Figure 3:** Crack growth in 7xxx series aluminium alloys for unpeened, glass bead peened and laser shock peened specimens.

Figure 4 shows the experimental results of the fatigue life as a function of laser power density. This result clearly shows that when the laser power density is approximately  $5 \text{ GW/cm}^2$  or higher, the fatigue life is dramatically reduced. Below this  $5 \text{ GW/cm}^2$  value, internal cracks were found at the  $3 \text{ GW/cm}^2$  level only in some of the tested specimens.

Figure 4 also shows clearly that when LSP does not lead to internal cracks, a 3 times increase in fatigue life can be achieved over un-peened specimens compared to 1.5 – 2 times for glass bead peened specimens at this high peak fatigue stress of 390 MPa. However, under “cracking” conditions the fatigue life is equal to or less than the un-peened mean value.



**Figure 4** Fatigue life as a function of laser power density on LSP 7050 Al specimens under spectrum loading at applied peak stress of 390MPa, where fatigue life of glass bead peened and un-peened (machined surface) 7050 Al specimens were included at the same loading conditions..



**Figure 5** The relationship between the predicted dynamic tensile stress during LSP, and peak surface pressure during the LSP process.

The exact causes of the internal crack at 3 GW/cm<sup>2</sup> level of laser power density are still being analysed. However, the experimental results indicated that the laser power density is one of main factors causing the internal cracking. Using the experimental results and numerical analysis, the critical condition was identified. Figure 5 shows the relationship between the predicted dynamic tensile stress and peak surface pressure during the LSP process. Clearly, when the pressure is higher than about 2.2GPa (corresponding to a laser power density of 4.65 GW/cm<sup>2</sup>), the local tensile stress can easily reach the critical tensile stress (~900 MPa), leading to the formation of an internal cracking. Put simply, the modelling suggests that the transition from uncracked to cracked in Fig. 4 matches the condition where the tensile stresses associated with overlapping shock tension waves equates to the material fracture strength.

In summary, the initial DSTO experimental results revealed a potentially significant technological risk in this investigation on 7050 aluminium alloy. The main factors promoting the internal cracking in LSP aluminium alloy are laser power (or intensity) and poor transverse material properties. The sample geometry may also play a certain role, but this has not been explored.

It is important to emphasise that although the internal cracking was found in the 7050-T7451 LSP specimens under test conditions aimed at revealing any technological risk factors, LSP clearly has great potential for fatigue life enhancement of components or structures if the process can avoid conditions which might promote internal cracking.

#### 8.4.14 Modelling of Defects and Damage in Aerospace Composite Structures (M. Scott, CRC-ACS)

##### 8.4.14.1 Overview

Defects in composite parts caused during manufacture, or damage induced in service, impose considerable costs on aircraft manufacturers and airlines. Analytical tools capable of accurately determining the effect on strength and stiffness of a given defect or damage can be used to reduce unnecessary repairs and scrapping of parts. Such tools could also be used to improve structural design practices and guidelines through the broad application of damage tolerance in design, improved structural repair techniques and manuals, and reduced testing for certification. This project is supported under agreements with Airbus Germany under the MODCOM program.

##### 8.4.14.2 Specific Goals

The first objective of this project was to develop a validated tool to predict the effects on mechanical properties of fibre waviness induced by manufacturing defects, fabric architecture and through-thickness reinforcement. The second objective was to develop a validated tool to predict impact damage and resulting residual strength for monolithic composite panels.

##### 8.4.14.3 Commentary

Prototype modelling tools have been developed to predict the stiffness and strength of composite laminates containing fibre waviness. To promote ease of use, all tools have been developed using Patran Command Language (PCL). The first tool developed is the Voxel Modelling Tool (VMT) for modelling the various waviness forms using a unit cell based approach. The second is the Analytical Stiffness and Strength Initial Simulation Tool (ASSIST) for modelling combined in-plane and out-of-plane fibre waviness. In addition, an interactive form of ASSIST, termed iASSIST, has been developed which allows users to interactively apply areas affected by fibre waviness to any pre-existing finite element model. A panel with a large waviness region defined using iASSIST is shown in Figure 1, along with the resulting buckling mode shape. Preliminary validation of the tools has been undertaken utilising previous experimental and theoretical results. Experimental data for composite laminates with surface cavities was also obtained. A modelling approach based on ASSIST was developed for this type of defect. Further work remains to complete validation and conduct parametric studies to determine the effect of fibre waviness on representative structures.

A prototype Impact Damage Assessment Tool (IDAT) has been developed to predict impact damage and resulting residual strength of composite structures. This tool is also written in PCL, and uses LS-Dyna for the impact and residual strength calculations. Currently, the tool can be used for the analysis of stiffened, flat or curved panels. These panels are generated parametrically by the tool and the impact conditions defined interactively by the user. The residual strength calculation is also automated, enabling the tool to be used by competent engineers without specialist training in LS-Dyna. Preliminary validation of IDAT has been undertaken using previous experimental data. Impact and residual strength testing on small specimens has also been performed for further validation. Parametric studies to investigate the effect of impact parameters on the damage behaviour and residual strength of representative composite structures remains to be conducted.

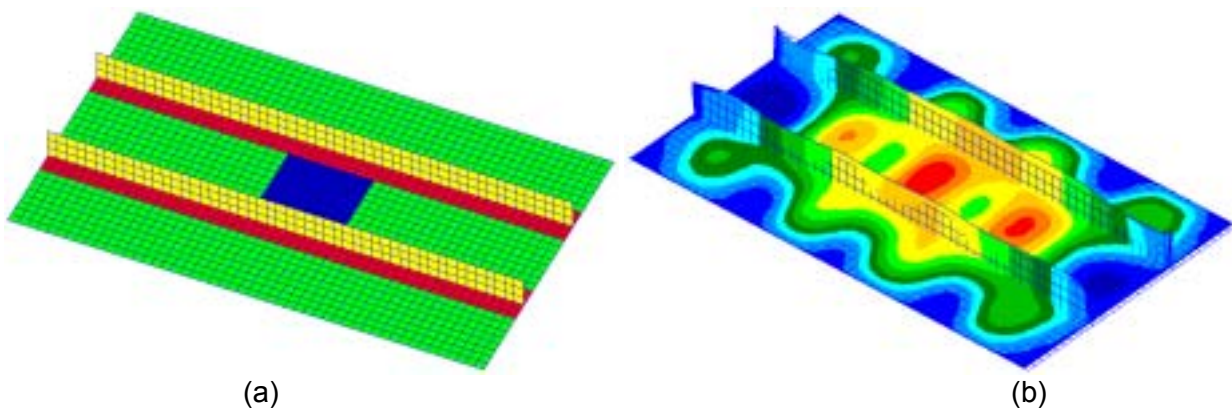


**Figure 1:** (a) Stiffened panel with patch of waviness defined in the skin and (b) the resulting compression buckling mode shape



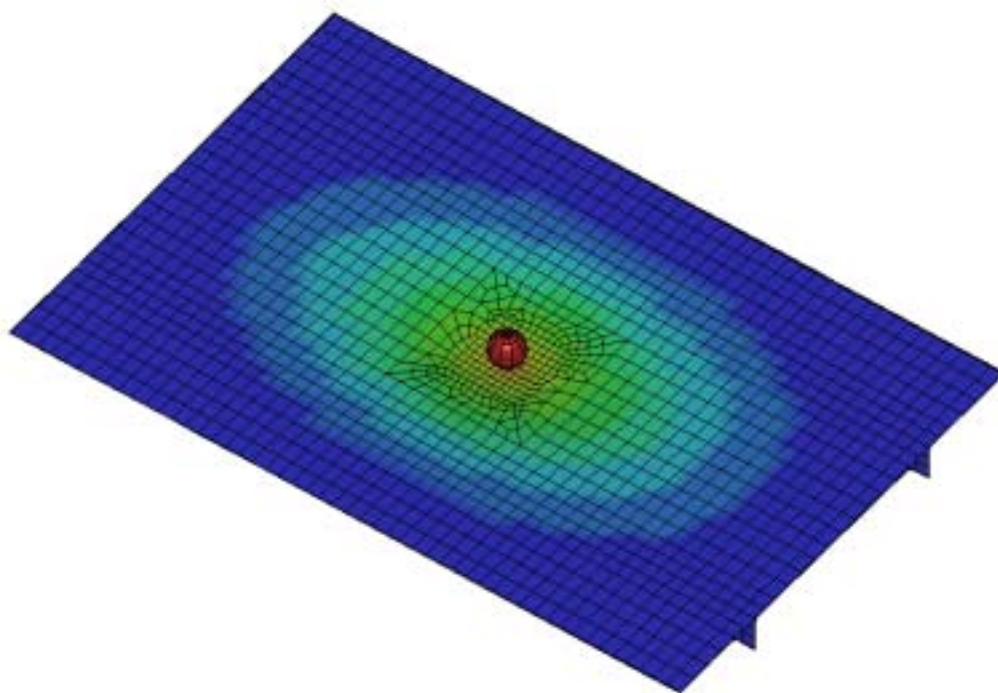


**Figure 2:** Impact damage simulation produced using IDAT

#### **8.4.15 Damage Resistance and Tolerance of Composite Replacement Panels (M. Scott, CRC-ACS)**

##### **8.4.15.1 Overview**

Previously, the CRC-ACS has developed a low-cost, high durability composite replacement panel technology. A demonstrator panel was designed and manufactured for the F-111 aircraft operated by the Australian Defence Force to replace a bonded aluminium honeycomb sandwich fuselage panel. Such aluminium panels suffer extensively from corrosion and are becoming difficult to replace as the aircraft is no longer supported by the manufacturer. However, one aspect that had not been considered was the comparative damage resistance and tolerance of the composite panels subject to impacts during fitment, operation and maintenance.

##### **8.4.15.2 Specific Goals**

The first objective of this project was to establish the damage resistance through test and analysis of typical aluminium honeycomb sandwich panels used on the F-111 aircraft. The second objective was to establish the damage resistance through test and analysis of the proposed hat stiffened composite replacement panels. The final objective was to establish the effect of impactor type and preload on the damage tolerance of the composite materials used in the replacement panels.

##### **8.4.15.3 Commentary**

Specimens representative of the aluminium panel and the composite replacement panel were impact tested at energies ranging between 1 J and 15 J with two hemispherical impactor tups to determine the damage resistance. It was found that the aluminium specimens suffered from significantly larger indentations and damage areas (see Figure 1). The specimens were then tested under compression to determine the damage tolerance.



Impact simulation of the aluminium sandwich specimens was conducted using a program called Sandmesh to generate the finite element model and LS-Dyna for the simulation (see Figure 2a). The model consisted of shell elements to represent the face-sheets, honeycomb core and adhesive. The comparison between the experimental and predicted damage depths and areas was excellent. Impact simulation of the composite specimens was conducted using Pam-Shock (see Figure 2b). Very good agreement was found with the experimental force-time histories, although the results were very sensitive to the boundary conditions applied. Excellent correlation with the delamination area was shown for a particular predicted damage level. These results provide a validated means to predict impact damage in other replacement panels developed in the future.

The effect of impactor shape on the damage characteristics of composite laminates was also investigated experimentally. Three impactors, all 12 mm in diameter, were used: hemispherical, ogival and conical.

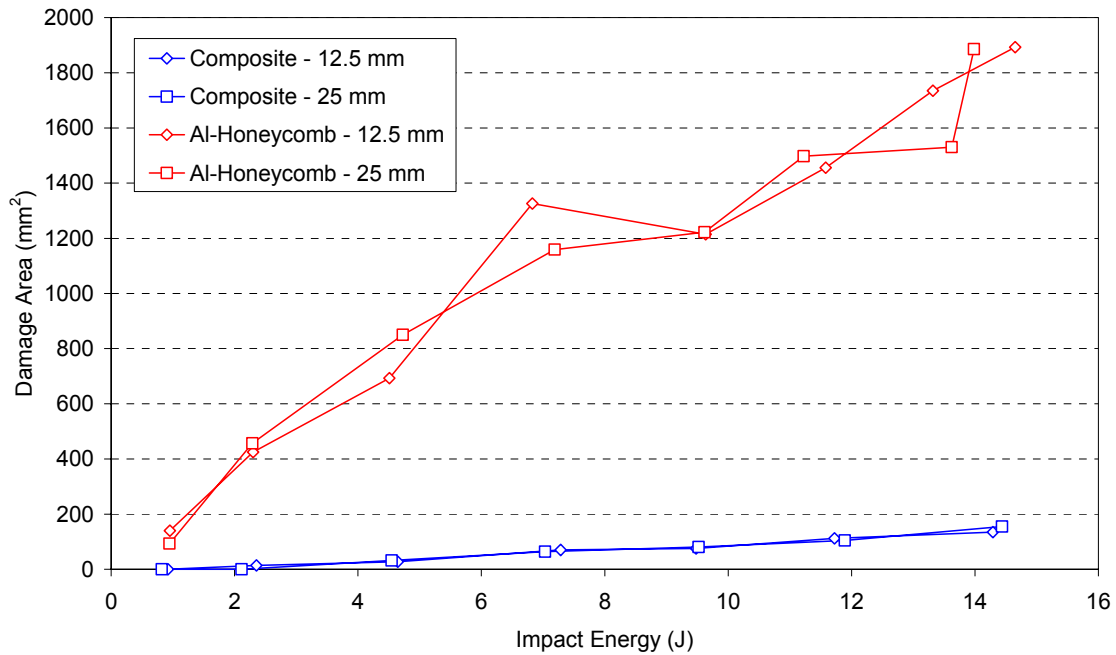


Figure 1: Variation in damage area for the composite and aluminium sandwich specimens

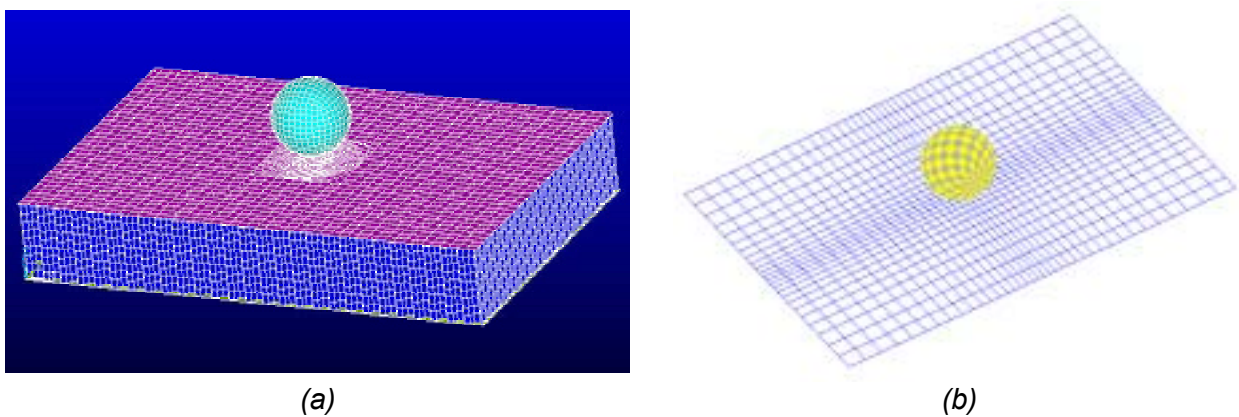


Figure 2: Finite element models for (a) aluminium sandwich and (b) composite impact specimens

## 8.5 FATIGUE INVESTIGATIONS IN NEW ZEALAND

### 8.5.1 C-130 Hercules: Fleetwide Cracking of Lower Wing Spar (M. L. Stevens, S. K. Campbell, P. C. Conor, G. Murphy, DTA, New Zealand)

In June 2003 The USAF and Lockheed issued an urgent Time Compliance Technical Order (TCTO) for the C-130 that mandated inspection of the lower wing spar near centre wing station 174 (CWS 174). Upon compliance with the required inspection the RNZAF discovered fatigue cracking in this area on all of its C-130 E\*/H aircraft.

The cracks were all relatively small (approx 0.09" max) and all discovered between CWS 168 and CWS 178. Of concern to the RNZAF was that signs of multiple site damage existed on some of the wings. Figure 1 shows schematics of the lower spar cap, indicating some of the cracking patterns observed. As can be seen from Figure 1 the crack initiation site and growth sequences varied from aircraft to aircraft. Although the cracking was most prevalent in the fastener holes located at the spar cap radius change, defects were also found at holes well away from the stress concentration.

At the time of discovery, the RNZAF were in the process of assessing its options to manage the remaining structural life of its C-130 fleet. Currently the RNZAF plans to operate its C-130 fleet for another 10-15 years. To achieve this, all RNZAF C-130s will undergo a series of refurbishments. In light of the cracking of the centre wing lower spar caps it was decided to repair the current cracking with a strap doubler as a temporary measure. The lower spar caps will be replaced as part of the upcoming refurbishment process.

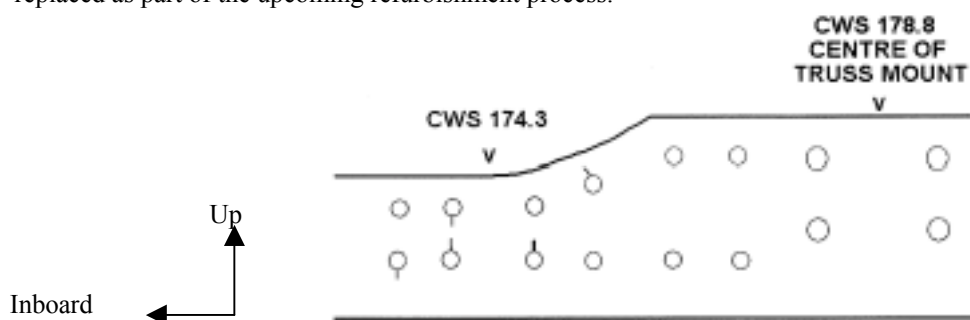


**Figure 1(a)** Example of cracking from Port wing of Aircraft 1

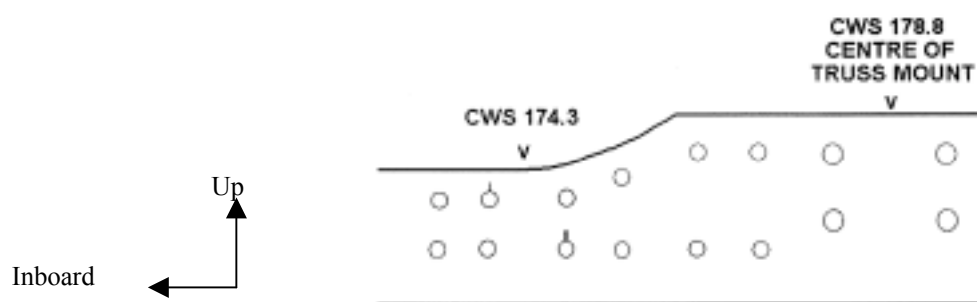


**Figure 1(b)** Example of cracking from Port wing of Aircraft 2

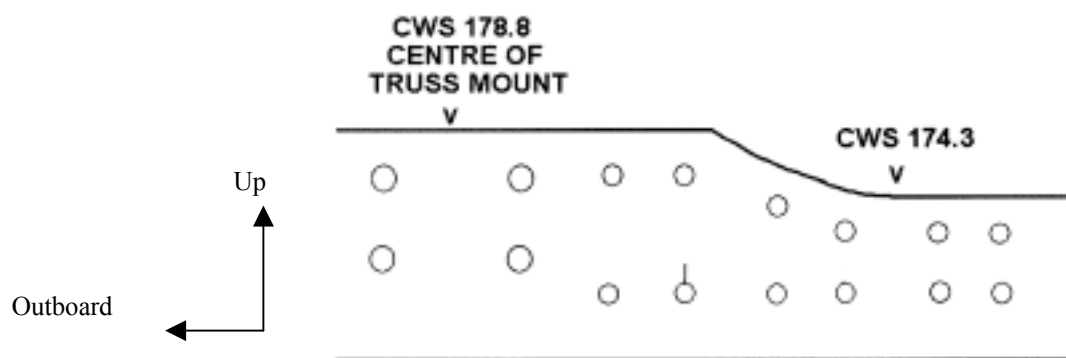


**Figure 1(c)** Example of cracking from Starboard wing of Aircraft 1

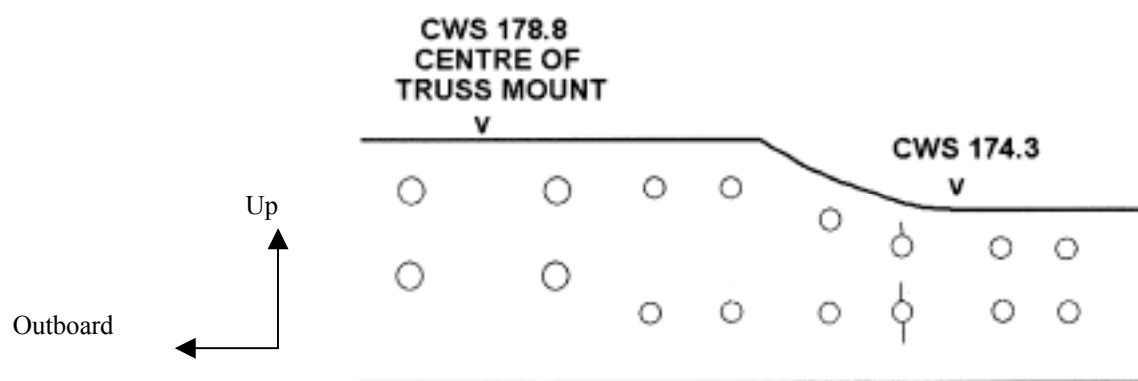


**Figure 1(d)** Example of cracking from Starboard wing of Aircraft 2

#### **8.5.2 Development of an Operational Usage Monitoring System using Commercial Data Recorders (M. J. Hollis, S. K. Campbell, D. C. Scott, J. D. Williams, DTA, New Zealand)**

The RNZAF C-130 Life of Type study conducted by Marshall Aerospace highlighted the need for more accurate usage monitoring of RNZAF Fleets. The Defence Technology Agency (DTA) was tasked with acquiring and developing a usage monitoring system suitable for installation in RNZAF fleets.

It was decided to develop a system based on commercially available data recorders and sensors. The system developed by DTA uses an eDAQ data recorder from SoMAT. The eDAQ is capable of recording multiple channels of data. For the RNZAF program, it has been configured to record four channels of strain data, one channel of normal acceleration data (measured near the aircraft centre of gravity), airspeed, altitude, cabin pressure and GPS data.

A prototype system was developed in conjunction with Safe Air Limited. The prototype was installed in an RNZAF C-130 in December 2004. The system is not yet operational as it awaits calibration flight trials that were postponed to allow deployment of the aircraft to assist the relief effort following the Boxing Day Tsunami.

### 8.5.3 Failure Investigation of Civilian UH-1H Main Rotor Blade, (A. D. James, P. C. Conor, DTA, New Zealand)

The RNZAF have previously reported an example of severe in-service fatigue of a UH-1H Iroquois main rotor blade (ICAF 2003). Currently there is a number of ex-military UH-1H helicopters in service within New Zealand. The Civil Aviation Authority of New Zealand was subsequently advised of an in-service fatigue crack of the main rotor blade of one of these aircraft. Due to the similarity of the failure to that experienced by the RNZAF, the Defence Technology Agency (DTA) assisted with the failure investigation.

The crack was visible on the under surface of the blade and extended through the leading edge, under the lower steel doubler and extended approximately 6 inches aft of the doubler (Figure 2). Upon removal of the doubler there was evidence of extensive disbonding and significant fretting on both the doubler and blade (Figure 3). To assist in exposing the fracture surface of the crack, saw cuts were made into the blade at the trailing edge and through the upper doubler, and the blade loaded in pure tension (Figure 4). In Figure 4, the inner end of the cracked blade has been loaded in tension to induce approximately the same degree of crack opening displacement as indicated by witness marks on the grip pad. The helicopter had evidently been flying with the crack in this configuration. The defect was much less visible when the rotor was stationary as the crack was closed by compressive forces in the lower blade surface.

The failure was verified to be similar to that experienced by the RNZAF. The exact cause of disbonding between the steel grip pad and blade in both the RNZAF and civil aircraft has not been categorically determined. It is considered that a range of loading conditions, bond degradation mechanisms and sub-optimal design all contribute to the observed cracking. Additional inspections have been instigated to ensure continuing airworthiness.



**Figure 2.** *View of the crack propagating beyond the doubler.*



**Figure 3.** Adhesive surfaces after removal of the grip pad (left). The fretting marks indicate the crack opening displacement experienced in flight.



*Figure 4. Application of a tensile load to simulate the crack opening displacement indicated by witness marks on the doubler. The aircraft was likely to have been flying with the crack in this configuration.*

## DISTRIBUTION LIST

A Review of Australian and New Zealand Investigations on Aeronautical  
Fatigue During the Period April 2003 to March 2005

Graham Clark

**DEFENCE ORGANISATION**

**Task Sponsor**                      **Chief AVD**

**S&T Program**

Chief Defence Scientist	}	shared copy
FAS Science Policy		
AS Science Corporate Management		
Director General Science Policy Development		
Counsellor Defence Science, London (Doc Data Sheet)		
Counsellor Defence Science, Washington (Doc Data Sheet)		
Scientific Adviser to MRDC Thailand (Doc Data Sheet)		
Scientific Adviser Joint		
Navy Scientific Adviser (Doc Data Sheet and Distribution List only)		
Scientific Adviser - Army (Doc Data Sheet and Distribution List only)		
Air Force Scientific Adviser		
Director Trials		

**Platforms Sciences Laboratory**

RLAM	
RLP	
RLFS	
L Molent	
R Locket (Aerostructures)	6 copies
K Watters	2 copies
M Heller	2 copies
G Hugo	2 copies
P Jackson	2 copies
LRF Rose	

Author: Graham Clark                      205 copies (sent to author at Fishermans Bend)

**DSTO Library and Archives**

Library Fishermans Bend  
Library Edinburgh  
Australian Archives

**Capability Systems Staff**

Director General Maritime Development (Doc Data Sheet only)  
Director General Aerospace Development

**Knowledge Staff**

Director General Command, Control, Communications and Computers (DGC4) (Doc Data Sheet only)

**Army**

ABCA National Standardisation Officer, Land Warfare Development Sector, Puckapunyal (4 copies)  
SO (Science), Deployable Joint Force Headquarters (DJFHQ) (L), Enoggera QLD (Doc Data Sheet only)



### **Air Force**

AIRCDRE D Tindal (DGTA) RAAF Williams  
 GPCAPT R Thomasson (DAIRENG) RAAF Williams  
 WGCDR J Agius (OIC-ASI) RAAF Williams

### **Intelligence Program**

DGSTA Defence Intelligence Organisation  
 Manager, Information Centre, Defence Intelligence Organisation

### **Defence Libraries**

Library Manager, DLS-Canberra  
 Library Manager, DLS - Sydney West (Doc Data Sheet Only)

### **UNIVERSITIES AND COLLEGES**

Dr K Shankar, Australian Defence Force Academy  
 ADFA Library  
 Prof R Jones, Dept of Mechanical Engineering, Monash University  
 Dr Lin Ye, Dept of Mechanical Engineering, University of Sydney  
 Hargrave Library, Monash University (Doc Data Sheet only)  
 Librarian, Flinders University

### **OTHER ORGANISATIONS**

National Library of Australia  
 NASA (Canberra)  
 AusInfo  
 Dr D Barton, SMS P/L

## **OUTSIDE AUSTRALIA**

### **INTERNATIONAL DEFENCE INFORMATION CENTRES**

US Defense Technical Information Center,	2 copies
UK Defence Research Information Centre,	2 copies
Canada Defence Scientific Information Service,	1 copy
NZ Defence Information Centre,	1 copy

### **ABSTRACTING AND INFORMATION ORGANISATIONS**

Library, Chemical Abstracts Reference Service  
 Engineering Societies Library, US  
 Materials Information, Cambridge Scientific Abstracts, US  
 Documents Librarian, The Center for Research Libraries, US

### **INFORMATION EXCHANGE AGREEMENT PARTNERS**

Acquisitions Unit, Science Reference and Information Service, UK  
 Library - Exchange Desk, National Institute of Standards and Technology, US  
 National Aerospace Laboratory, Japan  
 National Aerospace Laboratory, Netherlands  
 S Campbell Defence Technology Agency, Auckland NZ, 5 copies

SPARES (20 copies)

**Total number of copies: 311**

<b>DEFENCE SCIENCE AND TECHNOLOGY ORGANISATION</b> <b>DOCUMENT CONTROL DATA</b>					
				1. PRIVACY MARKING/CAVEAT (OF DOCUMENT)	
2. TITLE  A Review of Australian and New Zealand Investigations on Aeronautical Fatigue During the Period April 2003 to March 2005			3. SECURITY CLASSIFICATION (FOR UNCLASSIFIED REPORTS THAT ARE LIMITED RELEASE USE (L) NEXT TO DOCUMENT CLASSIFICATION)  <div style="display: flex; justify-content: space-between;"> <span>Document</span> <span>(U)</span> </div> <div style="display: flex; justify-content: space-between;"> <span>Title</span> <span>(U)</span> </div> <div style="display: flex; justify-content: space-between;"> <span>Abstract</span> <span>(U)</span> </div>		
4. AUTHOR(S)  Graham Clark			5. CORPORATE AUTHOR  Platforms Sciences Laboratory 506 Lorimer St Fishermans Bend Victoria 3207 Australia		
6a. DSTO NUMBER DSTO-TN-0624		6b. AR NUMBER AR-013-387		7. DOCUMENT DATE May 2005	
8. FILE NUMBER M1/8/1709		9. TASK NUMBER A20227B (AE/MGT - TTCP)		10. TASK SPONSOR CAVD	
				11. NO. OF PAGES 76	
				12. NO. OF REFERENCES 55	
13. URL on the World Wide Web  <a href="http://www.dsto.defence.gov.au/corporate/reports/DSTO-TN-0624.pdf">http://www.dsto.defence.gov.au/corporate/reports/DSTO-TN-0624.pdf</a>				14. RELEASE AUTHORITY  Chief, Air Vehicles Division	
15. SECONDARY RELEASE STATEMENT OF THIS DOCUMENT  <div style="text-align: center;"><i>Approved for public release</i></div>					
OVERSEAS ENQUIRIES OUTSIDE STATED LIMITATIONS SHOULD BE REFERRED THROUGH DOCUMENT EXCHANGE, PO BOX 1500, EDINBURGH, SA 5111					
16. DELIBERATE ANNOUNCEMENT  No Limitations					
17. CITATION IN OTHER DOCUMENTS <span style="float: right;">Yes</span>					
18. DEFTEST DESCRIPTORS  fatigue, fatigue tests, military aircraft, civil aircraft, research projects, Australia, New Zealand					
19. ABSTRACT This document has been prepared for presentation to the 29th Conference of the International Committee on Aeronautical Fatigue scheduled to be held in Hamburg, Germany, 6th and 7th June 2005. Brief summaries and references are provided on the aircraft fatigue research and associated activities of research laboratories, universities, and aerospace companies in Australia and New Zealand during the period April 2003 to March 2005. The review covers fatigue-related research programs as well as fatigue investigations on specific military and civil aircraft.					